

Integrated Corridor Management (ICM) Analysis, Modeling, and Simulation (AMS) for Minneapolis Site

Model Calibration and Validation Report

www.its.dot.gov/index.htm

Final Report – February 2010

FHWA-JPO-10-036

EDL Number 14943



U.S. Department of Transportation
Research and Innovative Technology
Administration

Produced by FHWA Office of Operations Support Contract DTFH61-06-D-00004
U.S. Department of Transportation
Federal Highway Administration

Notice

This document is disseminated under the sponsorship of the Department of Transportation in the interest of information exchange. The United States Government assumes no liability for its contents or use thereof.

1. Report No. FHWA-JPO-10-036		2. Government Accession No. EDL No. 14943		3. Recipient's Catalog No.	
4. Title and Subtitle Integrated Corridor Management (ICM) Analysis, Modeling, and Simulation (AMS) for Minneapolis Site Model Calibration and Validation Report				5. Report Date February 2010	
				6. Performing Organization Code	
7. Author(s) Yi-Chang Chiu, Brenda I. Bustillos, Vassilis Papayannoulis, Mark Hickman, Larry Head, Shuo Wang, and Vassili Alexiadis				8. Performing Organization Report No.	
9. Performing Organization Name and Address Cambridge Systematics, Inc. 555 12th Street, Suite 1600 Oakland, California 94607				10. Work Unit No. (TRAIS)	
				11. Contract or Grant No. DTFH61-06-D-00004	
12. Sponsoring Organization Name and Address U.S. Department of Transportation Research and Innovative Technology Administration (RITA) 1200 New Jersey Avenue, SE Washington, DC 20590				13. Type of Report and Period Covered Final Report	
				14. Sponsoring Agency Code HOP	
15. Supplementary Notes FHWA COTM: Dale Thompson, FHWA					
16. Abstract This technical report documents the calibration and validation of the baseline (2008) mesoscopic model for the I-394 Minneapolis, Minnesota, Pioneer Site. DynusT was selected as the mesoscopic model for analyzing operating conditions in the I-394 corridor study area, and the report provides details on the network development, traffic flow model calibration, origin-destination (OD) demand calibration, and model validation. In addition, the report provides a modeling methodology for simulation of transit, as well as the results of a sensitivity analysis, utilizing information from a known incident, undertaken to verify the ability of the validated model to replicate operating conditions for incident scenarios. In summary, the DynusT model for the I-394 corridor replicated the 2008 baseline operating conditions well as evidenced by the comparisons of observed and modeled volumes, travel times, and speed contours on I-394. Furthermore, the simulated known incident exhibited consistent traffic diversions, speed reductions, duration, and queue propagation with the actual data.					
17. Key Words Integrated Corridor Management, ICM, traffic simulation, modeling, mesoscopic models, AMS, traffic analysis, calibration, validation, incident, criteria				18. Distribution Statement No restrictions.	
19. Security Classification (of this report) unclassified		20. Security Classification (of this page) unclassified		21. No. of Pages 87	22. Price NA

Acknowledgements

The successful completion of this project could not have happened without the help and input from Minnesota Department of Transportation (Mn/DOT), Cambridge Systematics, Inc., Athey Creek Consultants, and Alliant Engineering.

Table of Contents

Executive Summary	1
Chapter 1 Introduction	2
1.1 MODELING FRAMEWORK.....	2
Chapter 2 I-394 and Arterial Network Modeling	5
2.1 I-394 CORRIDOR STUDY AREA DEFINITION.....	5
2.2 SIMULATION, ANALYSIS, AND PEAK-PERIOD DEFINITIONS.....	6
2.3 NETWORK CLEANUP AND VERIFICATIONS.....	7
2.4 TRAFFIC DATA COLLECTION.....	7
2.4.1 Freeway Data.....	7
2.4.2 Arterial Data.....	8
2.5 TRAFFIC FLOW MODEL CALIBRATION.....	9
2.5.1 Traffic Flow Model Calibration Methodology.....	9
2.5.2 Traffic Flow Model Type 1 Calibration (I-394 Corridor)....	10
2.5.3 Arterial Traffic Flow Model.....	15
2.6 TIME-DEPENDENT ORIGIN-DESTINATION MATRICES CALIBRATION.....	16
2.6.1 OD Demand Calibration Methodology.....	16
2.6.2 OD Demand Calibration Results.....	19
2.7 MODEL VALIDATION.....	21
2.7.1 Validation Criteria.....	21
2.7.2 Traffic Counts.....	22
2.7.3 Total Link Counts.....	24
2.7.4 Travel Times.....	25
2.7.5 Visual Audits – Individual Link Speeds.....	34
2.7.6 Visual Audits – Bottlenecks.....	36
2.8 TESTING AND VALIDATION WITH A PRIOR KNOWN EVENT.....	40
2.8.1 Methodology.....	40
2.8.2 Incident Scenario.....	42
2.8.3 Analysis Results.....	43
Chapter 3 Transit	53
3.1 TRANSIT CODING.....	54
3.2 TRANSIT OD MATRICES.....	60
3.3 PARK-AND-RIDE UTILIZATION.....	60
References	63
Appendix A. Time-Dependent Origin-Destination Matrices Calibration	
Methodology	A-1
STAGE 1 CALIBRATION – MATCH TOTAL COUNTS.....	A-2
STAGE 2 CALIBRATION – MATCH SPEED PROFILE.....	A-7
Appendix B. Metric/English Conversion Factors	B-1

List of Tables

Table 2-1.	Freeway Traffic Flow Model Parameter Values.....	14
Table 2-2.	Arterial Traffic Flow Model Parameter Values	15
Table 2-3.	Validation Criteria for I-394 Corridor	22
Table 2-4.	High Volume Link Statistics.....	24
Table 2-5.	Travel Time Criteria Validation for Entire Simulation Period.....	33
Table 2-6.	Travel Time Criteria Validation for Peak Period.....	33
Table 2-7.	Arterial Traffic Volumes	35
Table 2-8.	Scenario Characteristics and DynusT Running Modes.....	41
Table 3-1.	CUBE Transit Line File Structure.....	55
Table 3-2.	Route Definition of Line 672 Westbound in DynusT	57
Table 3-3.	Timepoint Definition in DynusT for Route 672 Westbound	58

List of Figures

Figure 1-1.	I-394 Subarea Extraction Process Illustration	3
Figure 1-2.	Modeling Framework.....	4
Figure 2.1	Subarea Network Cut on DynusT With Tagged OD Zones and Links (Left) and Google Maps (Right)	6
Figure 2-2.	Available Traffic Count Locations	8
Figure 2-3.	Modified Greenshields Model.....	9
Figure 2-4.	Sensor Volumes Along I-394 for 6:00 a.m. to 10:00 a.m. Simulation Period.....	10
Figure 2-5.	Sensor Locations on I-394.....	12
Figure 2-6.	Speed-Density Curve for A.M. Eastbound Sensor S282.....	13
Figure 2-7.	Flow-Density Curve for A.M. Eastbound Sensor S282.....	14
Figure 2-8.	Calibrated Speed-Density Curve	15
Figure 2-9.	DynusT Algorithmic Procedure	18
Figure 2-10.	Relative Gap Convergence for Calibration Iteration 72	19
Figure 2-11.	Origin Zone Percent Difference versus Trip Production	20
Figure 2-12.	Destination Zone Percent Difference versus Trip Attraction.....	21
Figure 2-13.	Simulated versus Observed Counts for Iterations 0 and 72.....	23
Figure 2-14.	TH-55, TH-7, and I-394 East and Westbound Travel Time Paths	26
Figure 2-15.	I-394 Eastbound Travel Times for Day of Interest.....	27
Figure 2-16.	I-394 Westbound Travel Times for Day of Interest.....	28
Figure 2-17.	TH-55 Eastbound Travel Times for Day of Interest.....	29
Figure 2-18.	TH-55 Westbound Travel Times for Day of Interest.....	30
Figure 2-19.	TH-7 Eastbound Travel Times for Day of Interest.....	31
Figure 2-20.	TH-7 Westbound Travel Times for Day of Interest.....	32
Figure 2-21.	Sensor Locations on I-394.....	34
Figure 2-22.	Volume Comparison on I-394 Eastbound.....	35
Figure 2-23.	Field Speed Contour Data for October 28-30, 2008	37

Figure 2-24.	I-394 Eastbound A.M. Speed Space Time Contour (Field Data: October 08 Averaged)	38
Figure 2-25.	I-394 Eastbound A.M. Speed Space Time Contour (Simulation)	39
Figure 2-26.	DynusT Baseline and Scenario Modeling Framework	40
Figure 2-27.	Three Activated Dynamic Message Sign Locations	43
Figure 2-28.	Speed Contour of Field Data for the Incident Scenario	44
Figure 2-29.	Speed Contour of Simulation Data for the Incident Scenario.....	45
Figure 2-30.	EB I-394 East of I-494	46
Figure 2-31.	NB I-494 TO EB I-394 Ramp.....	47
Figure 2-32.	EB I-394 TO NB I-494 Ramp.....	47
Figure 2-33.	EB I-394 TO SB I-494 Ramp (Detector 1871).....	48
Figure 2-34.	NB I-494 to Carson Parkway Ramp.....	49
Figure 2-35.	NB I-494 to Highway 55 Ramp.....	49
Figure 2-36.	SB I-494 South of I-394.....	50
Figure 2-37.	Baseline and Incident Case Volume Comparison (Vehicles).....	51
Figure 3-1.	Transit Schedule for Line 672.....	59
Figure 3-2.	Park-and-Ride Lot Average versus Estimated Usage (Vehicles)	62
Figure A-1.	Two-Stage OD estimation Framework.....	A-2
Figure A-2.	OD Demand Calibration Framework.....	A-6
Figure A-3.	Relationship between Demand, Capacity and Observed Flow	A-8
Figure A-4.	Cumulative Curves for an Upstream Detector and Downstream Detector	A-9

Executive Summary

The objective of the Integrated Corridor Management (ICM) initiative is to demonstrate how Intelligent Transportation Systems (ITS) technologies can efficiently and proactively manage the movement of people and goods in major transportation corridors. The ICM initiative aims to pioneer innovative multimodal and multijurisdictional strategies – and combinations of strategies – that optimize existing infrastructure to help manage congestion in our nation’s corridors. The objectives of the “ICM – Tools, Strategies, and Deployment Support” project are to refine analysis, modeling, and simulation (AMS) tools and strategies, assess Pioneer Site data capabilities, conduct AMS for the site, and conduct AMS tools post-demonstration evaluations. The modeling approach that emerged from the analysis of capabilities found in existing AMS tools, as well as from the ICM Test Corridor project, is an integrated platform that can support corridor management planning, design, and operations by combining the capabilities of existing tools. The integrated approach is based on interfacing travel demand models, mesoscopic simulation models, and microscopic simulation models.

This technical report documents the calibration and validation of the baseline (2008) mesoscopic model for the I-394 Minneapolis, Minnesota Pioneer Site. DynusT was selected as the mesoscopic model for analyzing operating conditions in the I-394 corridor study area, and the report provides details on the network development, traffic flow model calibration, origin-destination (OD) demand calibration, and model validation. In addition, the report provides a modeling methodology for simulation of transit, as well as the results of a sensitivity analysis, utilizing information from a known incident, undertaken to verify the ability of the validated model to replicate operating conditions for incident scenarios.

In summary, the DynusT model for the I-394 corridor replicated the 2008 baseline operating conditions well as evidenced by the comparisons of observed and modeled volumes, travel times, and speed contours on I-394. Furthermore, the simulated known incident exhibited consistent traffic diversions, speed reductions, duration, and queue propagation with the actual data.

Chapter 1 Introduction

In the aftermath of the I-35W Bridge collapse, between the University of Minnesota campus and downtown Minneapolis, on August 1, 2007, the Federal Highway Administration (FHWA) provided technical and decision support to Mn/DOT. A critical element of that effort was the development of the I-35W regional dynamic model, based on DynusT, to be used as a decision support tool to help evaluate and prioritize transportation needs and proposed strategies based on detour routes of post-collapse traffic conditions. Networks, trip tables, and other pertinent data were migrated from the regional travel demand model maintained by the Metropolitan Council serving the Twin Cities area. The regional travel demand model is a CUBE-based model, and it is comprised of 1,236 Traffic Analysis Zones (TAZ); nearly 5,000 nodes; and 12,000-plus links.

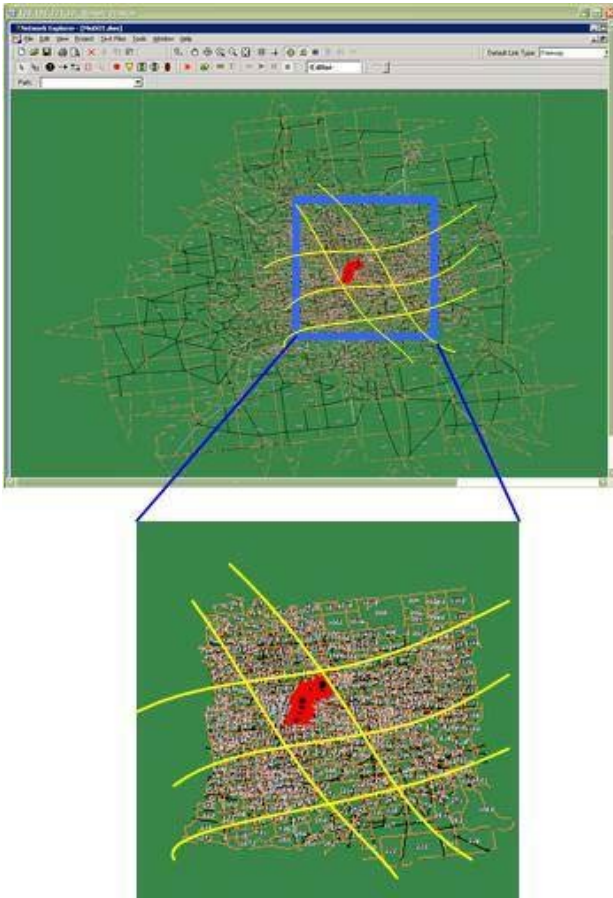
For the purposes of the ICM project, the I-35W Bridge DynusT model was utilized to extract a subarea (or subnetwork) for the I-394 corridor, as illustrated in Figure 1-1. A critical element of the subarea extraction process was the definition of the boundaries, so that the trip length for vehicles going through the corridor was preserved without being excessively shortened. To accomplish this task, a “select link” analysis was performed to determine origins and destinations of traffic traversing critical links.

The modeling framework for the I-394 corridor consists of three major components: 1) baseline model setup, 2) validation and calibration, and 3) pre-ICM and post-ICM scenario analysis. This technical report documents the calibration and validation of the baseline (2008) DynusT model for the I-394 Minneapolis, Minnesota Pioneer Site. In addition, the report provides a modeling methodology for simulation of transit, as well as the results of a sensitivity analysis, utilizing information from a known incident, undertaking to verify the ability of the validated model to replicate operating conditions for incident scenarios. Pre- and post-ICM scenario analysis will be provided under a separate document.

1.1 Modeling Framework

The setup of the baseline model starts with the conversion of the travel demand model (TDM), provided by the planning agency in the Twin Cities region. After converting the existing TDM model, additional data are acquired and entered into the model. These data include signal timing plans and intersection lane geometry configuration. The calibration of the regional model focuses on both traffic flow models and OD tables.

The calibration of the traffic flow model is aimed at matching the speed-density relationship exhibited in the collected field data. The calibration of the OD tables emphasizes the matching of link counts by adjusting the OD tables, originally provided by the planning agency. Once the regional model is calibrated, the select-link analysis is performed to determine the limit/boundary of the ICM network. The purpose of the select-link analysis is to understand the origin and destination for all the traffic traversing the ICM corridor. With this step, the boundary determined for the ICM network of interest retains most of the trips' lengths.

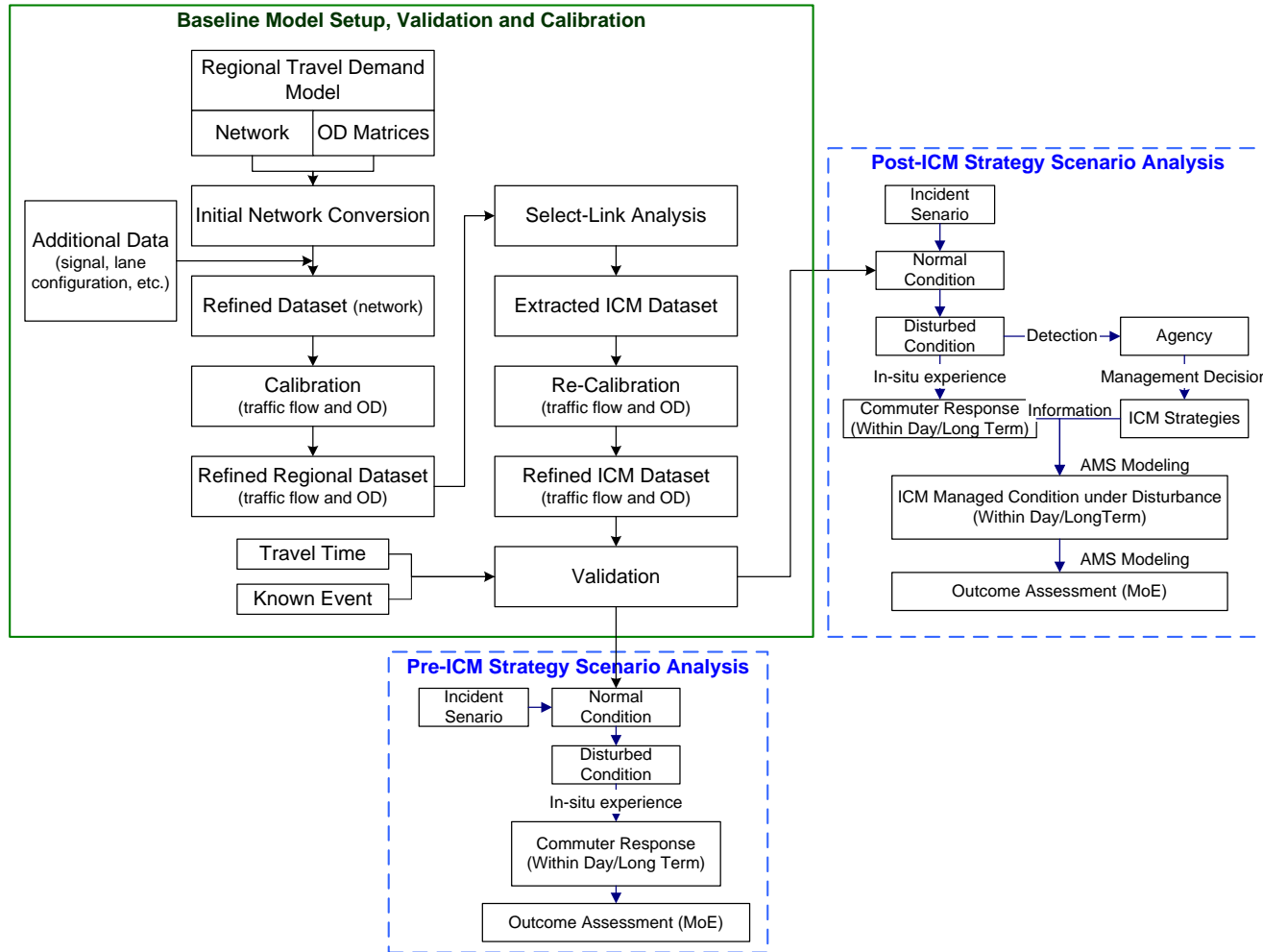
Figure 1-1. I-394 Subarea Extraction Process Illustration

[Source: Screen Capture DynusT software ©DynusT Lab.]

Given the extracted ICM network, a second round of OD calibration is performed. This step applies more detector data within the ICM network to further fine-tune the OD tables. Validation is performed using collected travel time and known event to ensure the validity of the calibrated model. At this step, the baseline model is ready.

The analysis of ICM scenarios is concerned with the impact of the incident scenarios of interest and the performance of the ICM strategies of interest. The pre-ICM analysis focuses on quantifying the impact of an incident without ICM strategies; whereas, the post-ICM analysis applies the same incident scenario with a selected number of ICM strategies. For the modeling of the pre-ICM strategy, the disturbed network condition is modeled by properly describing the travelers' response to congestion and the existing ITS technologies. In the post-ICM strategy analysis, the ICM strategies provide added opportunities for travelers to access information and/or make other decisions in response to incident-induced congestion. The outcomes of all studied strategy-scenario combinations are quantified in defined measures of effectiveness (MoE). The entire modeling approach is illustrated in Figure 1-2.

Figure 1-2. Modeling Framework



[Source: CS generated, original to this document.]

Chapter 2 I-394 and Arterial Network Modeling

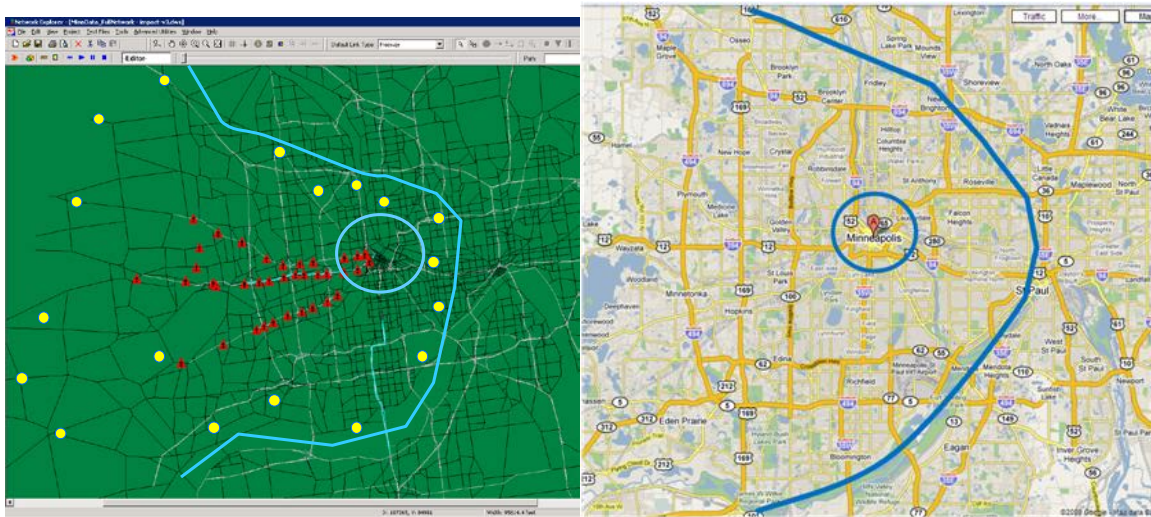
2.1 I-394 Corridor Study Area Definition

Before the I-35W Bridge regional DynusT model was spatially reduced to a subarea (or subnetwork) to reflect the I-394 corridor study area, care needed to be exercised to define the boundary of the reduced network so that the trip length for vehicles going through the corridor was preserved without being excessively shortened. This precaution avoided introducing significant bias to the modeling results. It was determined that the area of investigation must include links on the I-394 corridor along with links on highways running parallel or through it (e.g., TH-55 and TH-7). Utilizing a “select link” analysis process, the OD pairs accounting for the majority of the traffic traversing the tagged links are then recorded. The “select link” analysis requires a traffic assignment utilizing DynusT dynamic traffic assignment (DTA) capabilities. The assignment is run until a dynamic user equilibrium (DUE) is reached, where a DUE condition can be stated as:

For each OD pair and particular departure time, the experienced travel time on all used routes is equal and minimal, and travelers cannot improve their experienced travel time by unilaterally switching to another route [1].

Figure 2-1 displays the selected links with red triangles, while the majority of OD pairs traversing these links are displayed as yellow dots. These yellow dots were used to determine the boundary of the study area, showed by a blue line in Figure 2-1. Given the defined boundary, the reduction of the network was performed in DynusT graphical user interface (GUI) by selecting and deleting the portion outside the defined boundary. In this process, the zones encompassed by the subarea network were retained; whereas, the zones traversed by this boundary were redefined as external zones to the subarea network. To place the I-394 corridor study area in perspective, a Google map of the subarea is also provided in Figure 2-1.

Figure 2.1 Subarea Network Cut on DynusT With Tagged OD Zones and Links (Left) and Google Maps (Right)



[Source: Screen Capture DynusT software ©DynusT Lab and Google Maps.]

The resulting I-394 corridor study area is bound by I-494 to the north, the Mississippi River to the south, and downtown Minneapolis to the east; and includes special generators/attractors, such as the Minneapolis' Central Business District (CBD), the University of Minnesota, and the Metrodome Stadium. It is comprised of 558 zones (including 60 external zones); 2,837 nodes, 6,871 links, and 1.5 million vehicles.¹

2.2 Simulation, Analysis, and Peak-Period Definitions

For the I-394 corridor study area, the simulation period is defined to be 5:00 a.m. to 11:30 a.m., in which 5:00 a.m. to 6:00 a.m. is the “pre-loading” period. In the pre-loading period, vehicles are loaded to populate the network with a reasonable amount of traffic. The period of interest (analysis period) from which the results are analyzed lasts from 6:00 a.m. to 11:00 a.m. (300 minutes). The a.m. peak period is defined to be from 6:45 a.m. to 8:45 a.m. This peak period is determined by examining the 15-minute volume data collected along the I-394 corridor in the eastbound direction from 6:00 a.m. to 11:00 a.m. The time period in which the OD was calibrated is from 6:00 a.m. to 10:00 a.m. The 10:00 to 11:30 a.m. OD was prepared using the 9:00-10:00 a.m. OD matrix at a scale-down magnitude. This approximation was considered reasonable for the purpose of maintaining network loading after the peak period.

¹ The 1.5 million vehicles demand was further adjusted during the demand calibration process described in Section 2.6.

2.3 Network Cleanup and Verifications

After the I-394 corridor study area was defined, the verification and refinement of the network was initiated. To make the network easier to identify, feature points creating roadway curvature were added, and link lengths were adjusted. The number of lanes on I-394, TH-55, and TH-7, as well as on other selected freeways and arterials, was verified, along with geometrics and signal timings. The verification process was based on Google earth and Google maps, and information was provided by Mn/DOT. Overall, more than 100 intersections were carefully reviewed. Some sites appeared to be under construction on Google maps, which became difficult to verify. By consulting with Mn/DOT, detailed schematics and information of these construction regions were obtained, allowing for proper adjustments to the DynusT network. After all activities were completed, spot checking was conducted to identify and correct any remaining issues.

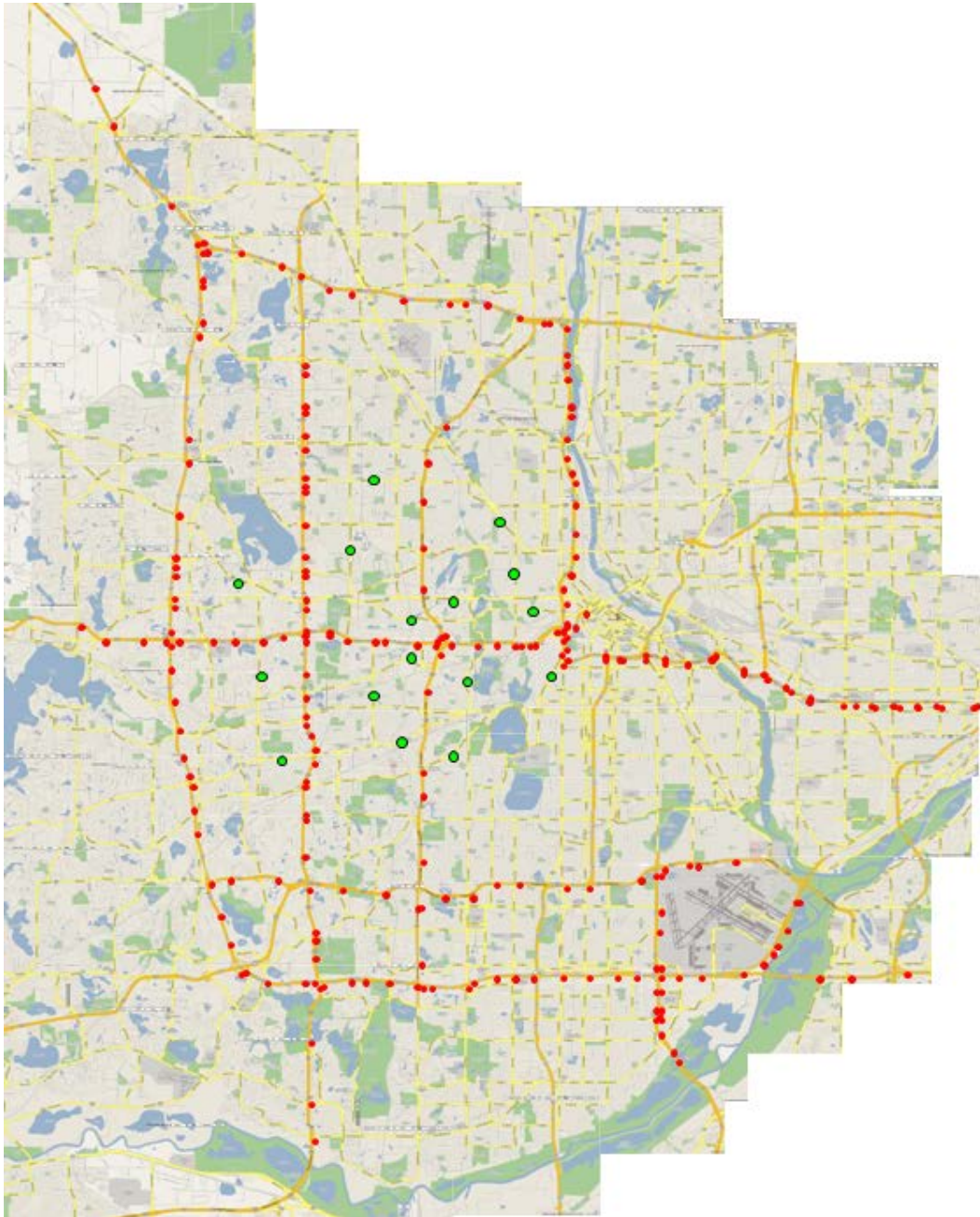
2.4 Traffic Data Collection

2.4.1 Freeway Data

A large portion of the data required for model validation is data that is automatically recorded by field sensors or monitoring devices, and stored on servers at either Mn/DOT or a local transit agency. In addition to this data, Mn/DOT collected travel time and arterial volume data on three “typical” days in October 2008 (i.e., Tuesday, October 28, 2008; Wednesday, October 29, 2008; and October 30, 2008). Given the data similarities among these three days, Wednesday, October 29, 2008, was selected to represent a “typical” day for the I-394 corridor study area. The Mn/DOT “data extract” tool [2] was used to compile a.m. period traffic data for the eastbound (EB) and westbound (WB) directions of the I-394 corridor, while travel time data was provided by Mn/DOT and their collaborating consultants.

Over 200 interstate and state freeway sensor locations were initially flagged as potential locations for traffic count data for the OD calibration and model validation procedures. The sensor locations were verified according to the “all detector report” [3] from Mn/DOT. The red circles in Figure 2-2 indicate the locations of all freeway sensors used for initial data collection. It was later decided to reduce the list of sensor locations due to either redundancy of neighboring sensors or the inability to extract data from malfunctioning sensors. Hence, the total number of freeway sensors utilized was 186.

Figure 2-2. Available Traffic Count Locations



[Source: Google Maps.]

2.4.2 Arterial Data

Arterial data could not be extracted from the Mn/DOT “data extract” tool; therefore, Mn/DOT and their collaborating consultants provided traffic count and travel time data for selected arterials. Traffic

counts were provided for a total of 16 arterial locations; mostly concentrated in close proximity to I-394, and are identified as green dots in Figure 2-2.

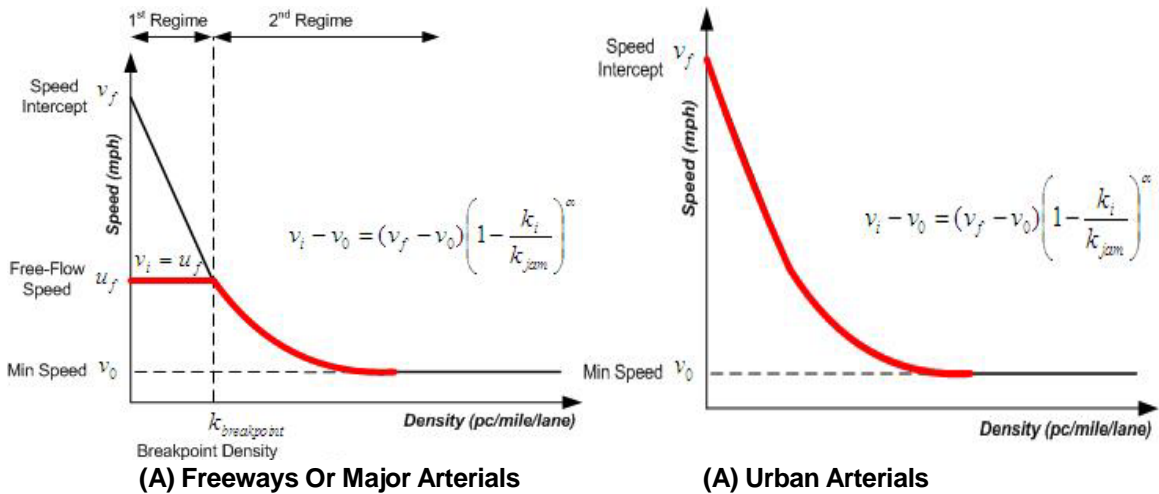
2.5 Traffic Flow Model Calibration

2.5.1 Traffic Flow Model Calibration Methodology

There are two types of traffic flow models identified in the DynusT simulation model. Type 1 is better suited for freeway or major urban arterial traffic flow behavior, because freeway links have greater capacity than other secondary arterials, and can accommodate larger densities near free-flow speeds. Type 2 is better suited for secondary arterial – type links, where speeds are more sensitive to density changes. Both flow model types are shown in Figure 2-3, and they are based on the modified Greenshields model, which follows the basic traffic engineering principles and relationships of speed, density, and flow. Equation (1) describes the modified Greenshields model.

$$v_i - v_0 = (v_f - v_0) \left(1 - \frac{k_i}{k_{jam}}\right)^\alpha \tag{Equation 1}$$

Figure 2-3. Modified Greenshields Model



Free-flow speed v_f , minimum speed v_0 , density breakpoint $k_{breakpoint}$, and jam density k_{jam} are estimated based on the collected data. The unknown variable α is the shape term, which gives the curvature of the speed-density curve as the density increases. By taking the natural log (ln) of Equation (2), the α can be estimated by performing a linear regression analysis of what is now a linear equation, as shown in Equation (2):

$$\ln(v_i - v_0) = \ln(v_f - v_0) + \alpha \left(1 - \frac{k_i}{k_{jam}}\right) \tag{Equation 2}$$

2.5.2 Traffic Flow Model Type 1 Calibration (I-394 Corridor)

Since the corridor of interest is I-394, it was decided to analyze the traffic flow characteristics along this corridor. This was accomplished by extracting the speed, density, flow, and volume count data from the freeway sensor information collected earlier. Figure 2-4 demonstrates the volume observed between 6:00 a.m. and 10:00 a.m. on Wednesday, October 29, 2008. The traffic sensors that provided the most data coverage along the corridor were selected. Currently, there are 13 sensors for the WB direction and 16 sensors for the EB direction. For Figure 2-4, sensors should be read from right to left, which resembles the direction of traffic. That is, “s273” is located near TH-169, “s279” is near TH-100. Accordingly, EB sensors in Figure 2-4(A) should be read from left to right. Illustrations of sensor locations are provided in Figure 2-5.

Figure 2-4. Sensor Volumes Along I-394 for 6:00 a.m. to 10:00 a.m. Simulation Period

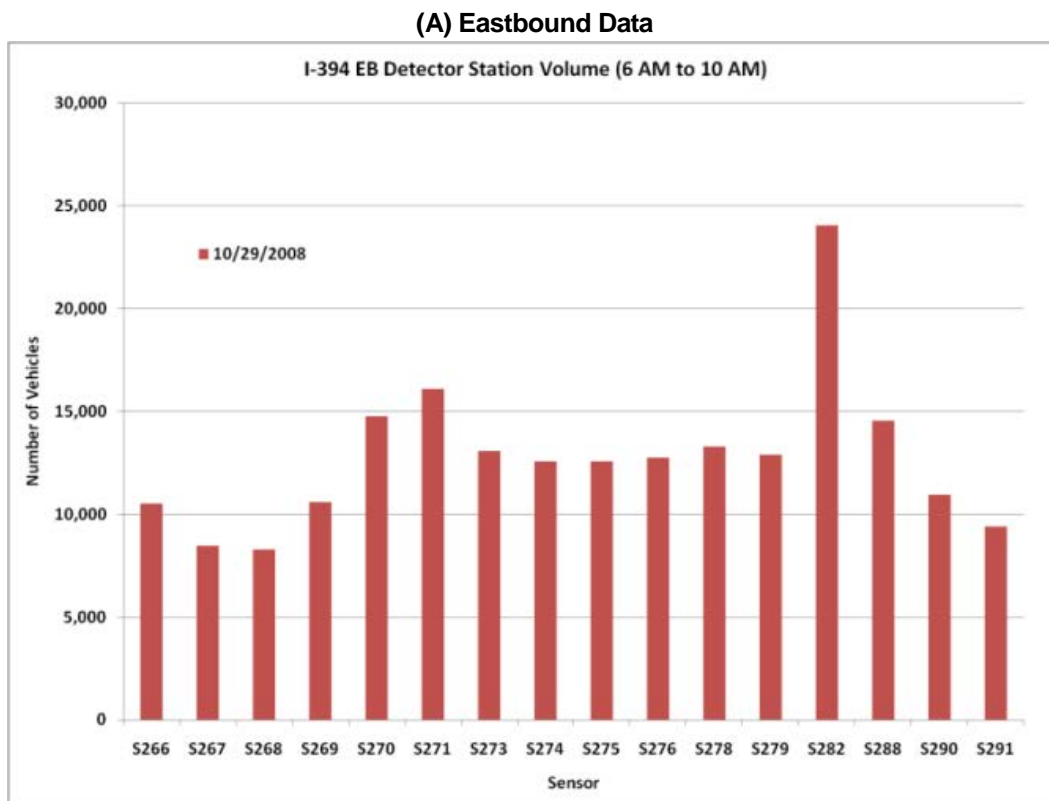


Figure 2-4. Sensor Volumes Along I-394 for 6:00 a.m. to 10:00 a.m. Simulation Period (continued)

(B) Westbound Data

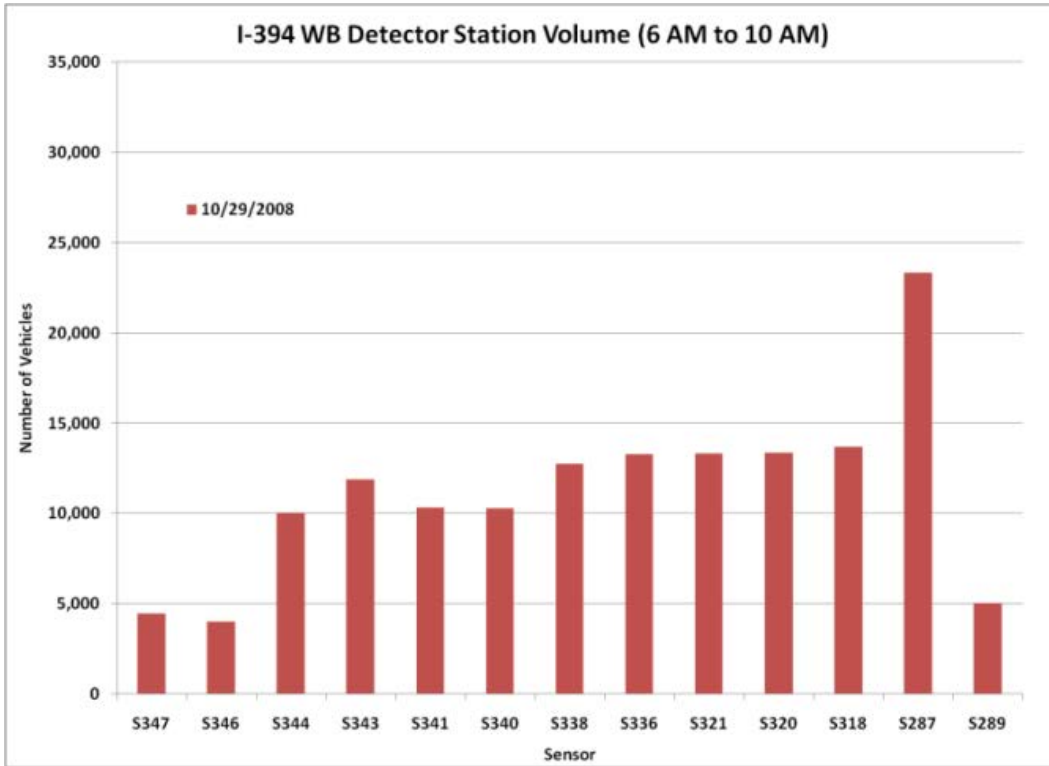
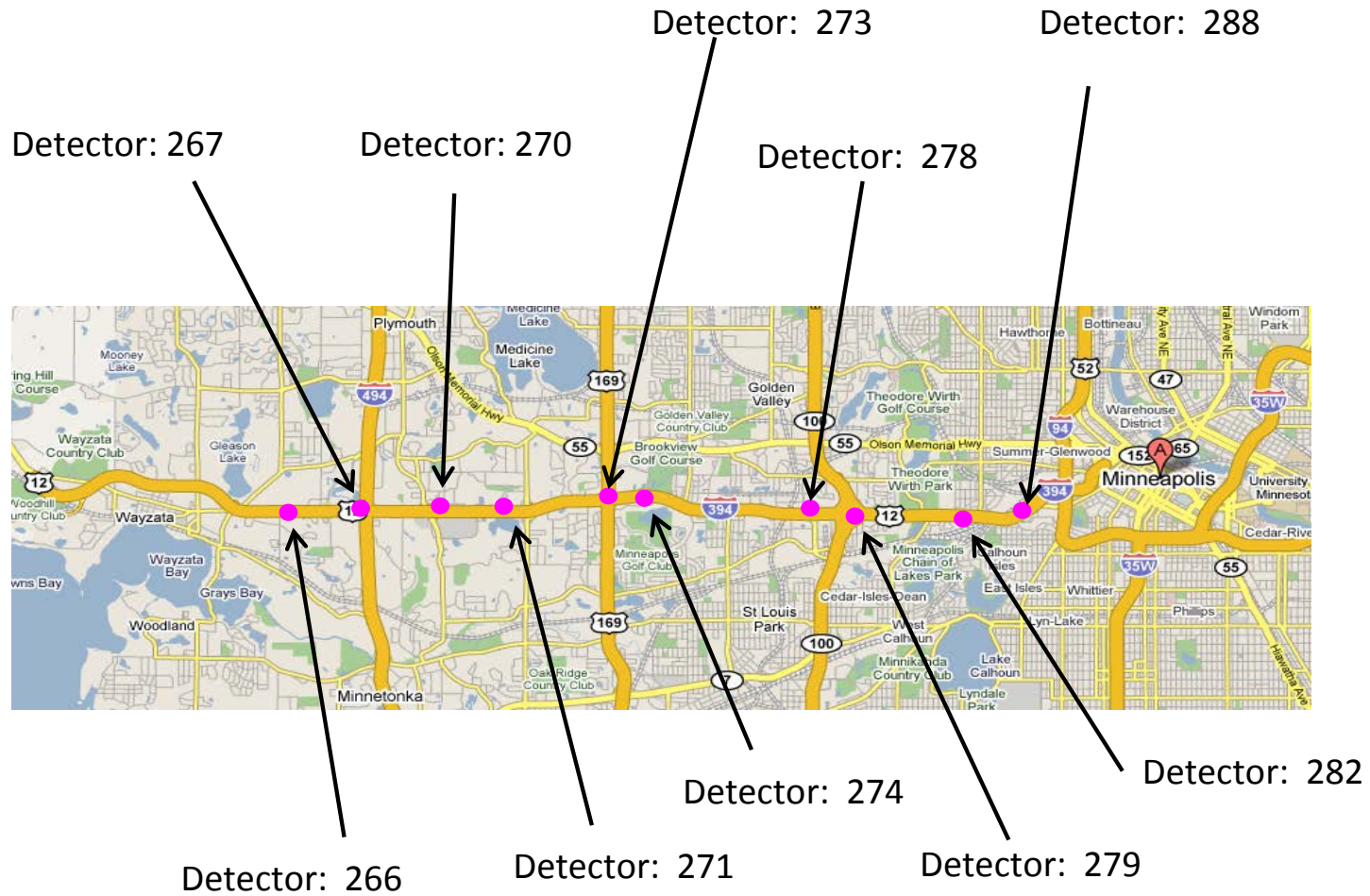


Figure 2-5. Sensor Locations on I-394



[Source: Google Maps.]

A more in-depth analysis of each I-394 EB sensor was performed to identify suitable data for traffic flow model calibration. The analysis was based on the speed-density and flow-density curves for each sensor. Figure 2-6 shows the speed, density, and flow relationships of traffic under various levels of congestion for EB direction detector station “S282.”

From Figure 2-7, free-flow speed v_f was estimated to be approximately 68 mph, while the minimum speed v_0 was estimated at 5 mph. The density breakpoint $k_{breakpoint}$ was approximated to be 20 veh/mile/lane. Different values of the jam density k_{jam} were used in conjunction with the calibration of the traffic flow model against the speed-density curve from S282 data. v_i and k_i were the data points forming the speed-density curve, while α is the unknown variable being solved.

Figure 2-6. Speed-Density Curve for A.M. Eastbound Sensor S282

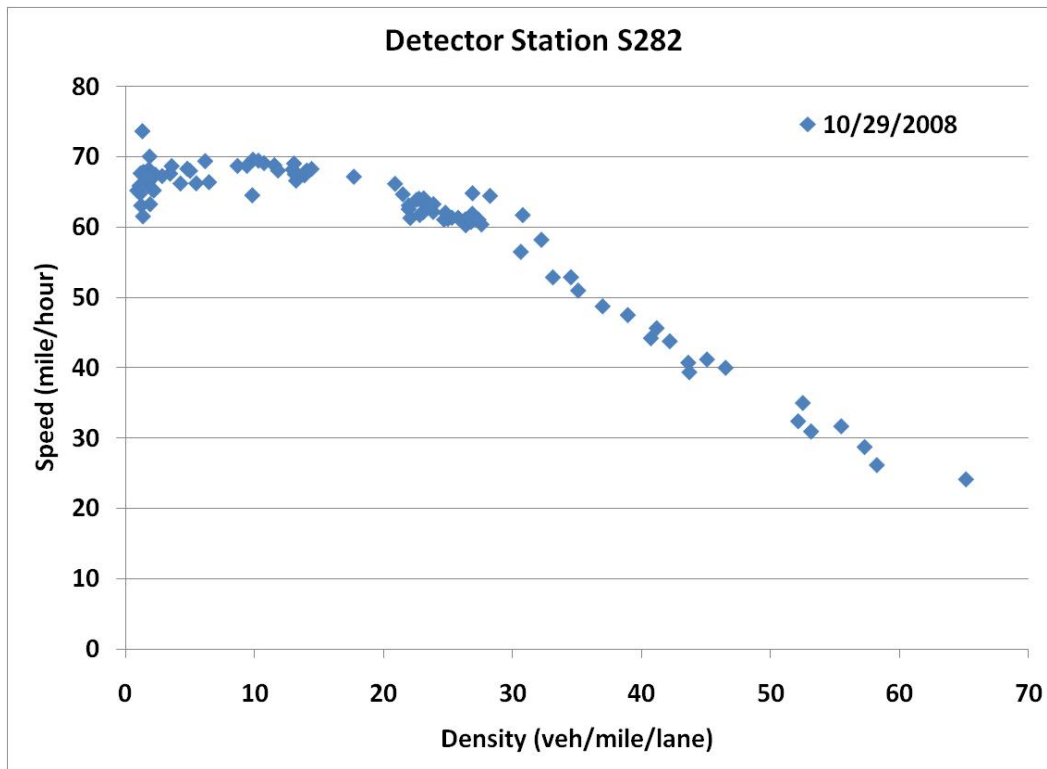
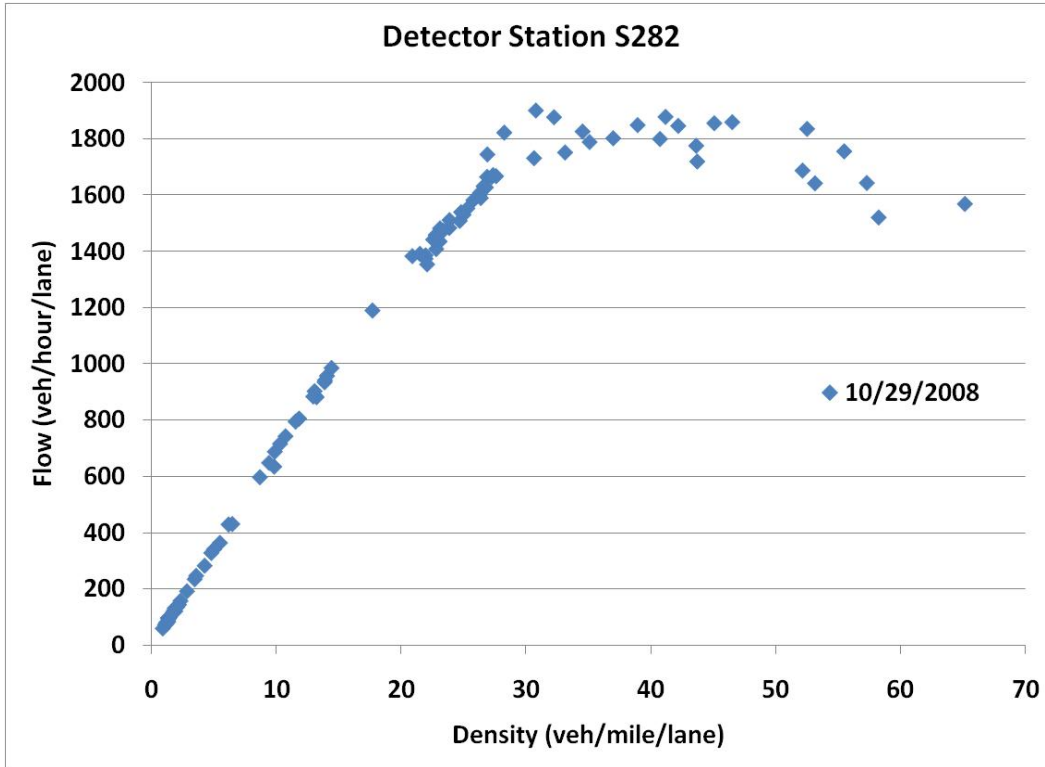


Figure 2-7. Flow-Density Curve for A.M. Eastbound Sensor S282

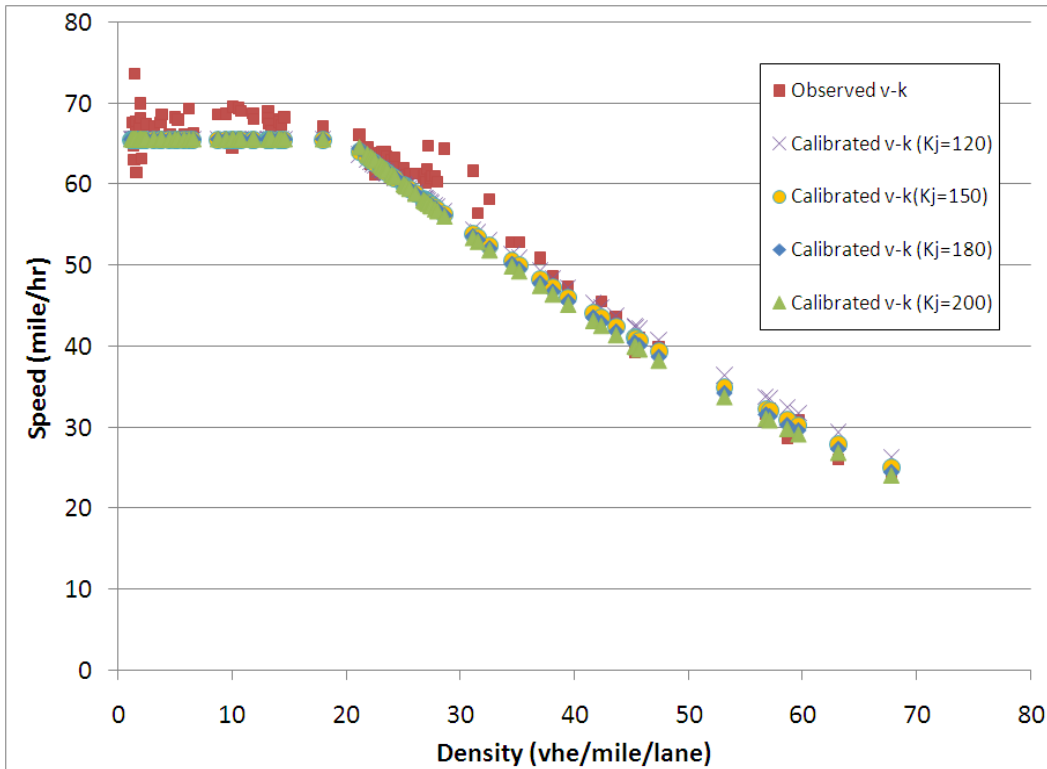


After multiple linear regression analyses under four k_{jam} values (120, 150, 180, and 200), $k_{jam} = 180$ veh/mile/lane and α value of 3.33 were found to be the optimal parameters with an R^2 value of 0.981129. Figure 2-8 illustrates the calibrated speed-density curve, while Table 2-1 summarizes, the calibrated traffic flow model parameters. This calibrated traffic flow model was applied to all freeway links and major urban arterials, such as TH-55 and TH-7 in the network

Table 2-1. Freeway Traffic Flow Model Parameter Values

Parameter	Value
v_0	5 mph
v_f	68 mph
$k_{breakpoint}$	20 veh/mile/lane
k_{jam}	180 veh/mile/lane
α	3.33

Figure 2-8. Calibrated Speed-Density Curve



2.5.3 Arterial Traffic Flow Model

No detailed arterial data, such as speed, density, and flow, was available; therefore, the arterial traffic flow model variables were assumed based on available data from secondary sources. These past arterial flow models proved to be quite stable and provided adequate estimation of arterial behavior. The final arterial traffic flow model parameters are given in Table 2-2.

Table 2-2. Arterial Traffic Flow Model Parameter Values

Parameter	Value
v_0	5 mph
v_f	Speed limit +-
$k_{breakpoint}$	N/A
k_{jam}	200 veh/mile/lane
α	3.55

2.6 Time-Dependent Origin-Destination Matrices Calibration

Even though the regional dynamic model had previously undergone one OD demand calibration, to fine-tune the regional demand trip tables, an additional 202 traffic counts were identified for the I-394 corridor study area. As such, the extracted trip table for the I-394 corridor study area was further adjusted based on these counts, utilizing a two-step OD demand calibration methodology developed by the University of Arizona.

2.6.1 OD Demand Calibration Methodology

The first step is to systematically match the total link volumes/counts over the entire analysis period (extended peak hours) by adjusting the OD entries through the optimization model. The second step is to properly represent the speed profile through the demand-supply concept based on the calibrated OD. There are two advantages to this approach: it reduces the problem to a manageable size, and it has a satisfactory convergence behavior.

The calibration process attempts to match simulated time-varying link volumes with observed link traffic counts collected from the field so that the difference between the simulated link volumes and observed link volumes is minimal. The calibration procedure is a bi-level optimization problem. The upper level is the one-norm linear program optimization problem minimizing total link count deviation, and the lower level is the DUE problem solved by DynusT (refer to Appendix A for a brief explanation).

This procedure calls for iterative interplays of DynusT and the calibration program. DynusT is executed with the given demand and run to DUE. A post-processing program is used to evaluate vehicle-based output data and accumulate information on vehicles (and their associated OD pair) whose paths traversed any link being evaluated. At this point, the link volumes are known. OD pairs that were found to have vehicles traveling through evaluated links are considered affected OD pairs. The link volumes, observed counts, and affected OD pairs are fed into a one-norm LP formulation and solver in order to estimate the OD matrix that aims to minimize the deviations of simulated and observed link counts. The total number of adjusted OD trips is then distributed to the time-dependent OD matrices according to the weighted ratios of each affected OD pair. The time-dependent OD demand tables are then rebuilt to reflect the changes, and the demand is fed into DynusT and rerun to DUE through another inner loop to evaluate the new demand. In this nested algorithmic process, each outer loop is called the OD iteration, within which each DynusT run includes multiple iterations until convergence.

As further illustrated in Figure 2-9, at each DUE iteration, a mesoscopic simulation (network loading) is run for the analysis period. The necessary information is then passed to the time-dependent shortest path and assignment algorithms, to update the vehicle assignment for each origin destination and departure time. This procedure is repeated for multiple iterations until the relative gap target value is reached.

The OD iterations continue until the maximum number of OD iterations are reached, or a pre-specified stopping criterion is met.

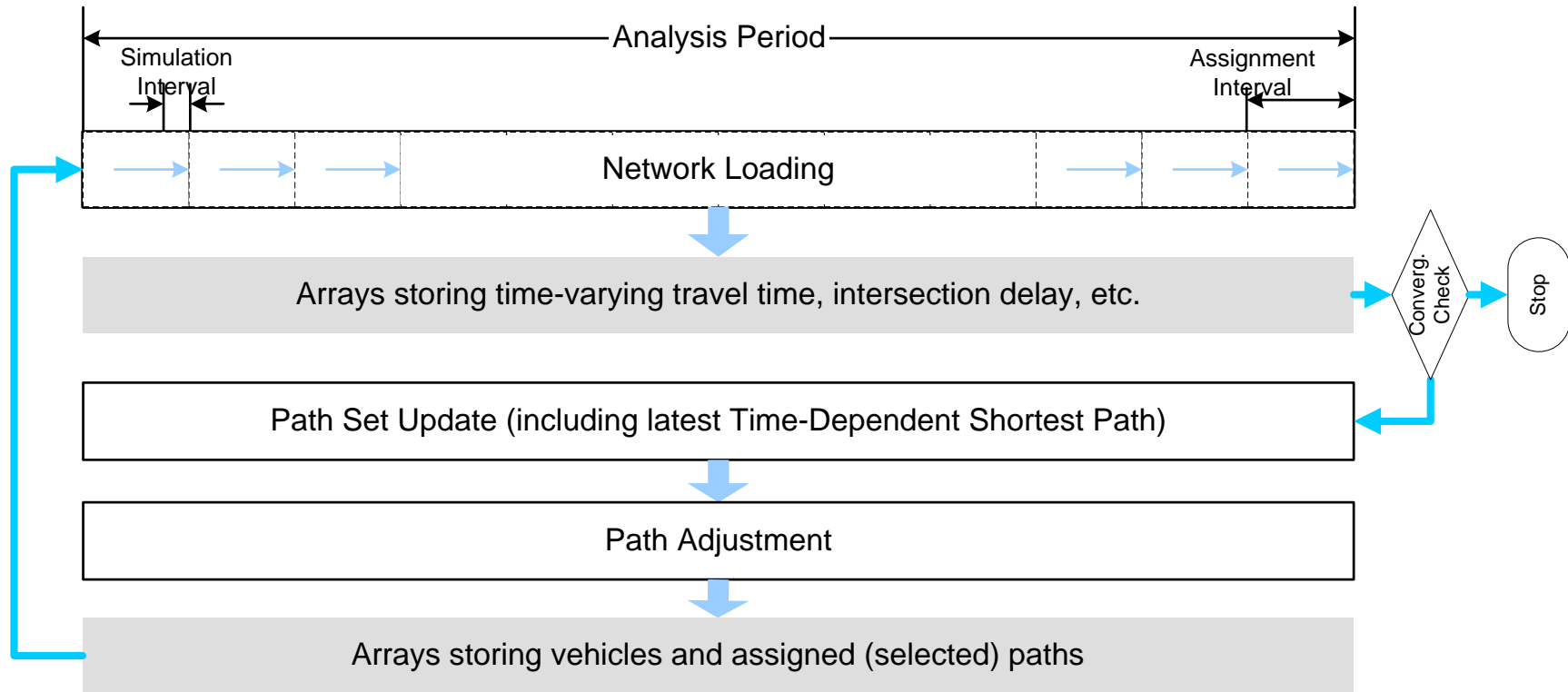
As discussed above, the convergence is measured by the relative gap, which is the sum of the difference between the experienced travel time for the used paths and the time-dependent shortest path for each origin, destination, and departure time. The typical definition of the total relative gap is:

$$rel_{gap} = \frac{\sum_t \sum_{i \in I} \sum_{k \in K_i} f_k^t \tau_k^t - \sum_t \sum_{i \in I} d_i^t u_i^t}{\sum_t \sum_{i \in I} d_i^t u_i^t}$$

Where t is an index for an assignment interval or a departure time interval, i is an index for an OD pair and k is an index for a path. Index i represents the set of origin-destination pairs and K_i denotes the set of paths connecting the origin-destination pair i . f_k^t represents the flow on path k departing at assignment interval t . τ_k^t is the travel time on path k for assignment interval t . d_i^t denotes the demand (total flow) for OD pair i at time interval t and u_i^t is the shortest path travel time for OD pair i and departure time interval t .

Note that at perfect equilibrium, the travel times on all used paths are equal to the time-dependent shortest path time, and hence the value of relative gap is to zero. Since the travel time on all used paths will always be greater than or equal to the shortest path, the value of relative gap will never be negative. In most DTA applications, the solution is assumed to have converged to an equilibrium solution when the relative gap is less than a pre-specified tolerance level (1 percent to 10 percent is the commonly reported convergence level for existing DTA models).

Figure 2-9. DynusT Algorithmic Procedure



The speed profile calibration is based on the concept of back casting the temporal demand pattern based on the observed traffic data. The temporal pattern of the demand curve is then used to adjust the temporal pattern in the vehicle and path file generated from the simulation run using the calibrated OD table. This speed profile calibration method has been shown to generate satisfactory speed profile calibration results.

2.6.2 OD Demand Calibration Results

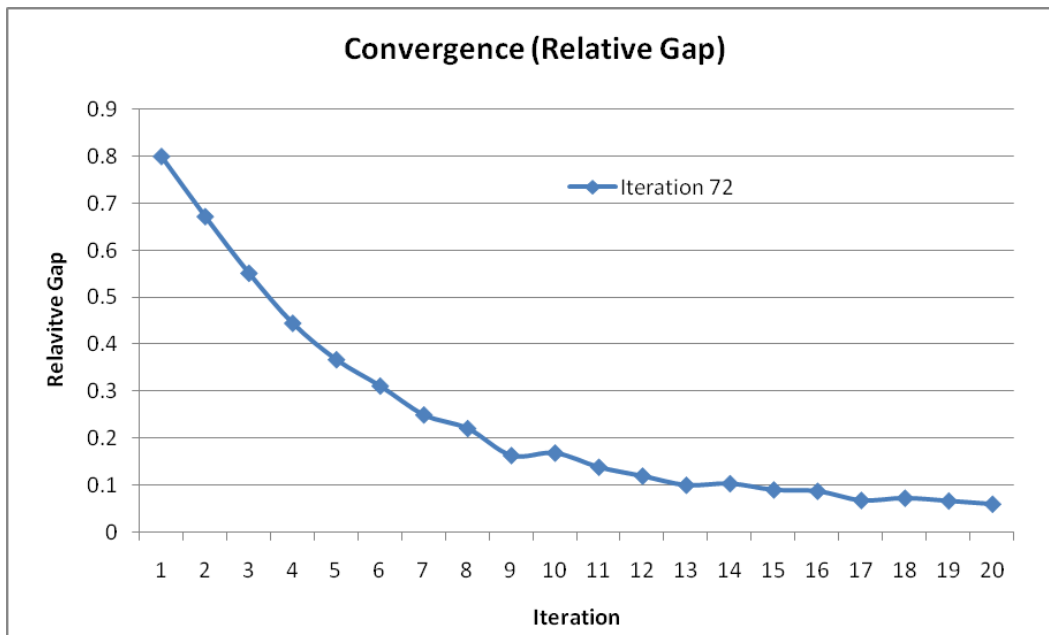
Baseline Network Convergence

The convergence of the DUE iteration is presented in Figure 2-10. Note that this is the 20-iteration relative gap value curve at the 72nd OD calibration iteration. From this figure, one can see that at the initial iteration, the relative gap function value is 0.7; meaning that, on the average, the experienced travel time of the used paths are 70 percent higher than the minimal travel time (shortest path travel time). As iterations progress, the relative gap value is gradually reduced to 0.05 (5 percent) at iteration 20. This convergence pattern indicates that:

There is a significant difference between path travel time and traffic condition between the initial iteration, which is based on incremental assignment, and the last converged iteration, which is true dynamic user equilibrium; any simulation approach that does not seek for convergence may significantly deviate from the desirable DUE condition.

This convergence pattern also indicates DynuST's DUE algorithm can stably improve convergence to a satisfactory level through iterations.

Figure 2-10. Relative Gap Convergence for Calibration Iteration 72

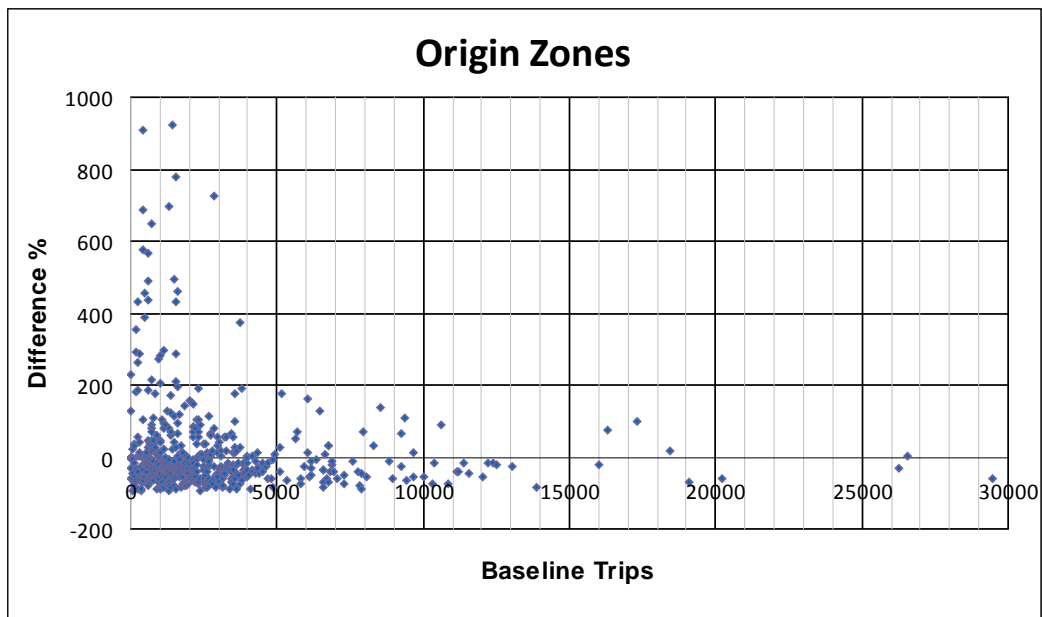


Comparison of Original and Calibrated OD Matrices

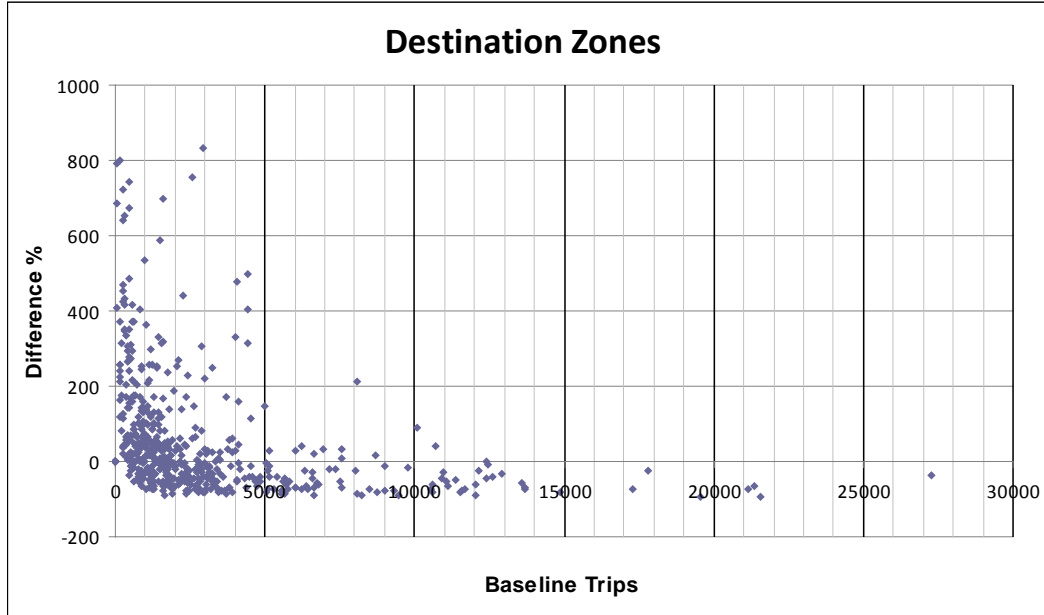
In the applied OD calibration methodology, the percent deviation for each OD calibration iteration is constrained by a user-specified limit. The overall deviation is then determined by the change made for each iteration. This allows adjustment to be made moderately for each iteration, but still permits changes to be made beyond the specified limit if doing so is advantageous to improve the matching of link counts.

In this section, the baseline (before calibration) OD matrix is compared to the latest calibrated OD matrix (Iteration 72). Total production from and attraction to a zone is determined for both the baseline and the calibrated OD matrices, differences are calculated along with percent errors. The results are presented in Figure 2-11 and Figure 2-12. Figure 2-11 puts the percent error in perspective along with the level of produced trips. Although the trips from some low-production zones may be modified considerably, less deviation is observed for higher production zones.

Figure 2-11. Origin Zone Percent Difference versus Trip Production



Similarly, total attraction to a zone is determined for the two OD matrices and differences are calculated along with percent errors, presented in Figure 2-12. Figure 2-12 demonstrates that higher attraction zones deviate much less than those with less than 5,000 trips.

Figure 2-12. Destination Zone Percent Difference versus Trip Attraction

It can be seen that after calibration the total number of trips was only slightly modified (from 1.5M to 1.6M), but some low volume OD pairs were modified considerably. This is considered reasonable since 1) the OD matrices are post-processed from the regional model DUE assignment through vehicle and path files and 2) the calibration performed for the regional model in 2007 is based on a limited number of traffic count locations for the I-394 corridor study area. Given the higher degree of variability in the original OD matrices, subarea cut process, and more extensive coverage of calibration sensors for the ICM network (more than 200 sensors), it can be expected that the change made to the OD matrices would not be, and should not be, limited.

2.7 Model Validation

2.7.1 Validation Criteria

The validation criteria from the analysis plan [4] are presented in Table 2-3. From the results discussed and presented in the following sections, the defined validation targets have been reached.

Table 2-3. Validation Criteria for I-394 Corridor

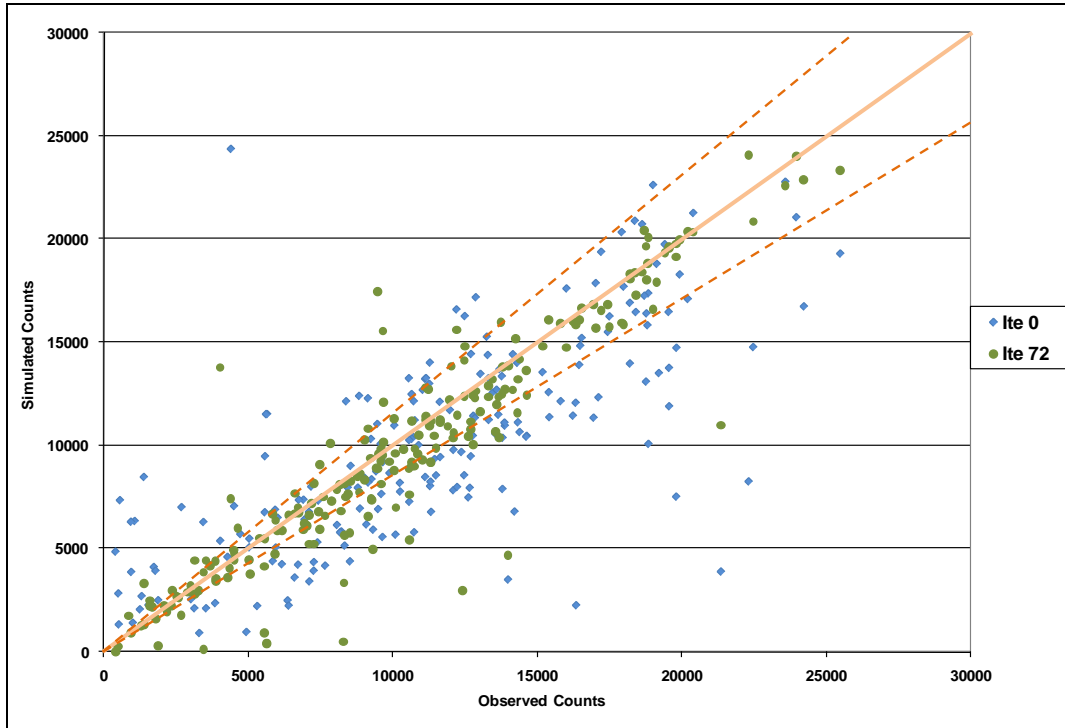
Validation Criteria and Measures	Validation Acceptance Targets	Results
Traffic flows within 15 percent of observed volumes for links with peak-period volumes greater than 2,000 vph	For 85 percent of cases for links with peak-period volumes greater than 2,000 vph	Target met.
Sum of all link flows	Within 5 percent of sum of all link counts	Target met.
Travel times within 15 percent	>85 percent of cases	Target met.
Visual Audits <i>Individual Link Speeds: Visually Acceptable Speed-Flow Relationship</i>	To analyst's satisfaction	Target met.
Visual Audits <i>Bottlenecks: Visually Acceptable Queuing</i>	To analyst's satisfaction	Target met.

2.7.2 Traffic Counts

Figure 2-13 shows the scattergram of observed and simulated counts on links. A 45-degree (solid) line represents a perfect match of observed versus simulated counts. The two dashed lines are the upper and lower bound for the 15 percent error band. It is evident from the figure that most of the links are within the 15 percent range. The calibration iterations improve the matching of the observed and simulated counts over the OD iterations. Approximately 1.5 million trips are generated before calibration. After calibration, approximately 1.6 million trips are generated, a trip increase of less than 7 percent.

Figure 2-13. Simulated versus Observed Counts for Iterations 0 and 72

5:00-11:30 a.m.



In addition to the scattergram above, two statistics were calculated for high volume links defined as links with volumes no less than 2,000 vehicles/hour, during the a.m. peak period. The first statistic was calculated as the percent of links with model volumes within 15 percent of the observed volumes. The second statistic reflects the total count-weighted average weighted error of these links.

The first statistic reflects the first validation criterion and is determined by calculating the error of individual links and computing the number of links that are within the 15 percent error to the total number of links; that is $e = g'/g$, where e is the matching criterion “% of links that is within 15-percent error” and g is total number of links and g' is number of links that has no greater than 15 percent error.

However, it needs to be pointed out that this statistic may ignore the fact that each link may have a different number of lanes and the actual volumes carried by each link could vary widely due to capacity differences. Better matching a link with a higher total volume (e.g., four-lane freeway) is more important than matching a link with a similar unit-per-hour per lane-flow rate, but a lower number of vehicles (e.g., a two-lane arterial or a one-lane ramp link). Without properly considering the effect of actual total counts for each link, low-total-count links may be overweighted when computing the performance measure. To this extent, the second statistic is proposed and calculated.

This statistic s calculates the total count-weighted average absolute error for all the high volume links. The weighted average absolute error for all these links should be less than 15 percent. This criterion

allows high-total-count links versus low-total-count links to be properly reflected in the performance measure. Mathematically, this criterion can be expressed as:

$$e = \frac{\sum_j n_j \epsilon_j}{\sum_j n_j} \tag{2}$$

Where,
 e: count-weighted average absolute error.

$\epsilon_j = \left| \frac{\bar{n}_j - n_j}{n_j} \right|$ is the absolute value of link count error. This is to prevent positive and negative errors from being canceled out, reducing the actual error.

n_j : Actual counts for link *j*.

\bar{n}_j : Simulation counts for link *j*.

Table 2-4 summarizes the results for the 112 links that meet the high volume threshold. It can be seen that 88.5 percent of the links are within 15-percent error, which satisfies the criterion set by the AMS analysis plan [4]. In addition, the count-weighted average error is 10.3 percent, which is less than the 15-percent target value associated with the first validation criterion.

Table 2-4. High Volume Link Statistics

	Links		Counts	
	Number of Links	Percentage of Links Within 15-Percent Error	Counts	Count-Weighted Avg. Absolute Error (Percentage)
2,000+	112	86.2	855,413	12.3

2.7.3 Total Link Counts

Computing the error for the total link count, is equivalent to following Equation 2 but changing ϵ_j to be $\frac{\bar{n}_j - n_j}{n_j}$ instead of the absolute value. One can see that when $\epsilon_j = \frac{\bar{n}_j - n_j}{n_j}$ is substituted into

Equation 2, Equation 2 becomes $e = \frac{\sum_j n_j \epsilon_j}{\sum_j n_j} = \frac{\sum_j (\bar{n}_j - n_j)}{\sum_j n_j} = \frac{\sum_j \bar{n}_j}{\sum_j n_j} - 1$, which is the definition of total link count error.

The error figure for the 112 links of interest is -4.4 percent. The same performance measure was applied to all 202 links yields -3.9-percent error. Both are within the 5-percent limit set by the experimental plan [4].

2.7.4 Travel Times

Probe vehicles collected travel times on TH-55, TH-7, and I-394 in both the EB and WB direction from October 28, 2008 to October 30, 2008, for a total of 143 runs. Refer to Figure 2-14 for vehicle paths on TH-55, TH-7, and I-394. Travel time comparisons for only the a.m. direction are evaluated since the simulation is performed for only the a.m. period.

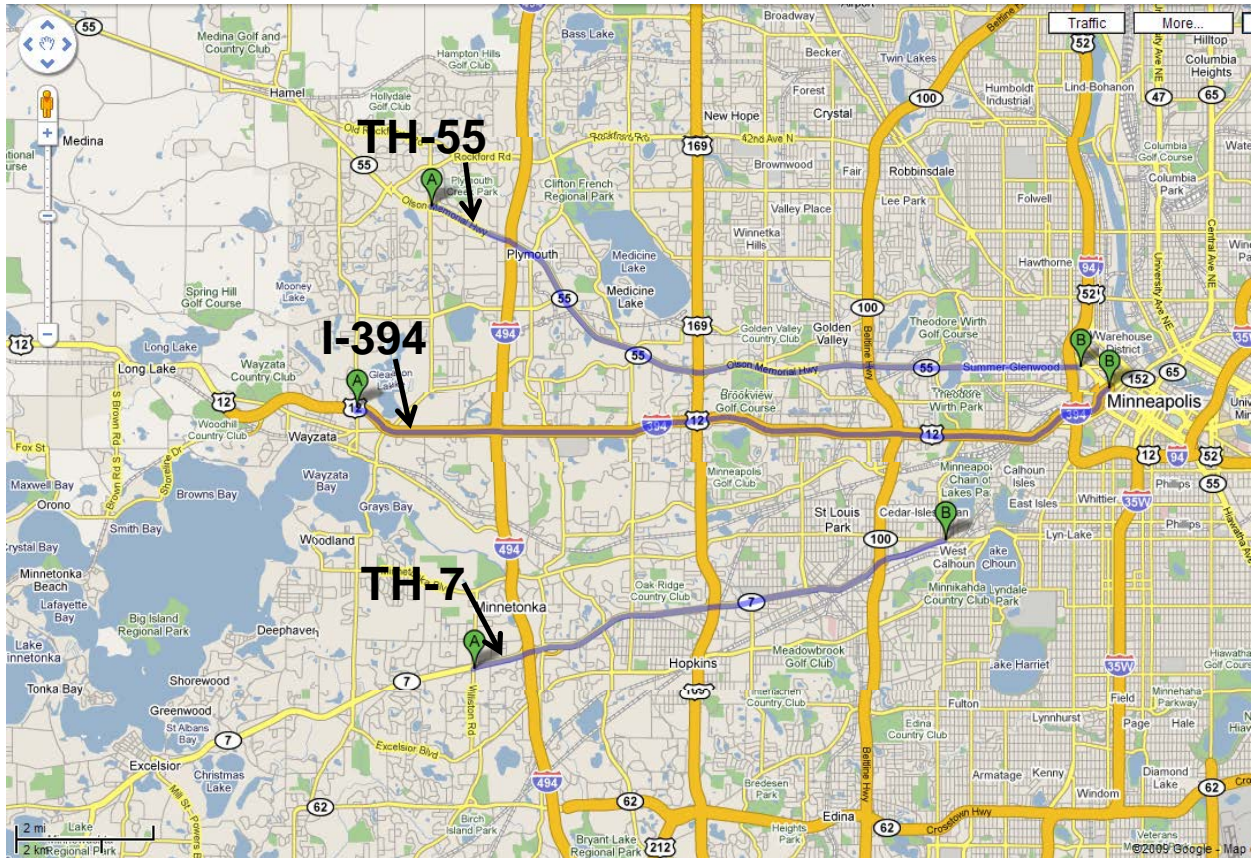
To ensure consistent comparison, simulation probe vehicles following the same routes and departure times as the actual probe vehicles were inserted to the DynusT vehicle and path files generated from the last converged DUE iteration. Then, one-shot simulation was performed using these vehicle and path files. After simulation, the experienced travel time (end time minus start time) for each inserted probe vehicle was extracted to compare with the experienced travel time for each actual probe vehicle.

Simulated total travel times for the paths on TH-55, TH-7, and I-394 are compared to the provided probe vehicle total travel times. As shown in Figure 2-15 through Figure 2-20, it is apparent that the experienced travel times for all probe vehicle departure times exhibit comparable temporal patterns compared with the observed data.

Figure 2-15 and 2.16 show the EB and WB travel times between the two end points on I-394. The EB travel times are approximately 12 minutes at 6:00 a.m., and gradually increase to above 20 minutes between 7:30 a.m. and 8:30 a.m. Three days of field data are plotted in the same figure and show that the simulated travel times clearly fall within the reasonable range of the field data. The WB trips are constantly maintained at approximately 12 to 13 minutes. The simulated travel times follow the same trend and are considered within the reasonable range, only slightly higher.

By checking with the scattergram for simulated and actual travel time – shown on the right for each figure – it can be seen that data points are mostly within the 15 percent band along the 45-degree line, giving a visual representation of the error range of the simulated travel times.

Figure 2-14. TH-55, TH-7, and I-394 East and Westbound Travel Time Paths



[Source: Google Maps, 2009.]

Figure 2-15. I-394 Eastbound Travel Times for Day of Interest

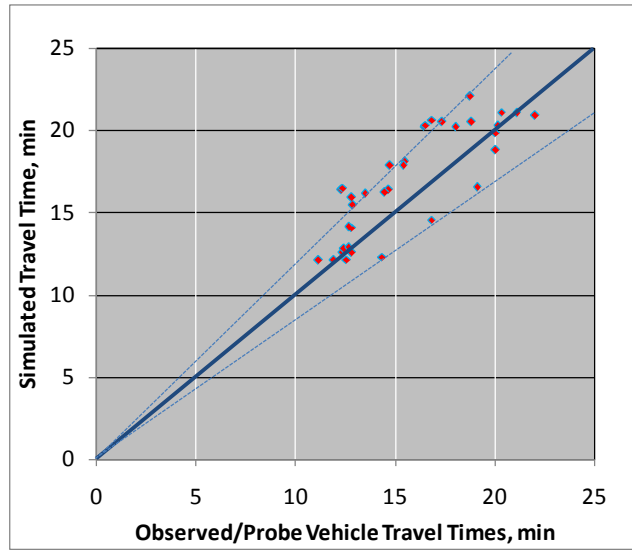
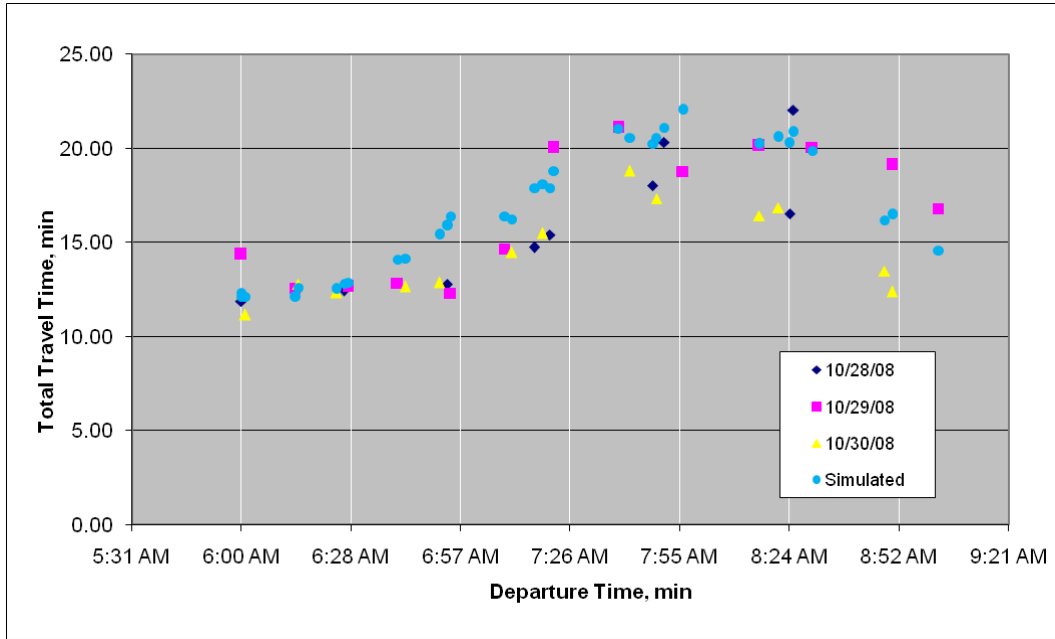
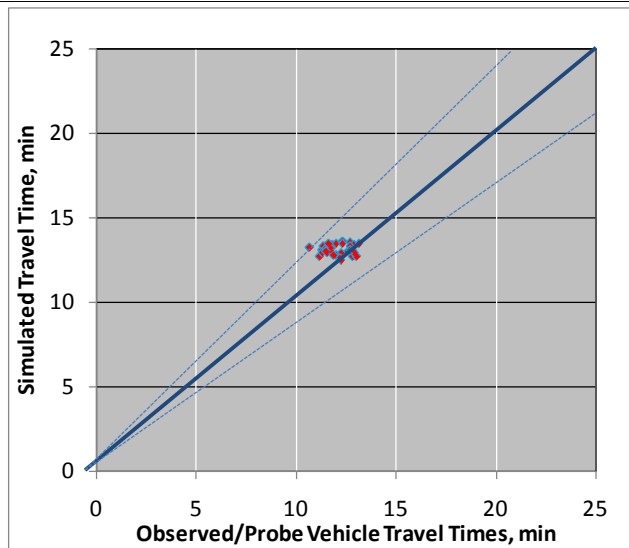
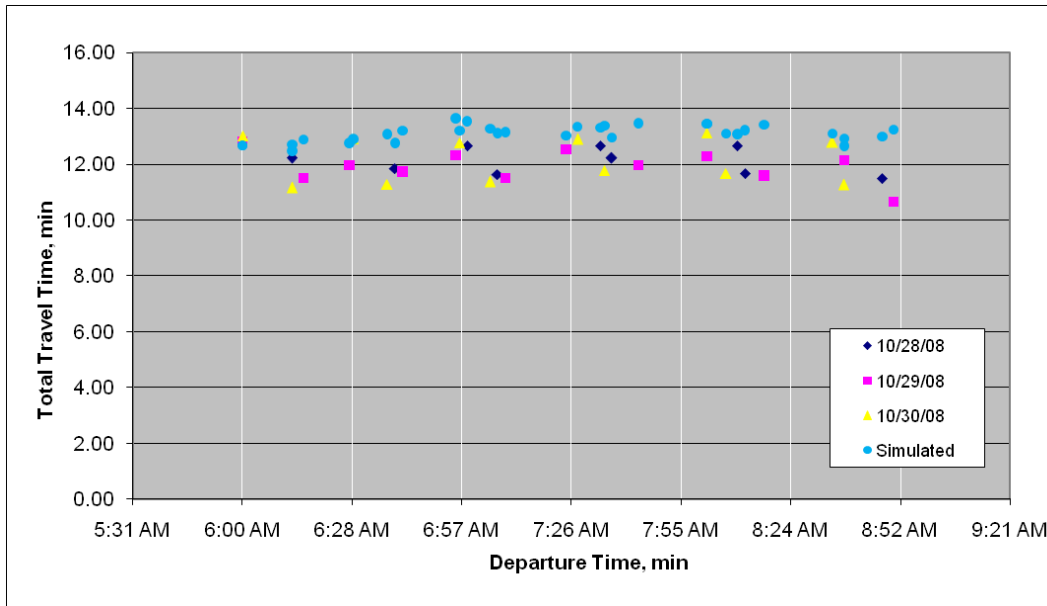


Figure 2-16. I-394 Westbound Travel Times for Day of Interest



Travel times for both EB and WB travel on TH-55 for the same time period are compared to the field travel time data in Figures 2.17 and 2.18. The EB travel times are approximately 14 minutes at 6:00 a.m. and gradually increase to 20 minutes between 7:45 a.m. and 8:00 a.m., and slowly reduce to 15 minutes after 8:30 a.m. The simulated travel times that follow the same temporal pattern and individual travel time points for both EB and WB trips are in the vicinity of the field data.

The scattergrams for both EB and WB directions show that the simulated travel times are mostly within the 15-percent range; however, WB travel times are slightly lower.

Figure 2-17. TH-55 Eastbound Travel Times for Day of Interest

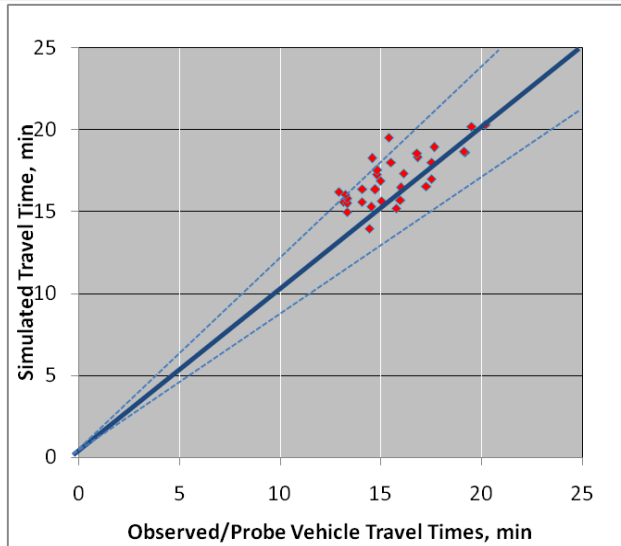
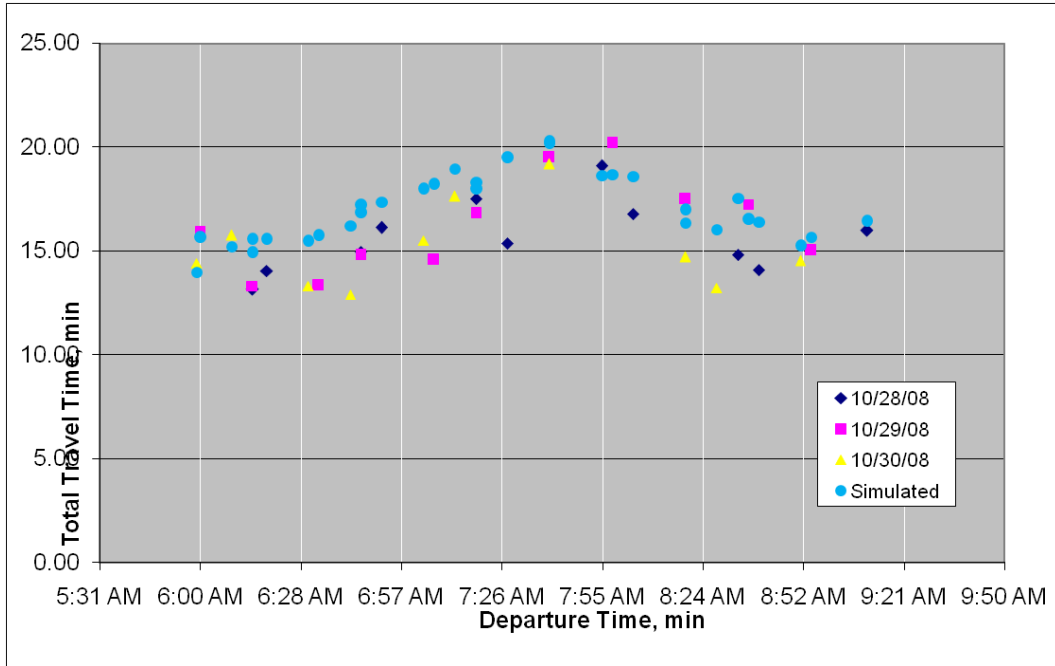
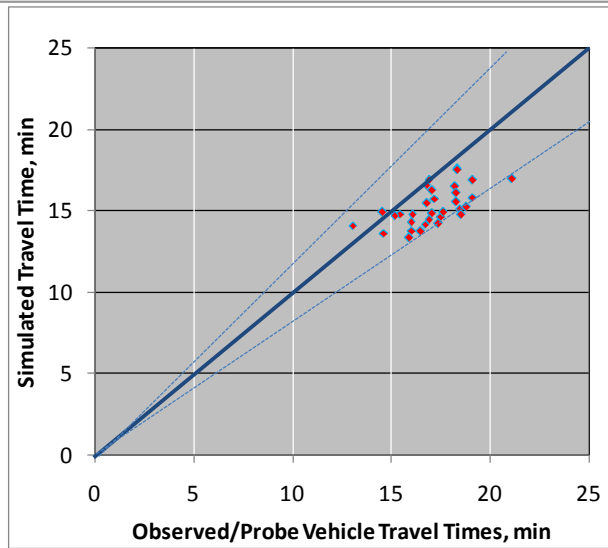
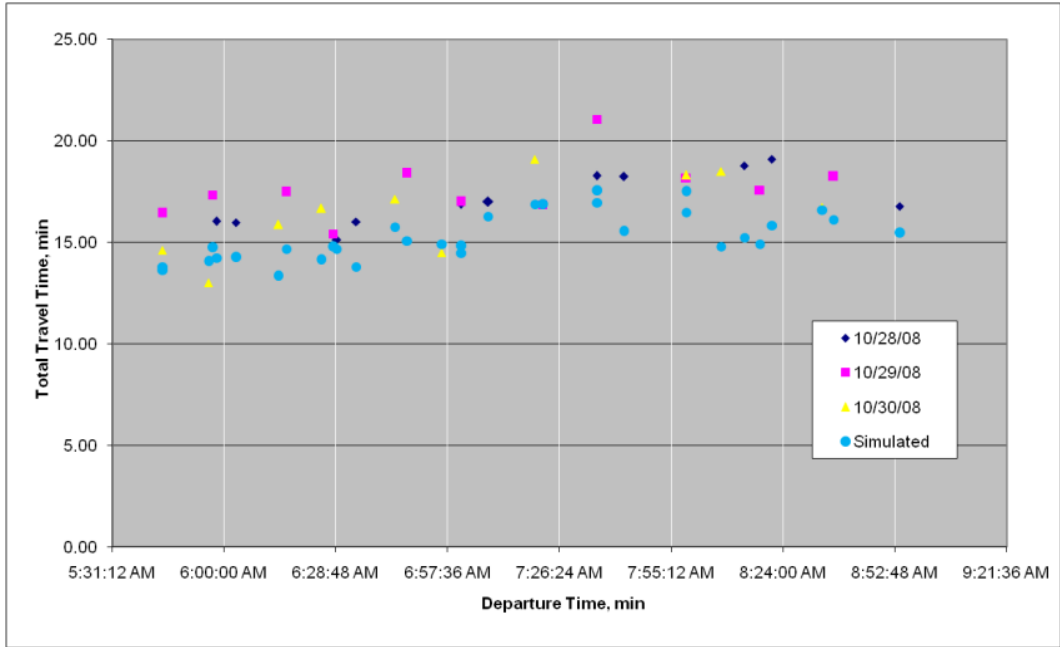


Figure 2-18. TH-55 Westbound Travel Times for Day of Interest



Travel times on TH-7 for both actual and simulated probe vehicles are displayed in Figures 2.19 and 2.20. The travel times are approximately 13 minutes at 6:00 a.m. and steadily increase to about 20 minutes at 8:00 a.m., followed by a gradual travel time reduction at 9:00 a.m. The simulated travel times fall within the range of the three-day data throughout the period of interest, except for EB traffic. EB traffic simulated travel times are slightly higher than field data just before 9:00 a.m. The WB traffic follows a similar temporal pattern to that of the EB traffic, except that travel times are within the 10- to 16-minute range. The simulated travel times clearly follow the same trend and fall within the field data range over the entire period of interest.

Figure 2-19. TH-7 Eastbound Travel Times for Day of Interest

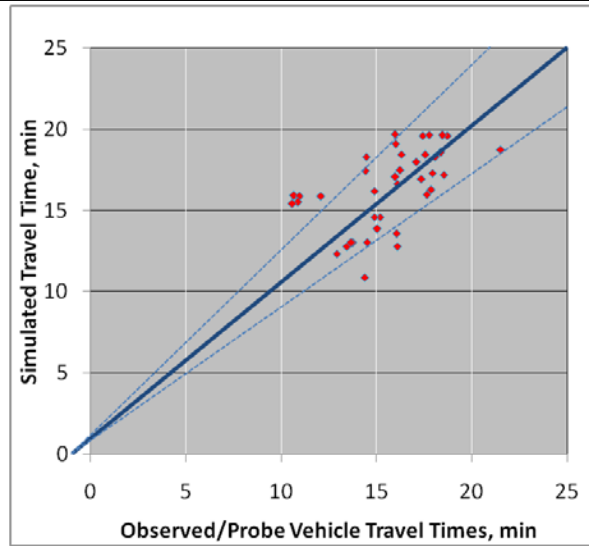
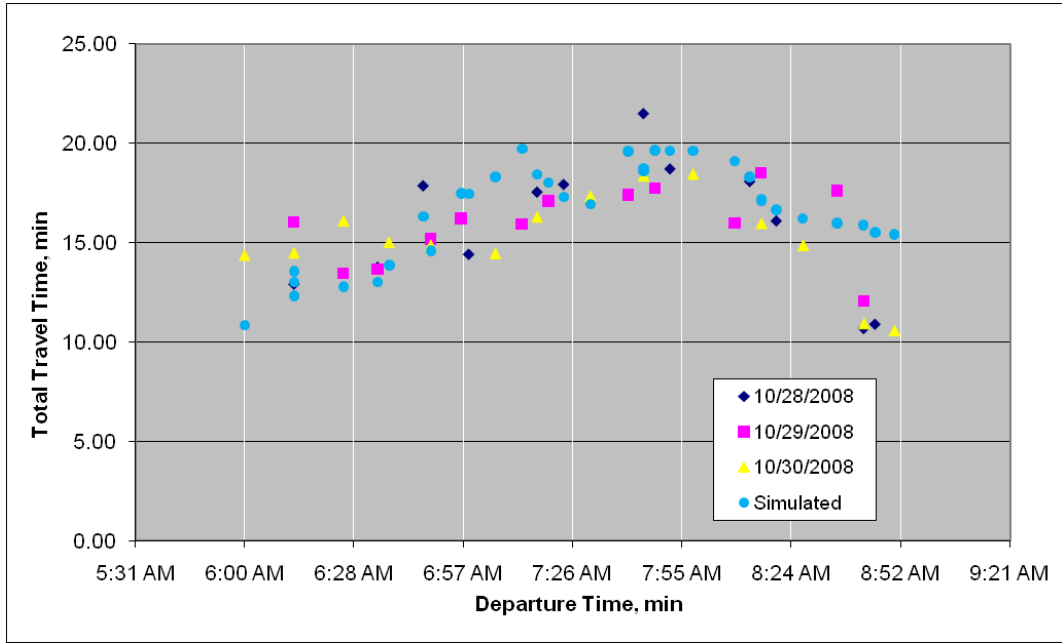
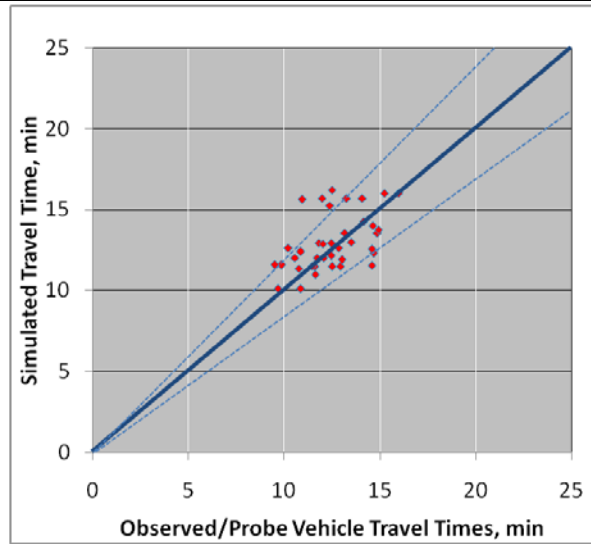
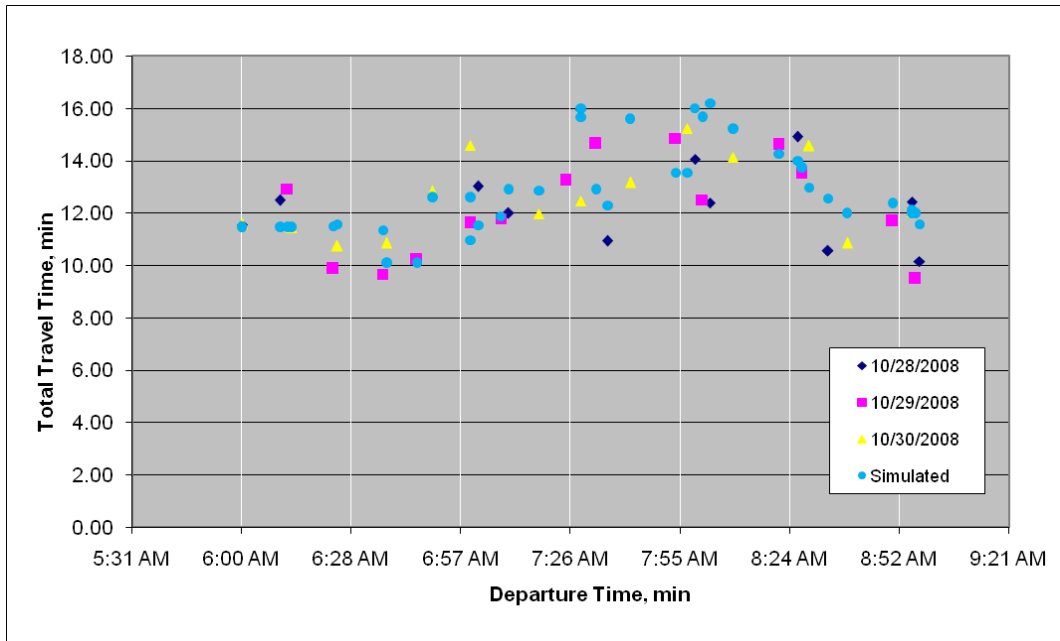


Figure 2-20. TH-7 Westbound Travel Times for Day of Interest



The accuracy of travel time estimation is further tabulated in Table 2-5. In Table 2-5, “Total Runs” means the number of probe vehicle runs Mn/DOT has performed on each corridor in each direction during the entire a.m. period. “Runs within #% Travel time” contains two values – the number of simulated vehicles falling into the #% error range, and the equivalent percentage in parentheses compared with the Total Runs.

Table 2-5. Travel Time Criteria Validation for Entire Simulation Period

	TH-55 EB	TH-55 WB	TH-7 EB	TH-7 WB	I-394 EB	I-394 WB
Total Runs	32	32	39	40	35	33
Runs within 15% travel time	21 (66%)	24 (75%)	28 (72%)	29 (73%)	22 (62%)	30 (91%)
Runs within 20% travel time	28 (88%)	30 (94%)	30 (77%)	33 (83%)	28 (80%)	32 (97%)
Runs within 25% travel time	28 (88%)	32 (100%)	33 (85%)	36 (90%)	33 (94%)	33 (100%)
Runs within 30% travel time	32 (100%)	32 (100%)	34 (87%)	37 (93%)	33 (94%)	33 (100%)

Taking TH-55 EB as an example, 21 out of 32 runs (66 percent) are within the 15-percent error range, 28 out of 32 runs (88 percent) are within the 20-percent error range, and all the runs are within the 30-percent error range. While 62 percent to 99 percent of simulated travel times fall into the ± 15 -percent range, significantly higher percentages of runs (77 to 97 percent) fall into the ± 20 -percent range. When considering +20 percent error limits, the accuracy percentages increases from 85 percent to 100 percent. Overall, the results indicate proper matching of experienced travel times from the calibrated model.

Similar results are presented in Table 2-6 for those runs only conducted within the a.m. peak period. It is observed that the accuracy remains satisfactory when looking at this narrower timeframe.

Table 2-6. Travel Time Criteria Validation for Peak Period

6:45 a.m. to 8:45 a.m.

	TH-55 EB	TH-55 WB	TH-7 EB	TH-7 WB	I-394 EB	I-394 WB
Total Runs	22	20	30	28	23	23
Runs within 15% travel time	14 (64%)	15 (75%)	22 (73%)	20 (71%)	11 (48%)	22 (96%)
Runs within 20% travel time	18 (82%)	20 (100%)	23 (77%)	23 (82%)	17 (74%)	23 (100%)
Runs within 25% travel time	21 (95%)	20 (100%)	25 (83%)	25 (89%)	22 (96%)	23 (100%)

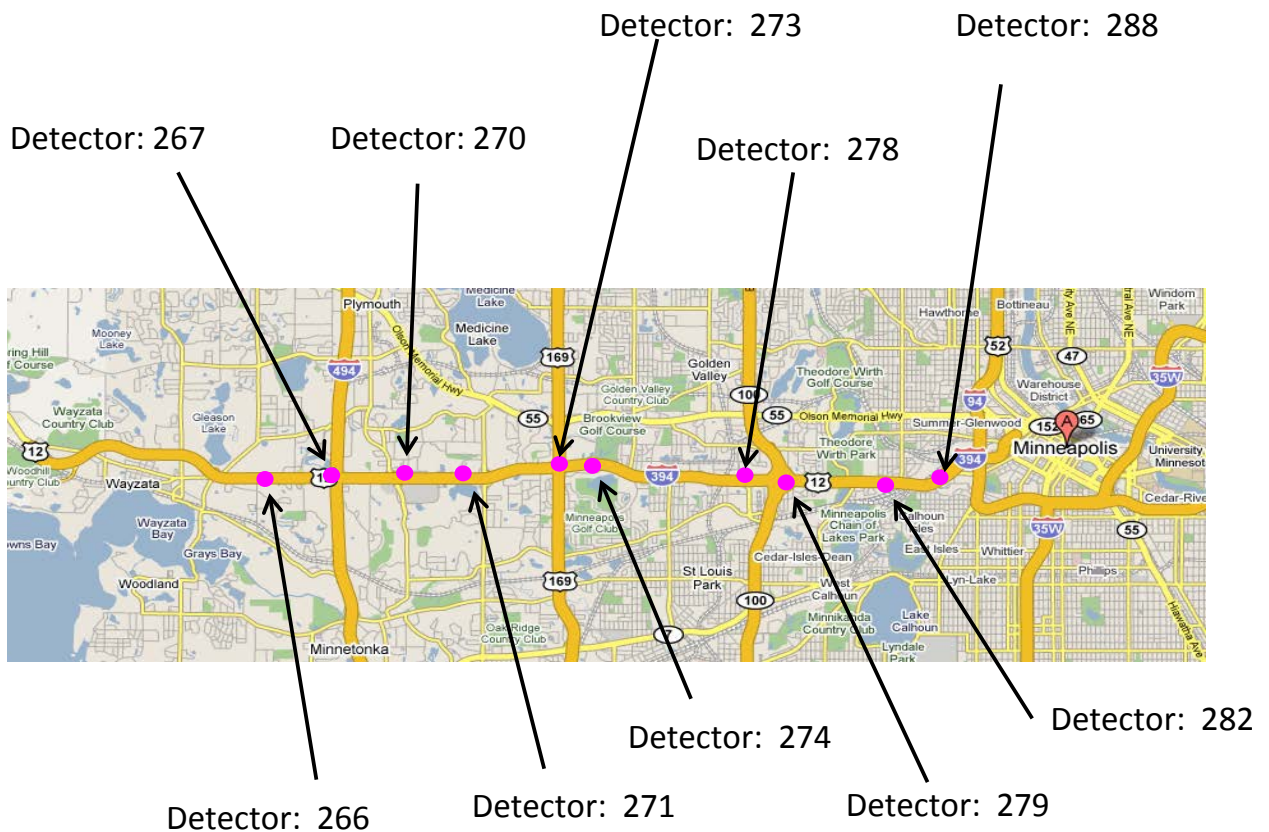
	TH-55 EB	TH-55 WB	TH-7 EB	TH-7 WB	I-394 EB	I-394 WB
Runs within 30% travel time	22 (100%)	20 (100%)	26 (87%)	26 (93%)	22 (96%)	23 (100%)

In summary, the baseline simulation satisfactorily validates results with actual travel time data in the corridors of interest.

2.7.5 Visual Audits – Individual Link Speeds

Figure 2-21 shows several sensor locations along I-394 that were examined to understand how well volume and speeds are matched on key locations along the ICM corridor. The following figures illustrate the simulated data compared with multiday sensor data. Overall, the simulated volumes and speeds satisfactorily replicate experienced volumes and speeds at most locations.

Figure 2-21. Sensor Locations on I-394



[Source: Google Maps.]

A few locations on TH-55 and TH-7 were selected and compared with synthesized field data. The synthesized field data is the 10 percent of the Average Annual Daily Traffic (AADT) from the Mn/DOT

travel demand model. Because these data are not real collected data, they are displayed in Table 2-7 without comparing the error range.

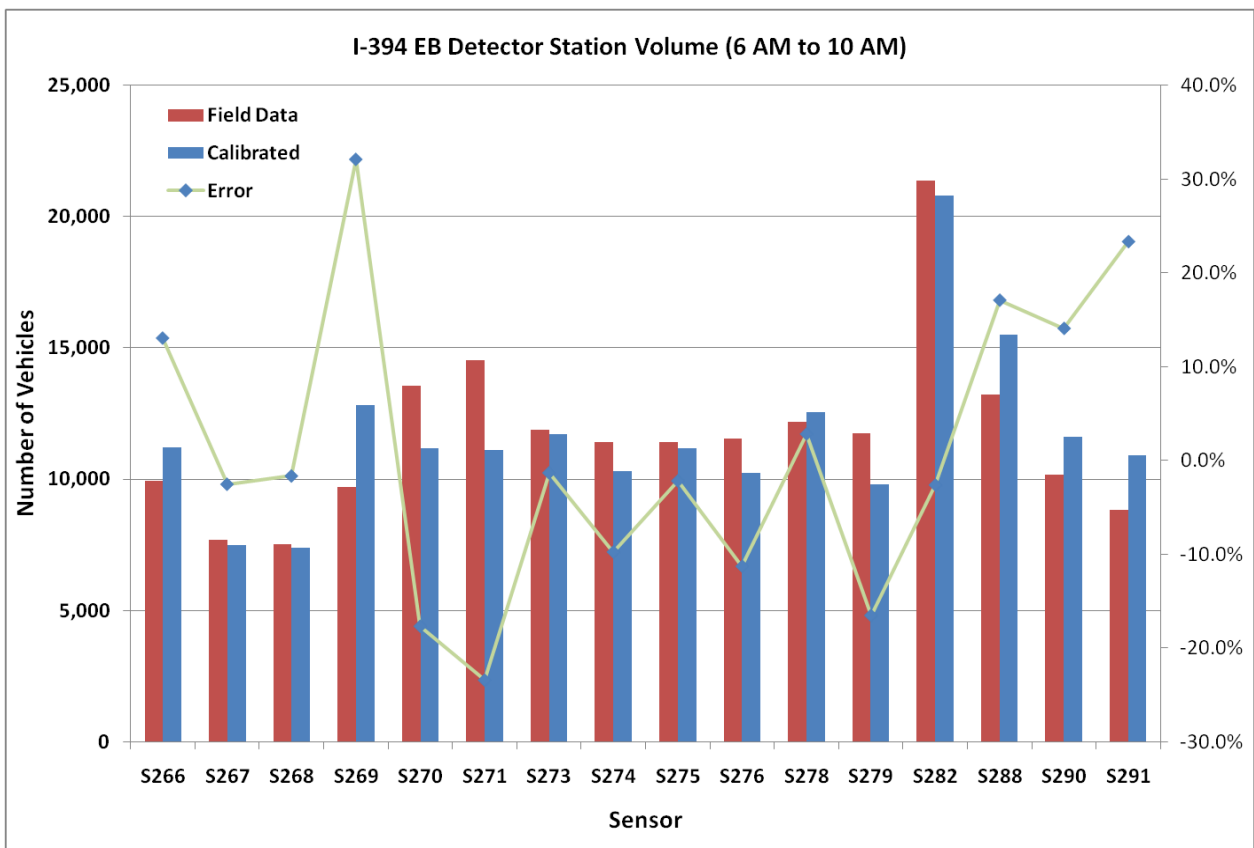
Table 2-7. Arterial Traffic Volumes

A.M. Period

Locations	Model Data	Synthesized Field Data
TH-55 EB East of 100	11,071	8,304
TH-7 EB West of 169	9228	7,594
TH-7 EB West of 100	7353	8,325

On the other hand, the simulated volumes versus actual volumes on selected sensors on I-394 are compared and illustrated in Figure 2-22. Volumes at all locations are generally in agreement with the sensor volumes. Twelve out of the 16 sensors (75 percent of total links and 88 percent of total volumes) are within ± 15 -percent error bound.

Figure 2-22. Volume Comparison on I-394 Eastbound



2.7.6 Visual Audits – Bottlenecks

Mn/DOT provided speed space-time contour data for Tuesday, October 28 through Thursday, October 30, 2008 (see Figure 2-23) and the October 2008 monthly average speed contour (see Figure 2-24) on the EB section of I-394 between I-494 and downtown. In these diagrams, the red represents speeds less than 25 mph, orange represents speeds between 25 and 40 mph, yellow represents speeds between 40 and 55 mph, and green represents speeds greater than 55 mph. Figure 2-23 illustrates obvious day-to-day speed variations. Wednesday, October 29 appears to be the most congested date with two obvious bottlenecks at Winnetka Avenue and east of TH-100 on EB I-394. The bottlenecks create spillbacks in the upstream direction (westbound) judging by the triangular congestion contour shape. For each triangle, the northeast-southwest contour line represents the congestion buildup shockwave propagating upstream due to increased inflow. The southeast-northwest contour line represents the congestion dissipation shockwave propagating downstream due to reduced inflow. The other two days have different congestion levels, but both locations remain the most congested locations on these two days. The speeds in all three daily datasets appear to fluctuate significantly more than the average monthly contour. This is an intuitive phenomenon, as the process of averaging would smooth out variations of the actual data.

DynusT simulation results were compared to Figure 2-23 and Figure 2-25. For discussion purposes, the focus is on only the section between TH-169 and TH-100 in the monthly average diagram. The Mn/DOT speed space-time diagram indicates that the congestion concentrates in this section starting at approximately 7:00 a.m. and lasts until 9:30 a.m. East of TH-169 and west of TH-100 have concentrated congestion during the same time period. East of TH-100 experiences mild congestion with speeds normally maintained between 25 to 55 mph. The direction of the shockwave during the onset of congestion shows that congestion starts early in the I-94 (downtown) area and spills westbound. The shockwave at the dissipation of congestion moves eastbound, indicating that the congestion was alleviated due to the reduced inflow to the section at round 9:30 a.m.

The speed space-time diagram plotted from DynusT simulation shows speed patterns that agree with those observed in the field data. Congestion is observed for the same sections and temporal extent, although speed recovery in DynusT appears to be slightly later than the field data. Congestion at the Colorado Avenue location is more congested than the field data. Congestion east of TH-169 (Winnetka Avenue or Louisiana Avenue area) is observed, but not to the extent of that observed in the field data. The temporal pattern for this congestion area is found to be in agreement with field data. At the I-94 and Dunwoody sensor locations, the DynusT simulation appears to be slightly more congested than the field data but only for a short time period.

It is important to point out that DynusT simulation represents traffic conditions for one typical day, which intrinsically exhibits a higher degree of speed fluctuation compared with the monthly average data. In other words, the degree of DynusT speed data fluctuation appears to be more comparable to the three daily datasets than to the monthly average dataset. However, DynusT data may not necessarily fit perfectly with any of the three datasets as real data fluctuates considerably. Forcing DynusT to exactly match any specific daily dataset may be impractical. The focus of the visual inspection is to discern if the simulation outputs exhibit similar bottleneck characteristics (e.g., location and duration) as shown in field data. To this end, it can be concluded that DynusT simulation data reasonably meet this criterion.

Figure 2-23. Field Speed Contour Data for October 28-30, 2008

The figure consists of three identical data tables stacked vertically, each representing a different day of the week: Monday (top), Tuesday (middle), and Wednesday (bottom). Each table contains 24 rows of time intervals from 6:00 AM to 11:30 AM in 15-minute increments. The columns represent various road segments and directions, including E of I-494, Plymouth Ave, Ridgewood Ave, CH 7A, Grand Ave, TH 160, University Ave, Wrynne Ave, Lovens Ave, Cottrick Ave, Xenia Ave, W of TH 100, E of TH 100, W of Wirth Ave, University Blvd, I-94, and Linden Ave. The data points are color-coded, with red indicating the lowest speeds and yellow/green indicating higher speeds.

**Figure 2-24. I-394 Eastbound A.M. Speed Space Time Contour
(Field Data: October 08 Averaged)**

Segment	W of I-494	E of I-494	Plymouth Rd	Ridgedale Dr	CR 73	Shelard Pkwy	TH 169	General Mills Blvd	Winnetka Ave	Louisiana Ave	Colorado Ave	Xenia Ave	W of TH 100	W of Wirth Pkwy	Dunwoody Blvd	I-94	Linden Ave
Detector	S268	S269	S270	S271	S272	S273	S274	S275	S276	S277	S278	S279	S280	S282	S288	S290	S291
Time																	
5:30 AM	65.2	69.9	68.7	69.6	70.6	70.7	69.2	70.5	67.6	64.0	65.8	65.5	69.9	67.4	70.0	53.7	49.0
5:35 AM	65.4	69.4	68.5	69.9	69.3	68.9	68.0	70.0	67.2	64.2	66.6	65.4	71.7	67.1	69.7	54.9	49.4
5:40 AM	66.2	68.8	68.0	69.7	69.1	68.4	67.9	69.9	66.8	63.3	66.9	66.0	72.5	68.3	70.2	57.4	50.9
5:45 AM	64.9	69.7	69.4	70.0	70.1	70.2	69.1	70.7	67.1	64.4	65.6	65.0	71.9	67.5	69.9	56.5	50.2
5:50 AM	65.1	70.6	69.6	71.0	70.3	69.8	69.1	70.9	67.0	64.6	67.3	66.4	72.5	69.6	70.5	56.1	48.6
5:55 AM	65.3	70.4	68.7	69.8	70.1	68.8	69.4	70.6	66.0	63.9	65.7	65.8	71.7	68.9	71.4	58.1	51.5
6:00 AM	66.1	70.7	69.3	70.4	69.6	70.6	69.8	70.6	67.4	64.2	65.1	66.2	72.0	68.0	68.6	58.1	51.3
6:05 AM	65.4	70.4	68.7	70.1	69.8	70.2	69.0	71.3	68.7	64.3	66.6	65.6	72.8	68.6	69.1	55.9	51.2
6:10 AM	65.3	70.3	68.7	69.8	69.2	68.8	68.7	70.8	68.9	63.8	66.7	66.4	72.7	68.3	68.9	57.1	50.8
6:15 AM	65.1	70.1	69.3	70.3	69.2	69.4	69.3	70.6	67.8	63.7	65.4	65.8	72.6	68.4	69.2	57.6	50.8
6:20 AM	64.0	68.5	68.7	69.8	68.6	69.3	69.1	70.5	67.9	63.3	65.8	65.3	71.8	68.0	68.5	56.9	50.2
6:25 AM	64.7	69.6	67.6	69.0	68.1	67.8	67.9	69.1	67.5	61.7	65.3	65.8	71.8	67.4	68.3	57.3	50.4
6:30 AM	64.7	68.7	67.0	68.5	67.8	68.8	67.8	68.7	66.2	61.7	64.0	64.4	70.8	66.1	67.4	56.2	50.3
6:35 AM	64.8	69.6	67.6	68.3	67.4	67.8	67.4	67.8	66.8	61.1	63.7	64.9	71.4	66.0	67.2	56.3	51.0
6:40 AM	64.5	68.9	66.5	67.7	67.1	67.3	67.2	67.0	66.0	59.5	64.0	64.2	70.7	65.6	65.8	56.2	50.5
6:45 AM	63.9	68.4	65.9	67.7	67.0	67.7	66.6	66.0	66.4	59.2	63.8	63.6	71.4	64.2	64.1	55.5	50.8
6:50 AM	64.2	68.6	65.8	67.1	66.6	67.3	66.4	65.9	64.2	58.4	62.7	63.7	71.6	64.4	57.3	54.8	50.7
6:55 AM	64.2	68.2	65.8	66.3	66.6	66.5	66.7	66.9	65.2	58.9	63.6	63.9	70.4	64.2	54.1	54.8	50.7
7:00 AM	64.6	68.2	65.8	66.3	66.7	66.9	66.7	65.5	64.5	58.1	63.5	63.2	71.6	64.4	54.2	54.2	50.5
7:05 AM	64.4	68.0	65.4	66.1	66.2	67.0	66.5	66.0	64.3	56.4	62.2	62.8	70.1	64.4	55.1	54.1	50.2
7:10 AM	64.1	67.8	65.0	66.1	66.1	66.0	65.1	64.2	61.6	51.3	60.9	62.2	68.3	61.8	55.4	53.9	49.9
7:15 AM	64.0	67.2	64.0	64.8	65.7	65.3	64.7	62.6	43.7	43.4	60.1	61.8	66.9	58.4	54.7	52.3	48.7
7:20 AM	64.4	67.0	64.2	64.0	65.5	64.5	64.4	60.0	34.0	40.4	57.2	60.7	65.0	55.5	49.1	53.0	49.6
7:25 AM	64.2	66.9	62.3	63.4	64.8	64.5	62.8	55.3	27.0	34.8	58.1	61.3	66.1	53.2	48.8	51.9	49.4
7:30 AM	63.9	66.2	60.8	62.5	64.3	63.1	62.4	37.2	24.7	34.5	56.5	61.0	65.3	49.6	48.2	51.6	50.0
7:35 AM	64.4	65.9	60.7	62.2	64.2	60.8	57.6	32.4	23.3	32.2	56.0	60.3	63.5	36.4	45.6	49.5	49.3
7:40 AM	64.5	65.5	60.6	62.1	64.6	61.6	59.0	25.6	19.9	31.7	55.0	58.4	59.4	34.8	44.0	47.0	48.7
7:45 AM	64.4	66.2	59.9	62.6	65.4	64.9	58.1	24.0	22.1	29.7	55.4	57.7	42.4	29.6	45.4	44.1	48.8
7:50 AM	64.2	65.6	61.3	62.2	64.6	66.0	54.4	25.5	23.6	33.1	54.0	53.9	24.0	31.3	44.8	37.6	48.3
7:55 AM	64.4	66.1	57.9	60.8	64.8	64.5	62.1	34.3	27.7	33.0	54.1	50.3	22.5	33.4	45.3	38.7	48.6
8:00 AM	64.5	66.7	63.0	63.5	65.6	65.8	64.1	50.6	28.5	28.5	54.7	54.1	27.8	30.3	43.0	43.4	49.2
8:05 AM	64.6	66.8	62.7	62.8	65.3	65.7	65.0	58.3	26.1	30.5	53.5	43.9	26.0	29.5	41.9	42.8	49.4
8:10 AM	65.5	67.4	64.3	63.5	65.5	66.4	65.6	60.1	28.4	30.4	52.9	39.1	19.0	31.3	42.5	43.0	48.6
8:15 AM	64.7	67.3	64.6	64.3	65.5	66.4	66.2	58.8	26.6	33.9	53.2	29.7	18.7	36.4	42.1	40.1	48.5
8:20 AM	64.3	66.5	64.4	65.4	65.2	66.5	65.4	62.4	42.9	35.9	54.8	28.0	21.8	35.1	42.3	38.2	48.0
8:25 AM	65.1	67.1	66.0	64.7	65.8	66.3	65.6	63.1	46.4	41.5	54.9	27.5	21.8	32.8	41.0	46.6	48.1
8:30 AM	65.0	67.4	65.5	66.2	66.5	67.4	66.7	65.6	57.5	54.8	55.6	25.6	22.6	30.2	41.4	49.1	48.2
8:35 AM	64.7	68.5	67.0	65.7	66.2	67.2	66.4	66.7	62.5	58.3	56.1	33.9	24.7	34.6	41.6	49.0	49.0
8:40 AM	64.9	67.6	66.7	65.9	67.1	68.1	67.0	65.9	62.6	57.9	57.4	25.7	23.0	34.1	40.2	50.3	49.0
8:45 AM	65.1	67.9	67.6	67.0	67.0	67.5	67.1	66.5	64.0	59.1	57.5	38.6	24.1	33.5	40.5	51.7	49.3
8:50 AM	65.4	68.9	67.1	66.2	66.5	67.2	66.4	65.9	63.6	58.9	61.4	57.3	21.9	32.7	41.8	51.1	48.9
8:55 AM	64.9	68.6	68.4	67.8	67.5	68.6	67.2	67.2	64.4	61.1	62.3	54.8	20.1	38.5	42.8	51.6	49.5
9:00 AM	64.7	68.5	67.5	67.5	67.2	68.0	67.0	66.9	65.5	60.9	62.1	52.5	24.8	37.3	43.8	53.5	49.5
9:05 AM	64.6	68.1	68.2	67.7	67.7	68.3	67.6	67.6	64.8	60.8	62.9	61.6	56.1	47.8	45.7	53.6	49.8
9:10 AM	64.3	67.5	67.7	67.1	66.6	67.6	66.8	68.0	64.0	59.7	61.4	61.3	65.6	54.7	47.9	54.6	49.8
9:15 AM	64.7	68.2	67.4	67.2	66.9	67.9	67.3	68.3	65.7	59.7	61.3	60.8	64.9	54.9	46.4	54.4	50.1
9:20 AM	64.4	67.8	67.1	67.3	67.3	68.1	66.6	67.5	64.9	60.4	61.1	61.1	67.2	59.5	49.1	54.4	50.1
9:25 AM	64.3	68.5	68.4	67.6	67.5	67.6	66.6	67.8	65.9	60.1	62.5	61.7	65.5	61.0	53.4	55.0	50.7
9:30 AM	64.1	67.9	68.1	67.7	66.7	68.4	67.1	68.7	66.4	61.1	63.7	62.3	67.3	60.9	54.1	54.9	50.5
9:35 AM	64.8	68.7	67.6	67.1	66.5	66.6	66.6	67.7	65.7	60.5	61.8	61.5	68.3	62.6	49.8	55.2	50.7
9:40 AM	64.2	67.5	67.4	67.4	66.8	67.3	67.1	67.9	66.4	60.5	61.8	62.2	68.3	63.0	50.6	56.0	50.3
9:45 AM	63.9	68.4	67.3	66.8	66.2	67.2	66.6	67.1	65.1	60.1	61.5	62.1	69.2	63.3	57.4	56.0	50.8
9:50 AM	64.6	67.8	68.4	67.3	67.3	68.1	67.1	68.0	66.8	61.1	62.1	62.0	68.2	63.4	58.6	55.5	50.2
9:55 AM	64.0	68.4	67.9	67.0	67.0	67.8	67.3	68.4	65.5	60.9	62.5	63.2	69.4	63.5	63.4	56.0	50.6
10:00 AM	64.7	68.1	67.2	67.1	66.9	67.5	66.3	67.0	66.3	60.7	62.2	62.3	68.0	62.6	64.7	57.2	51.4
10:05 AM	64.1	67.8	67.6	67.5	66.4	67.3	65.6	66.4	64.7	60.7	62.1	62.2	68.8	64.4	64.5	56.8	51.5
10:10 AM	63.8	66.4	66.7	66.2	65.5	67.3	65.8	67.7	66.5	60.9	61.7	62.2	68.2	64.0	66.6	57.6	52.3
10:15 AM	64.9	67.8	68.1	67.0	66.5	67.9	66.4	67.9	65.5	60.4	62.5	61.2	67.6	62.7	63.7	56.8	50.5
10:20 AM	63.6	67.2	67.2	66.3	66.0	67.2	66.3	67.7	66.4	61.2	62.4	61.6	68.2	64.0	64.8	57.2	51.3
10:25 AM	63.8	68.0	67.4	67.2	66.7	67.0	65.9	67.4	65.5	61.2	61.9	61.8	67.9	63.8	64.6	57.4	50.9
10:30 AM	63.7	68.3	67.6	67.7	66.3	67.2	66.8	68.0	66.6	60.9	61.3	61.9	66.9	62.7	64.6	56.9	50.7
10:35 AM	64.1	66.8	67.9	66.3	66.5	67.4	66.7	67.3	66.1	60.8	61.9	62.1	67.8	63.5	64.8	56.8	50.7
10:40 AM	63.6	67.1	66.9	66.5	65.4	66.2	66.0	67.5	65.2	60.3	63.4	62.9	68.2	63.5	65.1	56.7	51.7
10:45 AM	63.6	66.6	66.5	66.7	65.9	66.9	65.8	66.3	65.3	60.0	62.6	61.5	68.2	63.6	65.2	57.1	51.3
10:50 AM	63.6	67.1	67.9	67.1	66.0	66.9	66.1	67.5	66.8	60.4	61.5	62.3	69.1	63.5	64.6	56.9	50.6
10:55 AM	64.7	67.0	67.6	67.2	66.5	67.8	66.9	68.3	67.7	60.9	63.3	63.5	68.2	63.6	64.6	57.9	50.7
11:00 AM	64.2	66.9	67.6	67.5	67.0	67.2	66.6	67.5	67.7	60.8	61.9	62.0	68.1	64.6	64.2	57.1	50.8
11:05 AM	64.0	67.8	68.6	68.2	66.7	67.8	66.4	67.9	67.4	61.7	62.4	62.5	68.1	64.5	65.6	57.0	50.6
11:10 AM	63.3	67.4	67.5	67.5	66.4												

Figure 2-25. I-394 Eastbound A.M. Speed Space Time Contour (Simulation)

	W of I-494	E of I-494	Plymouth Rd	Ridgedale Dr	CR 73	Shelard Pkwy	TH 169	General Mills Blvd	Winnetka Ave	Louisiana Ave	Colorado Ave	Xenia Ave	W of TH 100	W of Wirth Pkwy	Dunwoody Blvd	I-94	Linden Ave
	268.0	269.0	270.0	271.0 ##272	273.0	274.0	275.0	276.0 ##277	278.0	279.0 ##280	282.0	288.0	290.0	291.0			
	4297->173 17090->51 5156->932 9321->932 9325->933 9334->935 9356->935 9355->936 9362->937 9374->938 9380->938 9384->939 9394->939 9396->517 5174->402 3698->968 4026->921																
5:30 AM	65.0	70.0	68.0	70.0	70.0	70.0	70.0	70.0	65.0	64.0	65.0	65.0	70.0	68.0	70.0	60.0	50.0
5:35 AM	65.0	70.0	68.0	69.9	70.0	70.0	70.0	70.0	64.9	64.0	65.0	65.0	70.0	68.0	70.0	60.0	50.0
5:40 AM	65.0	70.0	68.0	70.0	70.0	70.0	70.0	69.9	64.6	63.9	64.6	63.6	70.0	68.0	70.0	60.0	50.0
5:45 AM	65.0	70.0	68.0	69.9	70.0	69.9	70.0	70.0	64.9	63.9	64.8	63.8	69.7	67.8	69.5	59.9	50.0
5:50 AM	65.0	70.0	67.9	69.9	69.9	69.6	69.6	69.5	64.3	63.7	63.8	62.1	69.7	67.8	69.6	60.0	50.0
5:55 AM	65.0	70.0	68.0	70.0	70.0	70.0	69.8	69.1	63.9	63.5	63.8	62.0	69.8	67.9	69.8	60.0	50.0
6:00 AM	65.0	70.0	68.0	70.0	70.0	70.0	70.0	70.0	65.0	64.0	65.0	65.0	70.0	68.0	70.0	60.0	50.0
6:05 AM	65.0	70.0	67.9	69.8	69.9	70.0	70.0	70.0	64.8	64.0	65.0	65.0	70.0	68.0	70.0	59.9	50.0
6:10 AM	65.0	70.0	68.0	70.0	70.0	70.0	69.9	69.8	64.5	63.9	64.7	63.7	70.0	68.0	69.3	59.9	50.0
6:15 AM	65.0	70.0	68.0	69.9	70.0	70.0	70.0	70.0	64.9	63.9	64.8	64.4	69.9	67.9	68.2	59.7	50.0
6:20 AM	65.0	70.0	67.9	69.8	69.9	69.6	69.7	69.7	64.5	63.8	64.3	62.4	69.7	67.7	68.7	60.0	50.0
6:25 AM	65.0	70.0	68.0	70.0	70.0	69.9	69.7	69.0	63.8	63.5	63.6	61.9	69.8	67.8	68.2	59.8	50.0
6:30 AM	65.0	70.0	68.0	70.0	70.0	70.0	69.8	69.6	64.3	63.6	64.3	64.1	70.0	67.9	68.9	60.0	50.0
6:35 AM	65.0	70.0	68.0	70.0	70.0	70.0	70.0	70.0	64.4	63.8	64.5	62.0	69.8	67.9	68.2	60.0	50.0
6:40 AM	65.0	69.8	67.9	69.9	69.8	70.0	69.9	69.8	64.8	64.0	65.0	64.6	69.8	67.8	68.2	59.1	50.0
6:45 AM	65.0	70.0	67.9	69.8	69.3	69.5	68.1	64.0	58.9	63.4	64.9	64.7	69.8	67.9	69.4	59.6	50.0
6:50 AM	65.0	69.9	68.0	70.0	69.9	69.2	69.1	67.2	56.3	61.2	63.3	63.5	69.8	67.8	68.8	59.8	50.0
6:55 AM	65.0	69.9	67.9	70.0	69.8	69.2	69.9	58.8	53.9	58.1	57.9	64.2	69.9	67.9	68.8	59.8	50.0
7:00 AM	65.0	69.2	67.6	69.6	69.0	69.8	67.6	62.2	49.9	54.7	54.1	56.3	67.3	65.0	67.2	60.0	50.0
7:05 AM	65.0	69.8	67.7	69.3	69.6	69.9	66.7	56.8	48.8	54.6	54.8	59.4	67.9	64.0	65.0	53.2	50.0
7:10 AM	65.0	69.6	67.6	69.8	69.7	69.8	62.4	47.9	48.5	54.2	54.2	58.8	66.4	61.1	64.3	58.2	49.6
7:15 AM	65.0	70.0	68.0	70.0	70.0	70.0	68.2	57.1	38.6	48.2	51.6	57.4	66.3	62.4	65.9	53.8	50.0
7:20 AM	65.0	69.1	67.3	69.7	69.7	69.6	67.4	62.6	58.9	58.9	56.9	52.4	62.1	57.1	64.1	54.7	50.0
7:25 AM	65.0	68.8	67.1	69.5	69.4	69.2	56.2	40.4	41.7	52.6	53.6	51.2	66.7	60.2	62.9	55.5	49.9
7:30 AM	65.0	66.3	64.5	67.2	65.0	66.3	53.1	35.4	31.8	36.0	33.8	38.4	61.4	56.4	61.7	54.5	50.0
7:35 AM	64.4	66.1	64.8	67.0	65.5	65.3	20.2	26.5	28.3	21.9	18.1	33.0	46.2	46.7	59.2	53.8	49.8
7:40 AM	64.0	66.4	65.5	67.1	64.1	65.0	18.5	23.1	16.8	10.5	15.5	32.1	34.0	39.0	55.4	52.8	49.8
7:45 AM	64.8	67.6	65.8	67.8	66.5	67.3	25.3	21.2	9.2	10.9	16.0	28.4	22.1	37.0	54.7	53.5	49.3
7:50 AM	65.0	70.0	67.8	69.6	69.5	69.9	66.0	39.8	7.7	10.8	16.4	20.5	18.7	36.5	54.2	52.4	48.8
7:55 AM	65.0	69.9	67.9	69.9	69.7	69.8	70.0	66.1	8.9	12.0	15.8	15.4	17.7	36.5	57.2	57.9	49.7
8:00 AM	65.0	69.8	68.0	69.9	69.8	69.9	70.0	69.8	15.7	12.1	16.9	14.1	17.4	36.3	53.6	55.0	49.5
8:05 AM	65.0	70.0	68.0	70.0	69.9	70.0	69.9	69.9	61.6	11.3	13.0	15.4	18.0	36.3	51.6	52.1	49.1
8:10 AM	65.0	69.7	67.9	69.7	69.5	69.8	70.0	69.9	64.9	48.4	20.9	15.1	17.8	36.2	46.6	54.2	49.1
8:15 AM	65.0	69.7	67.9	69.7	69.3	69.8	70.0	69.9	65.0	63.7	56.2	16.3	17.6	36.2	43.7	47.6	46.9
8:20 AM	65.0	69.3	67.6	69.3	68.5	69.6	69.8	69.5	64.6	63.0	62.2	21.2	17.3	36.3	50.3	37.5	41.8
8:25 AM	65.0	69.4	67.7	69.3	68.8	69.5	70.0	69.9	64.9	63.7	63.2	22.3	17.4	36.4	48.3	38.5	44.4
8:30 AM	65.0	69.9	67.9	69.8	69.5	69.5	70.0	69.9	65.0	63.9	64.4	55.9	22.2	36.4	34.6	36.5	44.3
8:35 AM	65.0	69.6	67.9	69.9	69.8	69.6	69.9	69.9	64.9	63.8	64.2	64.2	23.2	33.5	27.0	31.4	44.7
8:40 AM	65.0	68.8	67.4	69.1	68.7	69.5	69.9	69.5	65.0	63.8	64.3	63.8	28.9	36.5	30.1	30.0	44.0
8:45 AM	65.0	69.5	67.7	69.7	69.6	69.6	69.9	68.5	65.0	63.6	63.6	63.1	38.5	54.3	30.1	31.8	44.2
8:50 AM	65.0	69.7	67.9	69.9	69.5	69.8	70.0	69.3	65.0	63.9	64.5	64.0	36.4	48.5	33.4	34.3	45.0
8:55 AM	64.9	69.1	67.8	69.5	68.4	69.3	69.8	69.1	64.6	63.7	64.4	64.3	61.8	52.0	30.2	33.7	43.0
9:00 AM	64.9	69.0	67.6	69.5	68.9	69.7	70.0	69.7	64.9	62.9	60.9	60.8	58.3	55.2	48.5	34.8	45.0
9:05 AM	65.0	69.8	67.9	69.6	68.7	67.1	69.9	69.1	65.0	63.7	64.0	64.1	61.1	49.2	50.3	41.3	45.0
9:10 AM	65.0	68.9	67.6	69.6	68.8	69.3	70.0	69.6	65.0	63.8	64.2	63.5	63.7	55.2	51.4	35.8	46.1
9:15 AM	65.0	68.9	67.6	69.4	68.9	68.9	69.9	69.7	64.8	63.4	63.0	63.5	61.2	56.4	63.2	47.6	46.2
9:20 AM	64.9	65.1	66.4	68.1	66.8	68.9	69.9	69.1	64.9	63.8	63.7	63.8	63.9	53.5	54.1	44.5	47.9
9:25 AM	64.5	59.7	63.0	65.9	63.7	64.4	69.3	68.0	64.7	63.6	63.5	64.0	66.5	63.6	56.8	38.9	45.1
9:30 AM	64.7	63.1	64.0	64.3	61.2	63.6	69.0	67.3	64.7	63.5	63.2	64.1	66.9	61.2	54.9	46.6	47.4
9:35 AM	65.0	67.8	66.9	68.1	64.9	61.6	68.6	67.9	64.4	63.5	63.5	63.5	65.1	59.3	58.6	40.9	45.7
9:40 AM	64.7	64.9	66.0	68.5	66.5	63.5	69.7	69.3	64.9	63.8	64.0	64.2	67.9	63.5	56.9	45.3	46.8
9:45 AM	64.5	63.7	65.6	67.4	64.8	61.3	69.4	68.7	64.8	63.4	63.4	64.5	67.6	64.5	63.5	47.4	47.3
9:50 AM	63.7	54.0	59.4	61.3	56.5	60.3	69.2	68.9	64.8	63.7	63.6	64.4	66.9	61.3	62.0	49.6	46.7
9:55 AM	64.4	58.3	61.2	62.4	55.5	50.1	66.3	65.1	62.1	62.5	60.8	63.3	64.6	58.3	60.1	48.1	47.6
10:00 AM	64.9	65.1	65.8	66.3	61.0	31.1	68.3	67.4	62.6	62.9	61.8	62.9	65.4	60.8	57.7	47.5	47.9
10:05 AM	65.0	65.5	65.5	67.7	65.2	38.4	68.3	68.0	63.5	63.0	61.8	62.5	63.3	55.2	56.1	49.8	49.0
10:10 AM	64.9	65.1	66.4	68.8	66.5	54.0	68.7	68.1	63.7	62.4	60.6	63.4	64.4	57.4	58.4	45.7	46.2
10:15 AM	64.9	63.7	65.3	67.1	64.4	63.4	67.5	66.3	63.5	63.1	61.6	63.4	64.9	55.6	57.0	44.2	46.1
10:20 AM	64.9	67.8	67.1	68.8	67.3	66.1	69.3	68.8	63.0	63.3	63.4	62.8	62.1	55.5	63.8	54.6	48.9
10:25 AM	65.0	68.8	67.3	69.1	68.9	69.0	69.7	69.3	64.2	63.4	63.6	63.2	65.0	55.8	62.6	53.2	49.1
10:30 AM	65.0	69.6	67.7	69.2	68.2	69.1	69.9	69.6	64.1	63.1	63.2	61.7	66.0	60.2	64.7	57.4	49.4

2.8 Testing and Validation With a Prior Known Event

2.8.1 Methodology

The overall modeling procedure for DynusT is illustrated in Figure 2-26. The highlighted area shows the process of modeling traveler reactions to an incident scenario. The baseline case employs the time-dependent OD matrices and is run to DUE. After the completion of the baseline case, the vehicle and path files containing all travelers are generated, along with a trajectory travel time file recording the arrival time at each node of the path for each individual traveler.

When analyzing the incident scenario, the analyst needs to decide whether an adjustment by the traveler will occur. If the incident is random with a short duration (several tens of minutes), then travelers may be able to react by changing their route or departure time only if they receive incident information. This is the “short-term reaction” to the incident. If the incident is persistent for several weeks or months, then travelers may learn from this situation and be willing to make a route and/or departure time change after days of learning and adjustment. This is the “long-term reaction.” Although travelers may adjust their routes or departure times in both short-term and long-term reaction scenarios, the underlying behavior mechanisms governing such decisions are rather distinct. In the short-term reaction case, if travelers have not accessed pre-trip or en-route information they may not be aware of the incident until they begin to experience congestion. Those who access or receive pre-trip information or en-route radio information and find their path is directly impacted by the incident may choose to take a different route even before encountering the incident-induced congestion. Those who become aware of the incident via dynamic message signs (DMS) may also choose to alter their routes.

Table 2-8 summarizes how different scenario situations call for either a short-term or long-term reaction mode in DynusT.

Figure 2-26. DynusT Baseline and Scenario Modeling Framework

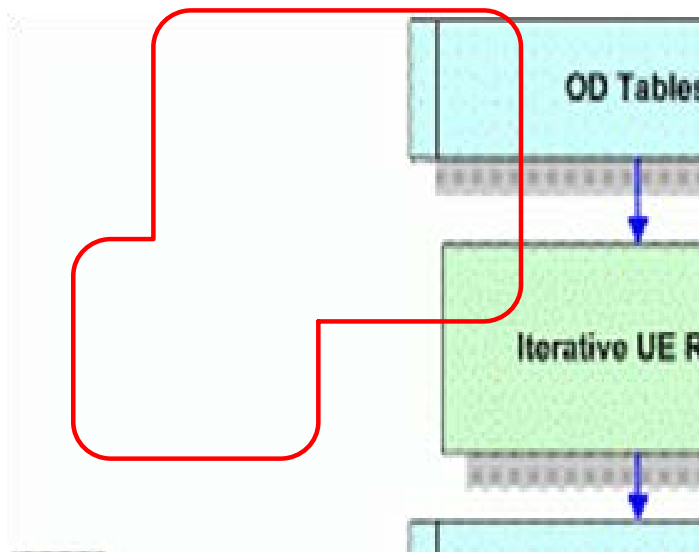


Table 2-8. Scenario Characteristics and DynusT Running Modes

Scenario Characteristics	Short-Term Reaction	Long-Term Reaction
Incident Persistent?	No	Yes
Travelers anticipate incident?	No	Yes
Travelers adjust departure time and/or route choice through learning and anticipation?	No	Yes
Travelers adjust departure time and/or route choice through pre-trip or en-route information and instantaneous reaction?	Yes	No
DynusT running mode	One-pass	Iterative DUE
DynusT running mode	One-pass	Iterative DUE

For the known event validation, the incident is a morning vehicle collision accident. This is considered a random incident in which no learning is involved; therefore, one-pass mode is employed. The modeling of reaction to the incident considers two aspects: 1) prevalence of information and reaction to information, and 2) reaction to congestion. The first aspect is addressed in DynusT via the provision of pre-trip information, which allows a traveler to choose a route when departing from the origin. En-route information allows a traveler with access to this information to make an en-route adjustment.

The second aspect, reaction to congestion, is primarily governed by the congestion responsive diversion behavior rule. It is postulated that travelers will continue to use their habitual routes if the delay is not out of ordinary. According to this diversion rule, travelers will tolerate the perceived delay as long as the total delay does not exceed their personal tolerance thresholds. In DynusT, this

threshold is randomly generated from an analyst-specified normal distribution function $N(\mu, \sigma^2)$ with a set minimal threshold value (e.g., no negative value). The delay for a traveler at current node P is calculated as the difference in perceived arrival time between the baseline (habitual) and scenario

cases, that is: $\epsilon_n^P = \max\{0.0, t_n^{p,s} - t_n^{p,b} + \epsilon_n^{p,s} - \epsilon_n^{p,b}\} \forall p \in \{1, 2, \dots, P\}$, where $t_n^{p,s}$ is the arrival

time at node P for traveler n in the scenario case and $t_n^{p,b}$ is for the same traveler n the arrival time at

node P in the baseline (habitual) case, $\epsilon_n^{p,s}$ is the perception error for traveler n at node P in the

scenario case, $\epsilon_n^{p,b}$ is the perception error for traveler n at node P in the baseline case, and P is the maximal number of nodes in the habitual path. In other words, when running the incident scenario, the analyst can specify DynusT to read the node arrival times for all travelers, which is calculated from the baseline DUE case. In the case of an incident scenario, some travelers will start to experience delays during simulation due to incident. Those who experience accumulative delays exceeding the

threshold $\epsilon_{n,i}^u \geq \bar{\epsilon}_{n,i}$ will then select alternative paths (the details of path calculation are explained in the later section).

Intuitively this diversion rule naturally captures the situation in which travelers, including those who are directly impacted by the incident (if their original path traverses the incident location) and those travelers who are impacted by the diverted vehicles and consider diversion if the induced delay is exceedingly lengthy compared to the habitual travel time. The diversion locations are not hard-wired – a traveler will initiate the diversion decision at the location where the perceived delay exceeds the personal threshold.

When travelers decide to choose an alternative route, they select a path starting from the diversion decision location to their destination. The path is then computed using travel time calculated from the baseline case updated with incident location information. This realistically considers the situation in which travelers may not know the instantaneous shortest path at time of decision, but they will try to use the prior knowledge to select a good diversion path.

2.8.2 Incident Scenario

The known event is a freeway incident, as described below.

- **Location:** Eastbound I-394 at I-494 (see Figure 2-27), crash occurred just east of the I-394/I-494 interchange, blocking the right most thru lane of I-394 (one lane blocked).
- **Date:** September 9, 2008.
- **Start time:** 7:13 a.m.
- **End time:** 8:03 a.m.
- **Time to clear lane:** 36.3 minutes (vehicles are moved to the side, but response still at the scene).
- **All clear time:** 49.3 minutes.
- **DMS assumptions:** Three DMSs were posted with congestion warning messages. The locations of these signs are illustrated on the Mn/DOT-provided DMS map (see Figure 2-27).

Consistent with the AMS Analysis plan and based on the Minneapolis Perception Tracking survey, a 15-percent usage of pre-trip information was applied to the entire population of travelers. Each traveler who accesses the pre-trip information will check if the incident is located on his/her habitual route, and if the estimated delay exceeds his/her tolerance. If so, the traveler will select a diversion route. Travelers without pre-trip information will stay at their habitual route. In other words, the 15 percent could be viewed as the market penetration of pre-trip information, but not the actual information induced diversion.

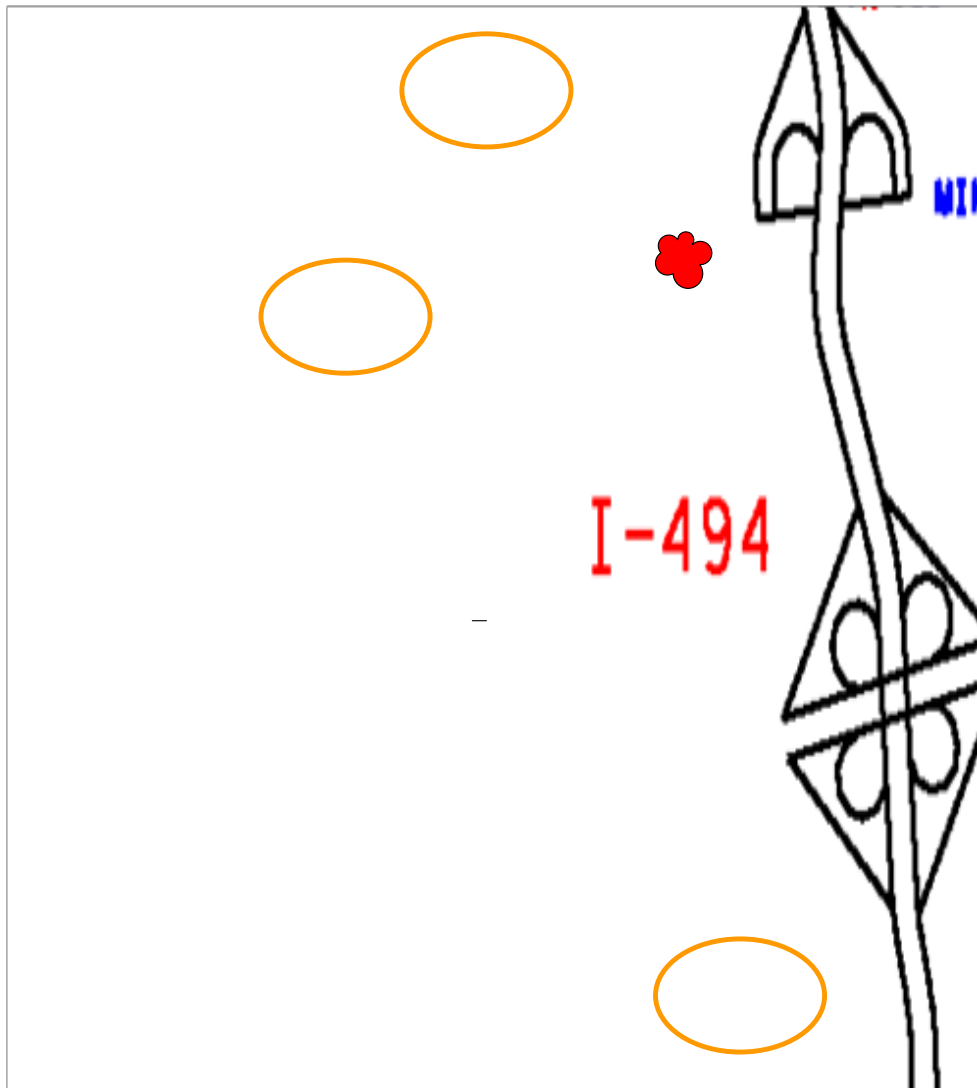
The AMS Analysis plan also cites that according to the survey, 29 percent of travelers have chosen to alter their route based on a DMS. All travelers having their route going through the incident site will evaluate the situation and consider diversion, if the estimated delay exceeds their preset delay tolerance.

The average delay tolerance threshold follows a normal distribution with mean equal to 20 minutes and standard deviation equal to 2 minutes.

2.8.3 Analysis Results

The speed contour of the field data of the incident scenario is shown in Figure 2-28. The sensor east of the I-394/I-494 interchange shows a speed reduction from 7:15 a.m. to 8:10 a.m. The traffic conditions at the two known bottlenecks appear to be worse than the monthly average. The congestion at Louisiana Avenue ranges from 7:00 a.m. to 9:00 a.m., and the congestion at west TH-100 starts at about 7:30 a.m. to 9:30 a.m. Both locations are downstream of the incident location; therefore, the higher congestion level can be attributed to higher demand at this particular date. Figure 2-29 shows the simulated speed contour for the same corridor. The contours show satisfactory resemblance of the traffic conditions at the same corridor.

Figure 2-27. Three Activated Dynamic Message Sign Locations



[Source: MnDOT.]

Figure 2-28. Speed Contour of Field Data for the Incident Scenario

Segment	W of I-494	E of I-494	Plymouth Rd	Ridgedale Dr	CR 73	Shelard Pkwy	TH 169	General Mills Blvd	Winnetka Ave	Louisiana Ave	Colorado Ave	Xenia Ave	W of TH 100	W of Wirth Pkwy	Dunwoody Blvd	I-94	Linden Ave
Detector	S268	S269	S270	S271	S272	S273	S274	S275	S276	S277	S278	S279	S280	S282	S288	S290	S291
5:30 AM	-1.0	69.4	69.6	67.6	68.9	74.2	70.0	68.6	66.3	66.0	66.7	65.5	69.5	66.3	76.4	58.3	48.3
5:35 AM	-1.0	65.9	68.3	71.0	71.4	69.4	70.7	71.6	66.8	61.1	64.2	64.3	70.4	66.1	74.7	50.5	52.7
5:40 AM	-1.0	70.7	68.5	66.3	69.3	72.2	70.3	71.2	63.8	64.7	65.9	67.1	66.3	70.4	76.5	56.9	48.4
5:45 AM	-1.0	65.8	66.6	67.6	69.4	69.8	71.9	74.3	67.7	66.0	65.5	64.2	70.0	67.8	79.0	51.3	56.5
5:50 AM	-1.0	66.3	67.6	68.5	68.8	68.1	66.8	67.9	65.2	64.1	64.6	64.1	70.5	66.7	77.0	57.2	52.2
5:55 AM	-1.0	68.1	65.9	65.8	68.7	66.6	67.1	69.2	66.0	64.0	65.7	66.5	69.4	69.1	77.5	55.5	50.1
6:00 AM	-1.0	66.1	68.0	68.1	68.4	68.1	69.2	69.1	65.5	62.5	64.7	66.3	73.2	69.0	78.9	56.3	50.5
6:05 AM	-1.0	71.4	69.5	70.5	70.6	69.4	69.4	69.8	69.4	64.4	67.5	65.5	72.8	68.8	78.7	55.6	53.5
6:10 AM	-1.0	64.4	65.9	67.0	68.6	68.9	70.4	71.0	68.9	64.0	67.2	64.6	70.9	66.3	75.4	57.1	50.1
6:15 AM	-1.0	70.1	65.4	67.1	64.9	65.5	65.6	68.3	66.2	61.9	64.7	65.4	71.3	66.4	78.0	55.4	49.4
6:20 AM	-1.0	64.4	67.4	68.0	67.2	67.3	68.0	69.5	66.8	64.6	65.6	64.9	71.8	67.5	78.4	57.7	52.4
6:25 AM	-1.0	69.9	67.3	68.4	68.4	68.5	67.9	68.5	65.2	60.8	64.4	64.4	70.4	67.4	78.4	56.5	50.6
6:30 AM	-1.0	69.3	68.2	67.6	68.6	68.8	68.4	69.6	67.7	62.4	65.3	64.2	70.7	67.3	74.4	56.1	53.7
6:35 AM	-1.0	66.9	67.7	67.9	66.6	67.8	68.0	70.3	66.8	62.7	63.5	63.0	71.6	65.0	76.4	56.2	51.7
6:40 AM	-1.0	66.9	66.0	67.7	67.3	65.8	66.7	67.6	65.5	60.5	64.0	64.6	70.3	66.3	76.5	57.9	51.8
6:45 AM	-1.0	66.9	66.0	65.6	65.3	66.5	64.8	65.1	63.2	56.5	61.8	59.7	66.7	61.9	74.6	56.2	52.0
6:50 AM	-1.0	65.8	65.7	66.2	66.1	67.6	66.4	65.9	64.6	60.8	65.6	64.1	70.0	62.7	70.8	55.8	50.8
6:55 AM	-1.0	65.7	67.1	63.2	66.0	64.9	61.2	66.5	60.8	51.7	61.6	61.5	70.5	65.4	64.5	55.9	51.3
7:00 AM	-1.0	64.9	61.6	59.2	64.6	63.2	54.5	55.8	26.2	44.0	63.5	64.8	71.1	61.7	68.6	56.5	51.0
7:05 AM	-1.0	66.1	63.7	59.8	62.1	62.8	60.8	44.6	21.3	37.4	59.1	59.5	65.2	58.8	75.6	55.5	52.2
7:10 AM	-1.0	65.2	63.6	64.4	66.0	61.7	57.7	23.8	20.9	36.4	60.7	58.1	65.3	60.6	72.3	56.5	51.0
7:15 AM	-1.0	35.4	52.5	62.5	61.3	62.7	45.9	21.6	18.9	34.5	61.8	59.3	65.0	41.4	69.5	55.2	50.5
7:20 AM	-1.0	18.2	63.0	66.7	66.7	64.3	33.6	22.0	18.6	35.1	55.6	55.8	50.8	45.9	66.7	54.5	53.9
7:25 AM	-1.0	17.1	63.0	68.1	66.4	64.1	50.5	25.7	18.1	29.4	56.7	38.4	19.3	51.9	63.1	50.2	48.5
7:30 AM	-1.0	16.4	64.6	66.9	66.4	63.6	55.9	21.3	19.8	30.5	58.1	29.5	26.1	47.1	63.3	42.5	46.9
7:35 AM	-1.0	19.2	64.6	68.8	67.4	68.7	64.0	21.5	15.6	29.2	55.5	34.0	32.2	47.6	56.0	41.9	48.2
7:40 AM	-1.0	19.5	66.7	70.2	68.2	67.4	66.0	34.5	18.4	31.2	56.9	28.5	25.2	51.6	45.6	41.2	48.4
7:45 AM	-1.0	19.5	66.5	68.4	66.8	68.9	64.5	49.6	19.8	34.2	51.5	17.2	20.8	52.7	49.7	34.5	48.2
7:50 AM	-1.0	17.2	54.4	60.1	62.0	63.7	60.5	56.8	22.8	31.2	32.5	19.3	20.8	52.3	50.1	24.6	46.8
7:55 AM	-1.0	18.5	54.9	57.8	62.9	63.5	48.3	27.0	19.5	29.8	31.0	15.2	22.9	52.2	49.7	20.5	47.0
8:00 AM	-1.0	23.9	49.7	57.7	59.3	60.1	44.4	28.1	17.8	24.8	35.7	23.0	19.7	35.9	34.1	20.7	46.8
8:05 AM	-1.0	39.2	49.1	55.5	61.6	54.9	23.1	12.1	17.5	29.8	48.0	21.8	24.0	40.1	51.0	21.3	47.6
8:10 AM	-1.0	54.5	55.4	62.4	63.2	24.8	20.2	25.0	20.3	29.4	54.1	27.7	19.2	42.9	35.6	21.5	46.6
8:15 AM	-1.0	65.7	50.0	52.2	60.5	36.0	26.1	23.1	20.7	31.3	47.7	24.5	24.7	36.5	45.3	21.9	46.9
8:20 AM	-1.0	64.9	62.3	61.4	64.0	39.6	20.2	20.9	20.8	38.9	44.3	19.8	19.9	43.0	40.4	25.4	46.6
8:25 AM	-1.0	66.4	64.3	65.0	65.3	57.5	23.2	26.4	26.3	33.0	38.0	15.8	18.6	32.8	60.3	22.8	46.2
8:30 AM	-1.0	67.1	66.0	66.5	64.6	67.2	51.7	28.1	22.7	31.3	26.6	16.6	20.6	35.0	43.3	21.2	45.0
8:35 AM	-1.0	64.9	66.6	66.1	65.8	67.4	64.4	16.0	22.0	36.0	34.2	17.3	24.1	49.4	59.7	21.3	45.9
8:40 AM	-1.0	66.7	68.9	68.1	67.3	68.5	61.0	35.7	22.6	37.5	44.4	19.9	23.3	51.8	51.3	35.3	47.3
8:45 AM	-1.0	65.2	64.1	66.3	66.6	68.7	60.4	30.6	23.8	52.0	41.4	26.5	24.3	54.8	61.1	48.9	49.1
8:50 AM	-1.0	64.5	66.5	67.2	65.5	66.8	65.6	29.1	26.8	49.5	53.8	17.4	20.3	58.6	61.9	50.1	49.1
8:55 AM	-1.0	65.1	67.4	66.9	67.4	66.3	64.0	46.0	20.8	30.0	50.8	35.5	27.2	56.7	70.9	51.6	49.3
9:00 AM	-1.0	66.6	70.0	68.2	67.1	67.1	66.1	35.2	20.2	37.1	52.5	57.9	30.8	55.2	70.6	53.2	50.9
9:05 AM	-1.0	66.5	68.3	69.2	67.8	70.3	66.4	60.7	26.6	50.7	63.3	60.7	29.0	50.6	66.7	50.6	47.8
9:10 AM	-1.0	64.4	66.0	65.2	66.0	70.6	69.5	68.8	60.5	56.9	59.7	63.2	54.2	46.0	69.5	38.1	45.6
9:15 AM	-1.0	64.2	64.0	62.3	64.0	66.1	65.6	64.0	63.4	58.8	61.9	62.1	46.4	30.0	67.9	54.0	49.4
9:20 AM	-1.0	66.0	68.7	68.1	66.8	67.8	66.8	68.6	63.8	61.1	61.8	52.7	25.0	47.7	63.6	51.2	48.7
9:25 AM	-1.0	64.2	66.2	66.0	65.0	67.4	66.5	66.9	65.4	62.0	62.2	58.8	22.9	51.9	65.4	53.3	47.0
9:30 AM	-1.0	66.1	66.0	66.3	64.6	64.8	63.1	63.5	64.1	60.4	60.2	60.8	62.3	55.0	55.8	55.8	49.4
9:35 AM	-1.0	64.0	68.2	67.2	66.8	67.7	67.4	67.9	65.1	58.5	60.0	59.5	67.8	62.8	48.3	55.6	51.5
9:40 AM	-1.0	65.2	66.5	66.0	66.6	66.3	66.8	68.1	64.0	61.4	66.0	65.9	72.2	64.5	48.2	53.6	47.6
9:45 AM	-1.0	63.2	64.9	65.4	64.1	63.3	62.0	65.4	62.7	59.3	63.9	63.6	69.9	65.1	53.5	55.0	48.5
9:50 AM	-1.0	66.9	67.2	65.9	66.5	67.1	66.3	65.9	61.7	61.5	59.4	59.9	64.6	63.0	62.1	50.9	46.9
9:55 AM	-1.0	66.0	68.6	68.0	69.3	70.4	68.8	69.5	65.5	64.5	62.1	62.2	67.3	65.4	76.2	52.8	50.3
10:00 AM	-1.0	62.7	67.2	65.1	65.8	64.8	64.8	64.2	62.8	59.8	61.2	60.4	66.7	64.5	74.0	55.5	52.7
10:05 AM	-1.0	62.7	65.4	67.9	68.1	71.3	69.5	71.1	68.0	60.4	60.5	60.3	64.5	62.9	71.1	53.6	49.5
10:10 AM	-1.0	66.1	64.2	65.2	64.4	64.6	64.0	67.2	64.1	62.4	65.7	64.8	71.7	65.6	74.9	59.6	54.3
10:15 AM	-1.0	62.7	68.0	65.5	63.9	65.2	62.9	66.6	65.3	61.7	65.4	64.8	69.2	64.7	75.0	55.4	48.1
10:20 AM	-1.0	65.2	69.0	70.2	67.5	67.6	66.2	67.3	63.2	61.1	59.9	60.9	69.1	64.2	71.7	56.8	50.7
10:25 AM	-1.0	65.1	41.4	38.7	427.8	192.7	64.3	42.9	62.9	62.4	64.9	64.4	69.1	64.3	74.2	57.4	50.1
10:30 AM	-1.0	60.1	62.5	62.8	63.3	62.6	62.0	63.1	59.9	59.3	57.7	61.3	66.8	62.4	72.9	54.8	51.1
10:35 AM	-1.0	61.2	62.5	62.6	61.7	60.7	59.9	61.5	58.6	56.3	59.3	57.9	62.9	61.0	68.1	52.9	51.0
10:40 AM	-1.0	64.4	63.5	65.2	65.0	60.7	65.4	66.1	61.9	61.2	61.9	60.7	66.8	60.5	71.1	54.8	47.5
10:45 AM	-1.0	64.7	64.6	66.0	65.2	66.5	65.6	64.7	61.9	59.1	62.5	59.0	67.1	60.6	75.4	56.4	49.2
10:50 AM	-1.0	55.8	60.2	62.7	64.5	66.9	65.0	66.7	64.9	61.4	61.3	62.8	69.1	64.7	73.2	54.9	47.1
10:55 AM	-1.0	62.0	66.0	63.4	63.2	63.5	61.4	63.5	60.2	56.2	58.8	59.2	68.5	62.9	74.0	56.1	50.2
11:00 AM	-1.0	64.5	65.8	65.8	65.4	66.4	64.1	65.2	65.8	60.1	61.1	61.1	66.9	59.8	71.0	59.5	47.6
11:05 AM	-1.0	65.9	68.7	68.6	66.9	67.9	66.6	68.0	63.0	61.7	61.8	64.1	69.5	65.9	72.5	58.0	52.0
11:10 AM	-1.0	66.8	67.6	67.7	67.2	68.9	68.7	69.5	69.0	61.6	61.0	62.9	67.3	66.0	75.3	54.8	49.5
11:15 AM	-1.0	67.2	66.6	64.9	65.1	66.5	64.7	65.1	61.7	59.4	61.3	62.6	65.4	60.3	72.2	56.6	49.3
11:20 AM	-1.0	67.0	69.7	70.0	66.7	67.6	67.1	67.3	65.9	61.3	66.1	64.7	68.5	64.0	73.2	56.6	51.6

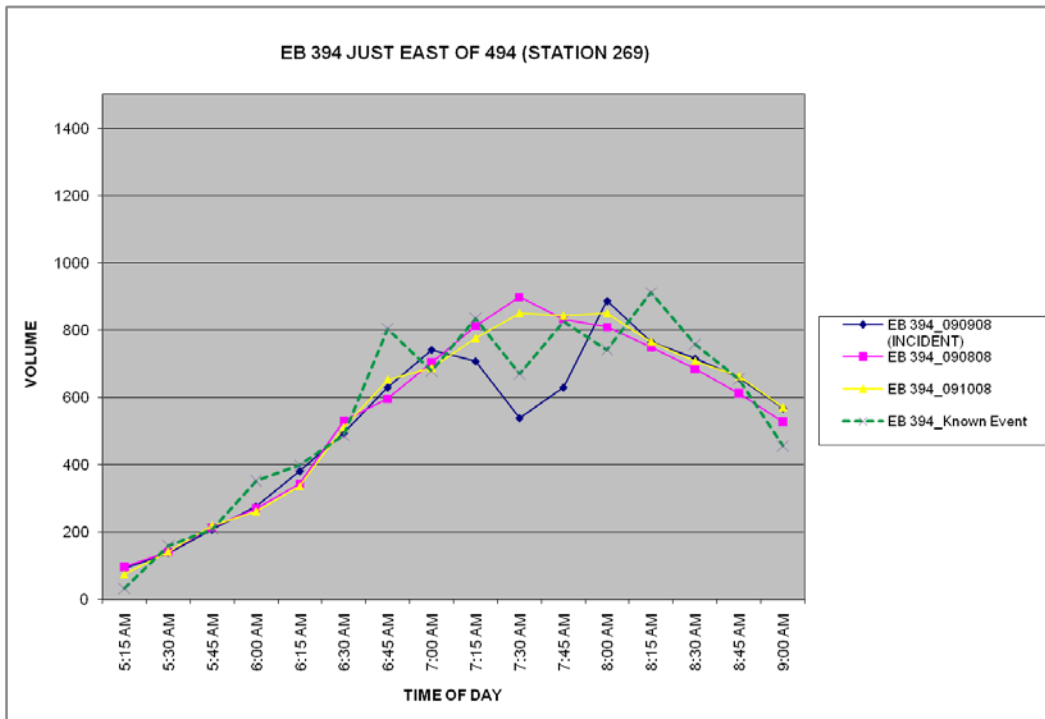
Figure 2-29. Speed Contour of Simulation Data for the Incident Scenario

	W of I-494	E of I-494	Plymouth Rd	Ridgedale Dr	CR 73	Shelard Pkwy	TH 169	General Mills Blvd	Winnetka Ave	Louisiana Ave	Colorado Ave	Xenia Ave	W of TH 100	W of Wirth Pkwy	Dunwoody Blvd	I-94	Linden Ave
5:30 AM	65	70	68	70	70	70	70	70	64.923	63.977	65	64.974	69.995	67.993	70	60	50
5:35 AM	65	69.98	67.836	69.64	69.795	69.858	69.87	69.863	63.234	63.95	64.988	64.952	70	68	70	59.965	49.998
5:40 AM	65	70	68	70	70	70	70	69.952	61.274	62.668	64.416	63.218	69.844	67.881	69.718	59.833	49.977
5:45 AM	64.997	69.969	67.982	69.994	70	69.933	69.997	69.992	63.041	62.607	64.904	64.185	69.484	67.468	69.215	59.893	49.999
5:50 AM	64.999	69.372	67.873	69.513	69.589	69.067	69.474	69.472	59.946	60.995	63.657	61.819	69.496	67.51	69.263	60	49.994
5:55 AM	64.999	69.798	68	70	69.901	70	69.435	68.357	58.089	60.201	63.426	58.951	68.881	67.219	69.413	59.848	49.933
6:00 AM	64.995	69.625	67.993	69.993	69.994	69.821	69.465	68.873	59.241	60.298	63.432	63.239	69.45	66.924	69.371	59.98	49.999
6:05 AM	64.998	69.876	67.935	69.901	69.936	69.929	69.652	69.551	58.804	61.128	63.782	59.869	68.796	67.107	68.986	59.987	50
6:10 AM	64.993	68.475	67.729	69.802	69.82	69.983	69.812	69.19	60.504	62.652	64.829	64.247	69.583	66.982	69.025	59.527	49.977
6:15 AM	65	68.668	67.939	69.715	69.106	69.181	67.701	63.807	50.621	59.237	64.805	64.297	69.608	67.478	69.853	59.775	49.995
6:20 AM	64.937	68.619	67.946	69.77	69.253	69.399	68.648	66.801	47.616	52.178	62.785	62.995	69.335	67.195	69.735	59.874	49.998
6:25 AM	64.995	68.413	67.851	69.887	69.599	68.839	66.873	61.334	44.814	53.321	59.961	63.456	69.203	67.223	69.057	59.831	50
6:30 AM	64.996	67.137	67.756	69.772	69.519	69.683	68.212	63.116	42.571	50.206	57.178	57	66.049	64.085	69.215	59.864	49.998
6:35 AM	64.951	68.8	67.813	69.193	69.459	69.87	68.772	63.788	45.267	48.317	57.571	61.235	67.332	62.49	66.93	59.561	49.92
6:40 AM	64.967	68.719	67.928	69.958	69.95	69.846	65.916	52.856	37.529	48.821	57.773	59.436	65.3	60.453	67.419	58.529	49.548
6:45 AM	64.998	69.742	68	69.987	69.843	69.946	68.767	64.546	35.31	42.973	55.836	59.59	66.286	62.279	69.066	59.613	49.884
6:50 AM	64.975	66.204	67.794	69.904	69.966	69.344	66.279	59.522	46.887	52.239	59.627	54.336	62.598	59.014	68.159	59.913	49.991
6:55 AM	64.914	63.1	67.086	69.406	69.317	69.378	64.658	47.841	30.027	43.659	55.01	53.389	65.699	61.713	67.765	59.879	49.893
7:00 AM	64.986	60.366	65.342	67.393	65.765	66.366	55.006	29.532	23.266	35.945	48.22	44.773	60.209	55.985	65.353	59.908	49.963
7:05 AM	64.443	59.374	64.902	67.228	65.973	65.914	20.144	18.848	20.884	35.328	43.863	39.337	47.184	45.364	63.443	59.624	49.942
7:10 AM	63.522	52.122	66.502	68.091	66.164	65.598	22.003	19.024	19.285	33.92	40.649	36.928	41.619	38.654	58.435	59.355	49.846
7:15 AM	54.986	24.521	67.997	69.988	69.916	69.974	62.847	39.228	17.816	33.246	43.157	38.888	25.315	35.268	59.781	56.831	49.313
7:20 AM	56.355	18.374	67.992	69.719	69.056	69.358	68.78	61.111	26.197	36.161	45.196	42.632	18.374	33.907	56.873	57.095	49.754
7:25 AM	55.926	18.028	67.913	69.629	68.88	68.936	69.173	67.518	44.246	37.265	42.504	39.505	16.287	33.849	59.342	54.076	49.347
7:30 AM	57.498	12.345	64.468	67.47	66.192	67.214	68.168	66.242	50.58	56.269	58.382	27.789	15.392	33.893	56.995	53.464	49.182
7:35 AM	59.642	12.94	62.139	63.714	60.378	60.164	57.715	49.81	39.651	50.932	52.952	29.057	15.242	33.805	56.687	54.557	49.767
7:40 AM	54.985	13.181	64.532	65.944	62.501	58.289	35.17	23.813	24.56	41.687	46.231	37.811	16.483	33.687	54.261	43.055	44.128
7:45 AM	54.178	11.578	63.046	64.352	59.681	61.701	25.889	20.055	21.157	46.576	49.179	55.083	22.366	33.8	52.296	44.686	45.096
7:50 AM	50.866	21.066	50.931	52.756	50.852	60.867	54.912	24.57	17.056	47.142	52.647	52.982	23.907	33.932	54.576	45.027	44.66
7:55 AM	55.335	27.588	48.975	42.064	35.631	49.281	49.983	26.768	13.962	38.014	45.81	50.063	19.948	33.747	52.73	43.12	45.374
8:00 AM	59.21	37.01	52.703	41.846	32.539	45.988	29.712	22.415	13.727	38.102	46.03	42.458	17.243	33.705	39.538	37.563	46.116
8:05 AM	62.817	51.271	58.984	48.303	31.366	37.85	14.543	20.602	13.409	36.117	44.42	27.482	15.735	33.823	36.412	38.088	44.918
8:10 AM	62.237	49.655	62.569	63.673	54.435	21.334	15.455	21.539	13.109	31.547	34.832	14.072	15.191	33.68	34.903	38.268	46.021
8:15 AM	62.792	42.098	54.402	54.649	49.683	25.547	16.24	21.174	13.177	25.99	17.513	11.984	15.428	33.803	42.091	37.536	43.814
8:20 AM	64.258	55.69	63.6	64.877	58.831	36.032	16.742	21.3	14.008	19.846	17.228	12.051	15.162	33.782	37.971	40.987	44.532
8:25 AM	63.118	54.032	62.975	64.221	61.914	63.352	25.492	21.409	14.341	24.415	20.899	10.137	14.497	33.469	34.055	39.807	45.042
8:30 AM	63.519	54.832	63.88	65.865	63.498	65.484	65.431	41.178	14.987	14.861	13.033	9.679	14.829	33.403	30.589	39.103	44.463
8:35 AM	63.448	54.232	64.312	64.572	61.181	64.715	68.762	62.391	16.245	9.472	12.378	11.915	15.613	33.677	34.681	36.586	45.073
8:40 AM	63.998	58.492	64.139	64.202	61.61	63.198	65.788	63.609	21.707	10.928	13.996	16.628	17.096	33.692	45.053	37.021	45.256
8:45 AM	64.489	56.828	65.54	66.431	63.488	64.101	68.078	64.835	46.783	31.944	35.716	17.956	16.351	33.76	54.216	42.125	45.431
8:50 AM	64.776	54.425	63.057	63.493	61.051	64.26	67.653	66.914	57.074	60.619	62.186	20.981	15.935	33.578	48.043	43.587	45.934
8:55 AM	63.702	50.207	63.494	64.928	61.239	63.663	68.873	67.993	57.093	56.293	59.033	59.206	26.531	33.592	41.329	45.53	48.182
9:00 AM	64.637	51.906	63.598	64.82	59.637	61.891	67.023	66.442	56.383	58.485	61.518	63.414	63.269	45.904	33.088	32.558	43.832
9:05 AM	64.831	55.915	66.085	67.778	64.39	65.236	67.685	64.915	56.913	59.211	61.854	63.942	64.253	59.683	50.28	32.262	43.265
9:10 AM	63.873	52.813	63.714	64.691	60.694	61.292	68.169	67.365	60.593	61.4	63.161	63.804	64.683	59.376	58.711	45.377	44.973
9:15 AM	63.429	48.886	62.029	62.773	59.619	62.419	67.869	66.476	56.784	57.481	60.48	63.104	63.046	57.35	62.213	48.15	47.12
9:20 AM	63.824	51.018	64.656	66.556	62.89	62.599	67.918	67.268	59.283	60.254	63.623	64.186	65.395	57.732	63.521	50.24	47.275
9:25 AM	63.528	49.072	62.005	62.63	58.935	59.92	63.049	62.552	56.414	61.04	63.605	64.101	66.581	60.344	62.258	51.474	49.27
9:30 AM	61.068	36.58	58.411	60.231	55.731	60.763	68.463	67.63	57.373	59.085	62.235	64.35	66.296	61.306	64.773	51.903	48.946
9:35 AM	62.929	40.98	59.02	60.761	54.963	53.971	65.62	64.46	52.304	58.932	63.315	64.175	66.605	62.548	66.306	53.669	49.727
9:40 AM	64.376	48.137	62.452	63.731	59.589	31.634	67.273	66.554	56.195	57.503	62.479	64.001	66.406	61.404	67.151	55.819	49.46
9:45 AM	64.343	46.423	58.86	59.825	55.972	41.486	63.504	63.337	50.651	57.654	63.286	64.53	67.05	61.146	67.122	53.868	48.633
9:50 AM	64.465	49.123	62.062	62.864	58.22	52.763	67.322	66.493	55.799	58.529	62.075	63.223	65.005	58.092	67.351	57.57	49.748
9:55 AM	64.567	54.388	64.592	65.26	63.054	54.965	67.236	65.861	55.298	58.607	63.313	63.551	66.761	62.989	69.183	58.07	49.494
10:00 AM	64.913	58.042	66.461	67.362	64.137	65.262	68.564	68.274	55.71	57.115	62.586	63.629	65.333	57.282	67.217	56.539	49.704
10:05 AM	64.963	63.819	67.104	68.026	65.949	64.536	68.552	67.332	53.987	57.54	63.497	63.467	67.752	63.706	66.615	56.447	49.474
10:10 AM	64.983	65.012	67.444	69.087	68.144	68.847	69.311	68.755	57.887	57.559	62.33	61.121	63.674	56.148	66.185	57.525	49.449
10:15 AM	65	64.979	67.364	68.916	68.839	69.355	69.66	69.006	58.183	60.931	63.643	62.077	66.67	60.615	64.814	53.909	48.464
10:20 AM	65	65.398	67.442	69.293	69.157	69.635	69.776	69.324	61.11	60.252	63.939	63.363	68.001	63.711	68.27	58.984	49.774
10:25 AM	65	65.207	67.732	69.863	69.632	69.711	69.687	69.154	58.886	61.194	64.347	63.232	66.482	61.305	68.015	58.408	49.727
10:30 AM	64.995	66.982	67.713	69.616	69.439	69.717	69.89	69.778	60.984	61.09	64.205	63.64	68.063	61.906			

Figure 2-30 and Figure 2-31 illustrate traffic flows for I-394, I-494, and selected freeway ramps for the incident date and two prior dates (September 8 and September 10, 2008). As shown in Figure 2-30, eastbound I-394, just east of I-494, exhibits steadily increasing flow which peaks between 7:30 a.m. and 8:00 a.m. with 15-minute volume at about 900 vehicles (1,100 vphpl). On the day of the incident, the volume drops to as low as 840 vphpl. After the incident is clear, the volume is restored to the same level. The simulation results are comparable. The temporal pattern is similar, and the reduction of traffic volume is observed at the same time. However, the volume drop is not as severe as the actual data.

Figure 2-30. EB I-394 East of I-494

Station 269



Examining the NB I-494 to EB I-394 ramp, the typical peak volume is 400 vehicles per 15 minutes (1,600 vphpl). The volume on the date of the incident exhibits flow reduction, implying that the DMS upstream of the NB I-494 results in some traffic being diverted. The simulation results show a similar pattern in the change of volumes.

Neither the field data nor the simulation results show a significant change in volumes at the EB I-394 to NB I-494 ramp, but a slight increase on the day of the incident can be observed. The simulation does not show that type of increase, but overall the level of volumes and the temporal pattern is consistent with the field data.

Figure 2-31. NB I-494 TO EB I-394 Ramp

Detector 1649

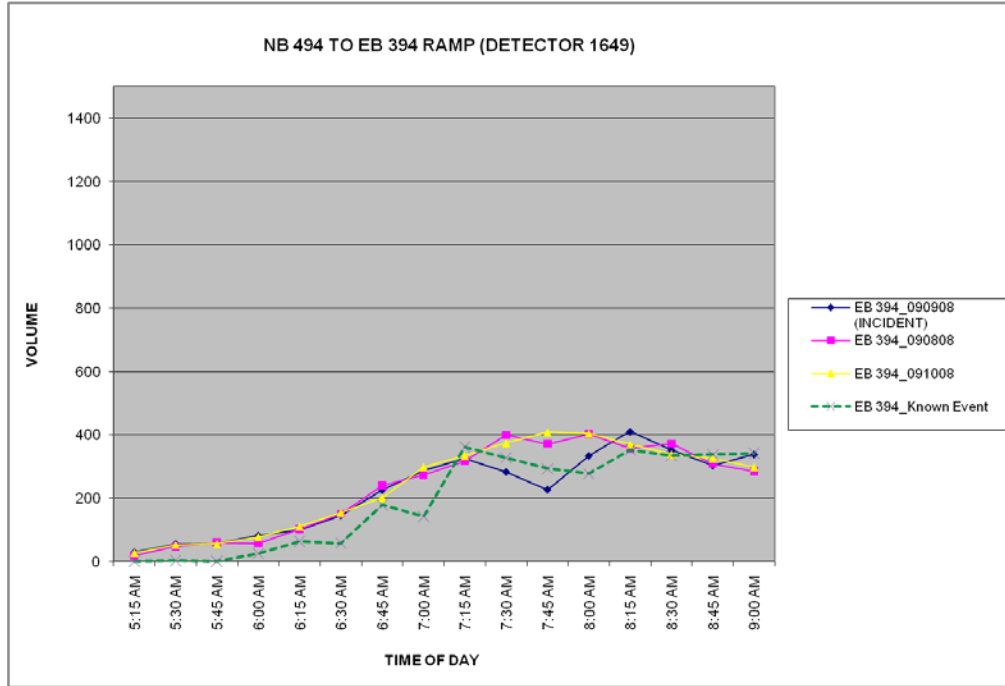
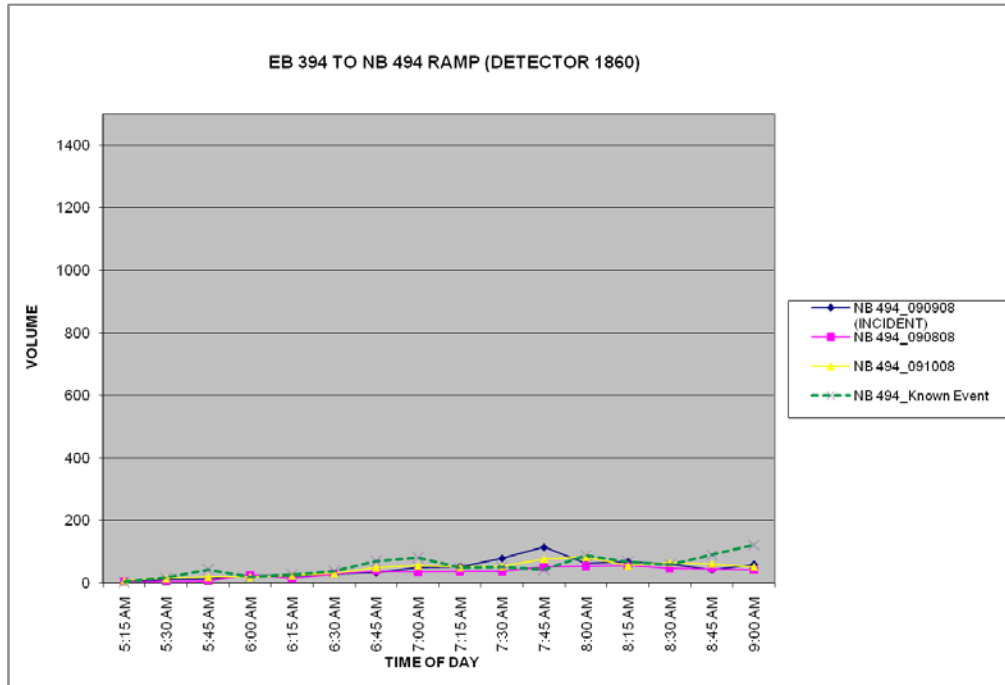


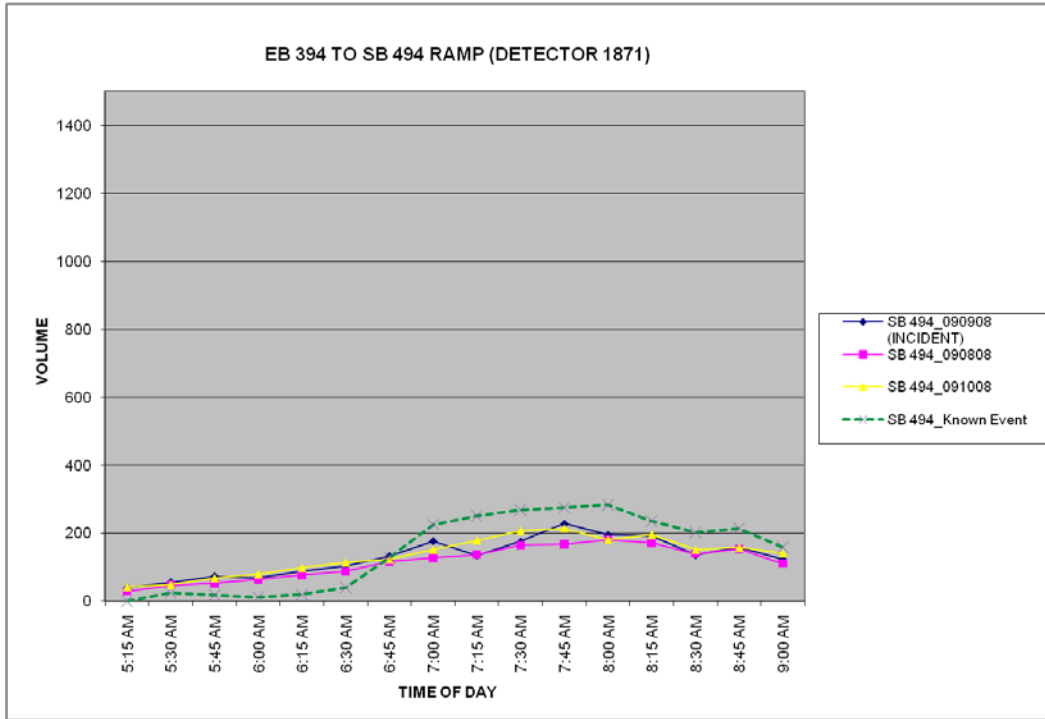
Figure 2-32. EB I-394 TO NB I-494 Ramp

Detector 1860



On the day of the incident, the traffic volume on the EB I-394 to SB I-494 ramp does not show significant change compared to the two reference dates. This implies that there is no evidence that drivers took the diversion route SB on I-494. The simulation slightly overestimated the volume at this ramp, but the overall temporal pattern is consistent.

Figure 2-33. EB I-394 TO SB I-494 Ramp (Detector 1871)



Looking at the NB I-494 to Carlson Parkway data, the field data for all three days show a similar temporal pattern with the peak volumes of about 340 vehicles per 15 minutes (1,300 vhppl). The simulation results follow a very similar temporal pattern between 5:00 a.m. to 7:15 a.m., but slightly underestimate the volume afterward. Nonetheless, the overall order of magnitude and temporal pattern between simulation and field data are comparable.

Northbound I-484 to the Highway 55 ramp does not show noticeable volume changes between the incident date and the reference dates, implying that the incident does not lead to diversions passing through this location to Highway 55. The simulation results appear to underestimate the field data, but the volumes match well from 7:45 a.m. onward.

Figure 2-34. NB I-494 to Carson Parkway Ramp

Detector 2912

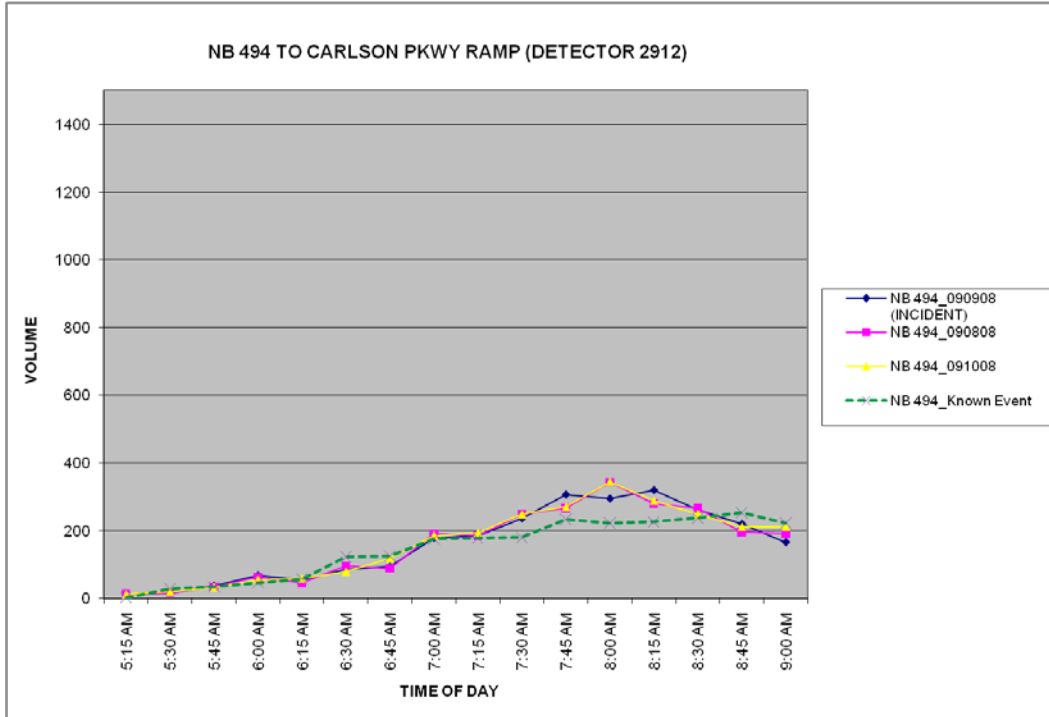
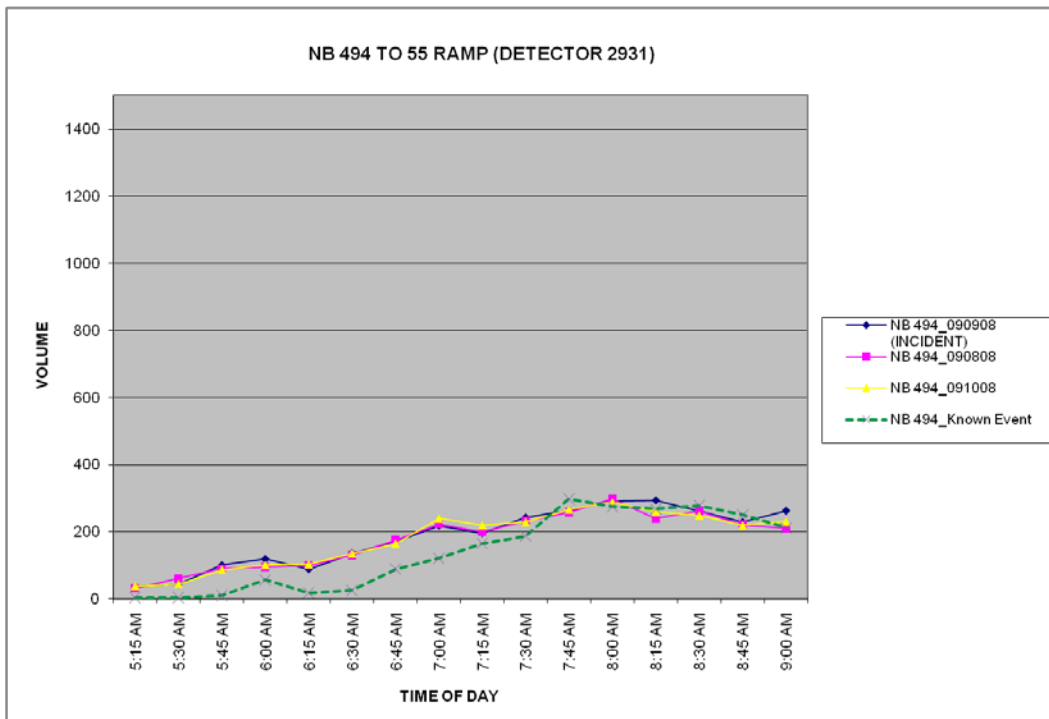


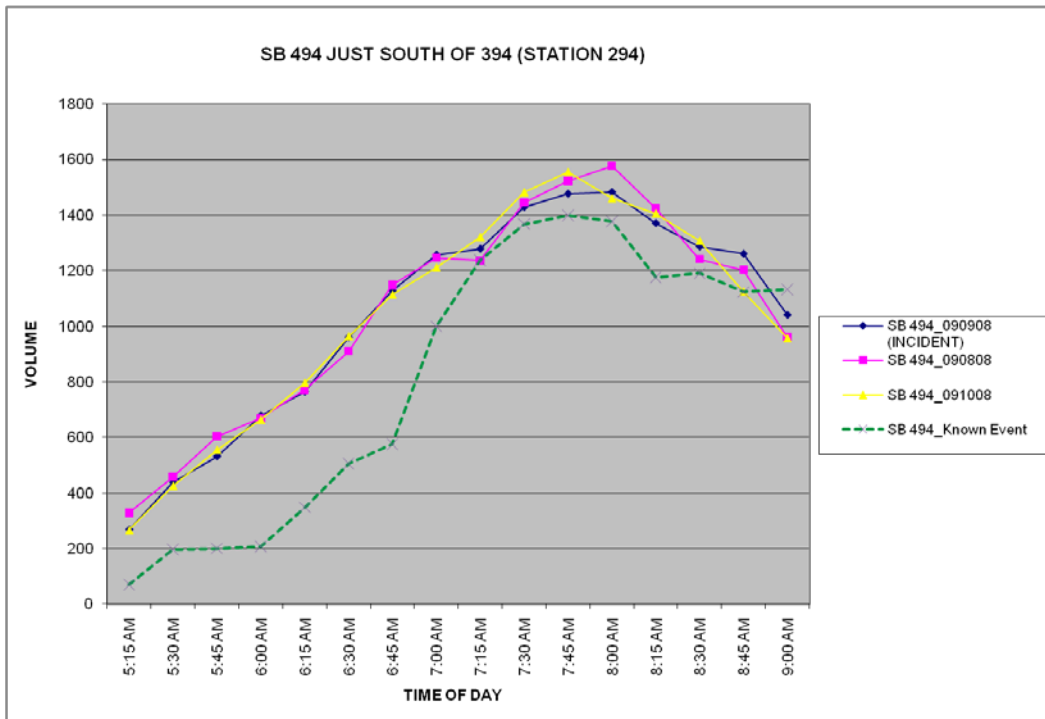
Figure 2-35. NB I-494 to Highway 55 Ramp



In Figure 2-36, the field data show a minor reduction of SB I-494 traffic on the incident data compared to the two reference dates. However, the difference is rather small. The simulated volumes are considerably below the field data prior to 7:30 a.m. The difference becomes much smaller from 7:30 a.m. onward, and the results exhibit similar temporal pattern and magnitude compared with the field data.

Figure 2-36. SB I-494 South of I-394

Station 294



In addition to the speed contour and the flow profiles, a diversion schematic, as shown in Figure 2-37, was developed to illustrate volume changes between the validation (no-incident) and the known incident models. As it can be seen from Figure 2-37, the incident settings in DynusT appear to produce intuitive diversion pattern at the locations where diversion is expected. The diversion appears to be moderate due to the moderate severity and duration of this known incident.

Figure 2-37. Baseline and Incident Case Volume Comparison (Vehicles)

5:30 a.m.-9:00 am.



[Source: Google]

In summary, the simulated speed contour exhibits an analogous pattern compared to the actual field data, indicating that the DynusT simulation results properly reflect the incident situation on the I-394 corridor. The additional flow profiles and volume comparisons in the vicinity of the incident location indicate that the overall simulation results exhibit comparable patterns to the field data.

Finally, Table 2-9 summarizes the U.S. DOT known incident validation guidelines as related to the simulated results.

Table 2-9. Scenario Characteristics and DynusT Running Modes

Scenario	Results
<p>Freeway bottleneck locations: Should be on a modeled segment that is consistent in location, design, and attributes of the representative roadway section.</p>	<p>The incident link has been modeled on the freeway 394 location with consistent geometric and traffic configuration with the actual roadway section.</p>
<p>Duration of incident-related congestion: Duration where observable within 25%.</p>	<p>Comparing Figure 2-28 and 2-29, the simulated incident duration ends at 8:15 a.m., which is consistent with the actual data.</p>
<p>Extent of queue propagation: Should be within 20%.</p>	<p>Comparing Figure 2-28 and 2-29, the simulated and actual queue propagations appear to be consistent.</p>
<p>Diversion flows: Increase in ramp volumes where diversion is expected to take place.</p>	<p>The simulated diversion appears to be comparable with the results examining Figures 2-30 to 2-36.</p>
<p>Arterial breakdown when incident: Cycle failures or lack of cycle failures.</p>	<p>The cycle failure has not been observed in both the actual data and simulation. Concluded from Figures 2-30 to 2-36, this incident induces only moderate amount of diversion, and no severe impact to arterial was expected nor observed.</p>

Chapter 3 Transit

Mode shift in the I-394 Corridor could be influenced by adverse traffic conditions (incidents or heavy demand) or by ICM strategies (such as traveler information systems). Modeling of mode shift requires input of modal travel times, which are calculated by network segment and at key decision points, and cost by mode. Prior to the ICM project, DynusT did not have any capabilities for modeling mode shifts, and transit modeling was limited, primarily to transit vehicles assigned on pre-specified paths (i.e., on fixed routes) with pre-determined dwell times at stops along each route. Travelers assigned to transit, or travelers with intermodal trips (auto access to transit), were not specifically modeled. However, through the ICM effort, UA developed an approach to enhance transit modeling in DynusT, and provided the Minneapolis AMS team with the means to broadly establish transit baseline data for the corridor that could be used to assess potential auto-transit diversions under various incident scenarios.

The approach provides DynusT with the capability to: 1) model mode choice between auto and transit using time-dependent travel times, costs, and other factors affecting the utility of auto and transit; and 2) model transit vehicle loading and usage of park-and-ride lots. One important element is the consideration of distance from the destination, since traveler information could entice users of the corridor to change their mode. For example, travelers may take transit instead of their vehicle, if they receive the information before their departure from home. Alternatively, they may decide to park their car at the nearest park-and-ride lot and switch to transit, if they receive en-trip information of an incident. Finally, they may choose to continue driving if they receive en-trip information of an incident, and they are either close to their destination or driving to the nearest park-and-ride lot significantly increases their time. The approach developed by UA can be summarized as follows:

1. Alternatives are represented by utility functions with three variables measured during simulation – travel time, fare, and accessibility. The travel time attribute applies to both existing and alternate routes and is primarily assessed from experience (e.g., prior UE run), but it could account for available ATIS information.
2. Fare is represented as cents per mile for simplification purpose, but the methodology can accommodate more complicated fare structures.
3. The accessibility measure is measured by two attributes – distance to park-and-ride facility and distance to final destination. The distance to nearby park-and-ride facility can be determined by querying the shortest path algorithm that is regularly executed. In this case, the origin is the location of the vehicle (could be en-trip or pre-trip), and the destination is the park-and-ride facility. Similarly, the distance to the final destination can be calculated by querying the distance label from the shortest path for candidate locations.

The application of the aforementioned approach, though, requires the modeling of individual travelers who are represented in the model in the form of OD tables. As it was indicated in Section 1.2, the vehicular trip table for the I-394 corridor study area was extracted from a DynusT application previously developed for the I-35 Bridge. Transit demand trip tables though were available only through the regional travel demand model, which represents an area significantly larger than the I-394 corridor study area. While the Minneapolis metropolitan planning organization's (MPO) subarea

procedures allow for the extraction of vehicular demand trip table, similar procedures are not available for the transit component of the travel demand model. In addition, on-board surveys that could have been used to develop the transit trip table for the I-394 corridor study area were not available.

Therefore, it was decided to develop transit demand tables for the transit routes associated with park-and-ride facilities, and thus to provide the I-394 corridor model with a baseline transit dataset and the capability to model potential incremental diversions to transit (up to the maximum capacity of the park-and-ride lots) under various incident scenarios. Specifically, during pre- and post-ICM incident scenarios, the baseline transit trip tables will be assigned along with the vehicular trip tables, and the park-and-ride usage will be accumulated. The utility functions representing mode alternatives will be assessed during the simulation either due to pre-trip/en-route information or congestion, and drivers could divert to transit if transit is a more attractive option and the park-and-ride capacity has not been met. Given the relatively low transit utilization in the I-394 corridor, the process is envisioned to be evoked during severe incident congestion.

The development of the transit trip tables was supported by a plethora of data received from Mn/DOT, Metro Transit, Plymouth Metrolink, Southwest Transit, and the Metropolitan Council. These data included the following:

- The transit line file, from CUBE, for the 2006 baseline year;
- The 2008 transit schedules for routes serving the I-394 corridor area, including Metro Transit, Plymouth Metrolink, and Southwest Transit;
- The 2006 TP+ transit OD matrices for local and express routes (separately), and separated by access mode (walk, park-and-ride, and kiss-and-ride);
- The 2008 complete boarding and alighting data, by stop, where automated passenger counters (APC) were available;
- The 2008 total boardings and alightings, aggregated across the full route, for routes without APCs; and
- The locations, number of parking spaces, and average number of spaces used at each of the park-and-ride lots.

The following sections provide a detail description of the various elements required for the development of the OD transit trip tables, as well as an assessment of the estimated park-and-ride utilization.

3.1 Transit Coding

The 2006 CUBE transit line file was obtained from the Metropolitan Council, and the file was in the typical transit line format pertinent to travel demand models. Based on this information, transit routes were coded into DynusT with each possible route variation coded separately by direction (e.g., different branches of a single route or limited and express services). With information provided from the transit line file, the headways, frequencies, distance between stops, dwell times, and departure times of each bus run were added to the routes in DynusT. As a result, individual paths for bus trips in the network are generated within DynusT. This takes the form of a designated vehicle (bus) path in DynusT, with a specified start time from a route terminus.

From the 2008 schedules, the following 47 routes were extracted that are of interest to the I-394 corridor study area:

- **BlueXpress** route: 490;
- **Plymouth Metrolink** routes: 740, 741, 742, 743, 747, 771, 772, 774, 776, 777, 790, 793, and 795;
- **SouthWest Transit** routes: 680, 685, 690, 691, 692, 694, 696, 697, and 698; and
- **Metro Transit** routes: 9, 587, 589, 604, 615, 643, 649, 652, 663, 664, 665, 667, 668, 670, 671, 672, 673, 674, 675, 677, 755, 756, 758 and 764.

Additional effort requiring manual adjustment of the route locations, frequencies, and schedules was needed to adjust the 2006 CUBE transit line file to account for changes in routes between 2006 and the 2008 baseline. Current schedules from Metro Transit, Southwest Transit, and Plymouth Metrolink transit network were also checked to ensure consistency with the routes and schedules in the 2008 baseline.

On the supply side, the simulation requires route “trajectories” (sequences of nodes). Specifically, the simulation requires several files with the same data structure, since they contain information for different time periods (e.g., peak hour, off-peak, night). It was necessary to manually convert each node for each of pertinent routes in the CUBE file into common node numbers from the DynusT network. Table 3-1 shows a sample of the CUBE transit line file structure. (lanes versus three lanes blocked).

Table 3-1. CUBE Transit Line File Structure

Line 672 Westbound

Transit Line
LINE NAME="672W," MODE=7, OWNER="M," ONEWAY=T, FREQ[1]=36, FREQ[2]=0, FREQ[3]=0, N=9196, 12599, 6039, 12585, 12530, 12531, 12596, -12526, 12528, -12529, 12565, -12527, -12547, 12541, -12562, -12570, 12523, -12524, 12580, 5217, 5223, 5224, -8724, 4021, -4022, -4023, -4024, -9686, -9680, -9683, -3699, -9660, -9656, -9677, -9389, -9379, -9373, -9375, 9378, 9368, 9366, 9316, 9361, -9364, -9353, -9359, -9349, -9350, -9357, -9358, -9333, -9336, -9326, -9320, -8851, 6677, 8768, -8440, 8769, 8439, 8771, 4284, -4290, -4291, -5019, -5020, -6487, 6488, 8436

Route 672 westbound, shown in Table 3-1, has three route variations. Figure 3-1 shows the actual schedule for this route, and one may note in the lower right schedule box that the westbound schedule has three possible sequences of time points. Each possible sequence is coded as a route variation (or “Scheme”) within DynusT. In addition, during the transit coding, some issues were encountered and were addressed as follows:

1. In the fall 2006 CUBE file, some bus stop nodes were not listed in the original road network in DynusT. Additional nodes and associated transit routes were created in DynusT to properly reflect the transit route information.
2. The ridership from the APCs for 2008 were used to estimate the transit demand at each stop. Boarding and alighting times were approximated as four seconds for

each boarding and three seconds for alighting to determine total dwell times at each stop.

3. The transit system is essentially a schedule-based system. The actual route schedules (rather than simple frequencies or headways) were coded directly into DynusT.

An example of the full transit route coding in DynusT for Scheme A for Route 672 westbound is shown in Table 3-2. This table shows the sequence of node numbers (i.e., the bus path) for Scheme A in DynusT. It should be noted that there are slight differences when compared to Table 3-1, which could be attributed to: 1) the route was modified slightly between 2006 and 2008; 2) not all nodes from the CUBE line file are included in this route variation; and 3) there were new nodes added to DynusT along this route. Nonetheless, many of the node numbers are similar.

In addition, Table 3-2 includes an indicator for “Stop type”; this value is 1 for timepoints and 0 for other stops along the route. The final line, the “Stop #,” is actually the timepoint number along this route. For comparison with the schedule in Table 3-1, Table 3-3 condenses the full DynusT route representation to simply the timepoints for each of the three route variations (Schemes A, B, and C) for Route 672 westbound.

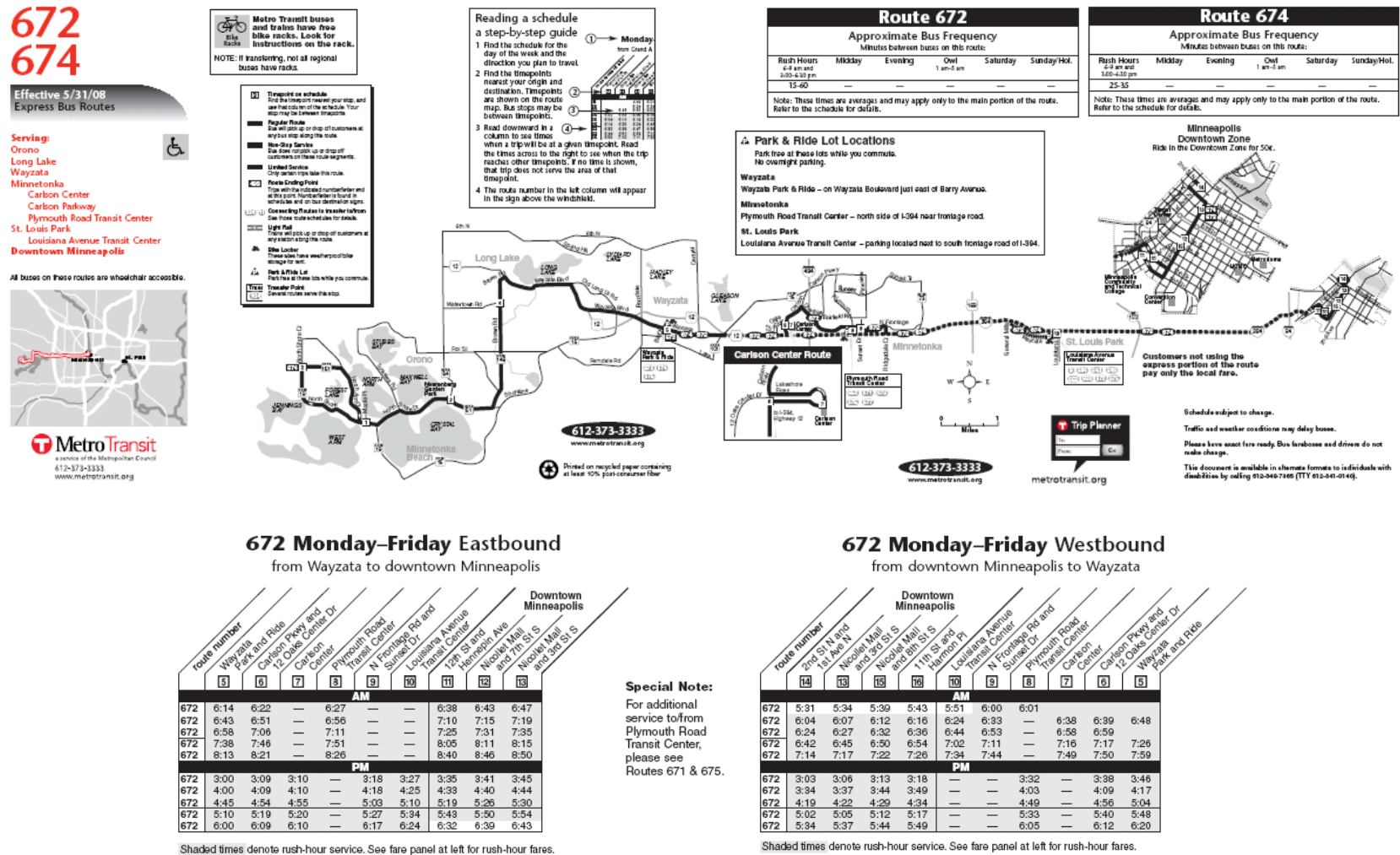
Table 3-2. Route Definition of Line 672 Westbound in DynusT

Scheme A										
Node PK	1	2	3	4	5	6	7	8	9	10
Node Number	12611	12613	9196	9197	12601	6044	12531	12515	12514	12516
Stop type	1	0	0	0	0	0	1	0	0	0
Stop #	14						13			
Node PK	11	12	13	14	15	16	17	18	19	20
Node Number	12517	12518	12524	5217	5224	8724	4022	4023	4024	9686
Stop type	1	0	0	1	0	0	0	0	0	0
Stop #	15			16						
Node PK	21	22	23	24	25	26	27	28	29	30
Node Number	9680	9683	3699	9660	9656	9677	17355	9389	9379	9372
Stop type	0	0	0	0	0	0	0	0	0	0
Stop #										
Node PK	31	32	33	34	35	36	37	38	39	40
Node Number	9365	17354	9361	9316	9366	9368	9366	9316	9361	17354
Stop type	0	0	0	0	0	1	0	0	0	0
Stop #						10				
Node PK	41	42	43	44	45	46	47	48	49	50
Node Number	9364	9353	9359	9349	9350	9357	9358	9847	9848	9850
Stop type	0	0	0	0	0	0	0	0	0	0
Stop #										
Node PK	51	52	53	54	55	56				
Node Number	9853	9326	9328	8443	8851	6677				
Stop type	0	1	1							
Stop #		9	8							

Table 3-3. Timepoint Definition in DynusT for Route 672 Westbound

Route ID: 672		Route Type: 1							
West	DynusT Node								
	Stop 14	Stop 13	Stop 15	Stop 16	Stop 10	Stop 9	Stop 8	Stop 7	Stop 6
Scheme A	12611	12531	12517	5217	9368	9326	9328		
Scheme B	12611	12531	12517	5217	9368	9326	9326	9328	4290
Scheme C	12611	12531	12517	5217	9368	9326	9326	9328	

Figure 3-1. Transit Schedule for Line 672



[Source: ©MetroTransit.]

3.2 Transit OD Matrices

The DynusT version utilized during the initial validation stages did not have a transit component and therefore no attempt was made to validate the model for transit volumes. Nevertheless, a tool was needed to identify the current park-and-ride lot utilization and how it may change due to the ICM scenarios. As such, the current transit demand was estimated for 39 out of the 47 routes in the I-394 corridor, utilizing Origin-Destination Matrix Estimation (ODME) techniques, and parking utilization was derived from the estimated alighting and boarding volumes. These 39 routes were selected because they serve a park-and-ride lot in the corridor (the remaining 8 routes do not serve a park-and-ride lot). Routes for which OD matrices were estimated included the following:

- Seventeen (17) routes that had APC data (boarding and alighting counts at each stop): 9, 589, 643, 649, 652, 663, 665, 667, 668, 671, 672, 673, 674, 675, 677, 758, and 764.
- Twenty-two (22) routes that only had total ridership counts: 490, 604, 615, 664, 670, 680, 685, 690, 691, 692, 694, 696, 697, 740, 741, 747, 771, 772, 776, 777, 790, and 793.

Generally, the APC data give the stop names, the number of passengers boarding, the number of passengers alighting, and the resulting bus loads by vehicle trip (or “run”) from the fall of 2008. Where both boardings and alightings by stop were available for a bus route, a transit OD matrix was generated using the method of [5] as elaborated in [6]. For these routes, the OD matrix is actually an assignment of trips to an origin stop and a destination stop; this is a so-called “unlinked” transit trip, since the true passenger origins and destinations, and any route-to-route transfers, are not known.

For the 22 routes where only the total boardings and alightings are given, there is no specific reference to the stop where passengers boarded or alighted. For park-and-ride routes, these data were deemed useful, in that one might assume that the boardings occurred primarily at the park-and-ride lots and that the alightings occurred downtown, or wherever the route ended. Yet, assumptions had to be made as to the geographic distribution of boardings and alightings for this data. Lacking more detailed information, it was assumed that the total boardings were uniformly distributed among likely park-and-ride lots (e.g., if there were 16 boardings and 2 park-and-ride lots, it was assumed 8 boardings at each lot). A similar assumption of a uniform distribution was made for alightings among likely destinations (i.e., stops downtown or at specific route termini). Under these assumptions, it was possible to generate route-level OD matrices, using the method of [5] as elaborated in [6].

Finally, in some cases, there were some local routes with total boardings and alightings, but again without reference to the stop where passengers boarded or alighted. In these cases, it was not possible to ascertain the distribution of boardings and alightings along the route, and therefore OD matrices for these routes were not generated.

3.3 Park-and-Ride Utilization

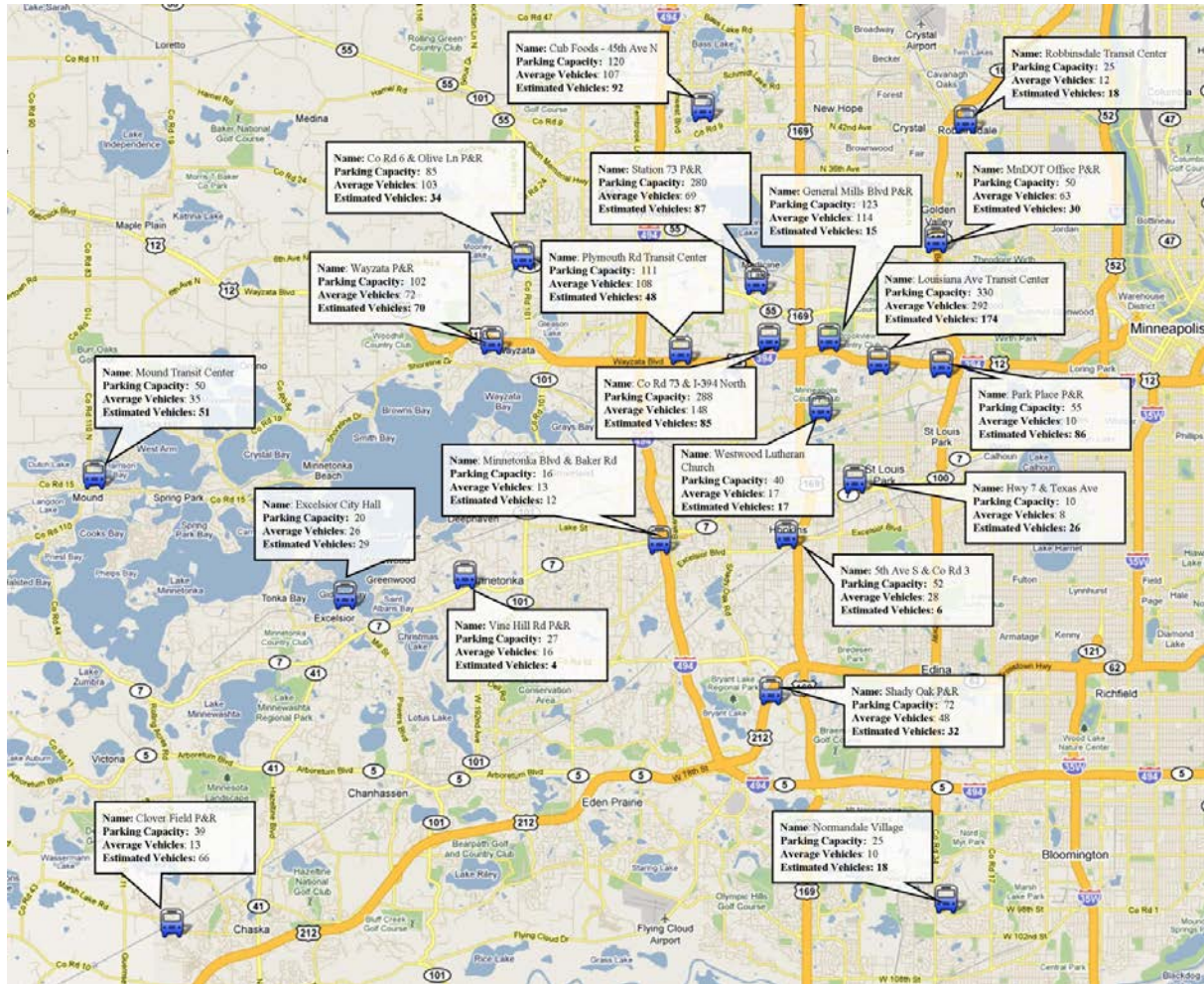
Existing capacity, and usage for these park-and-ride lots was provided by Mn/DOT and is shown in Figure 3-2, as the “Parking Capacity” and “Average Vehicles,” respectively. Estimated usage was calculated based on boardings, as estimated from the OD matrices developed in Section 3.2 based on the assumption that

90 percent of the transit riders will arrive by car to the park-and-ride lots; and the remaining 10 percent will arrive by walking, bicycling, kiss-and-ride, or other transit feeder services. In addition, for those vehicles parking in the park-and-ride lot, an average occupancy of 1.2 persons per vehicle was assumed. Based on these assumptions, the estimated demand (vehicles) is 1,000 compared to average usage of 1,312.

For the purposes of modeling transit diversions during an incident, the primary concern is in the availability of spaces in the park-and-ride lots, particularly along the I-394 corridor. Given the relatively low transit utilization along the I-394 corridor, the methodology outlined below is envisioned to be used in analyzing the park-and-ride utilization during major incident scenarios.

- The transit OD tables developed in Section 3.2 will be used to establish a temporal utilization profile for the park-and-ride lots.
- For each OD transit trip table, it will be assumed that 80 percent arrive by car with 1.3 occupants per car. These vehicles will be emitted to the park-and-ride lots based on the temporal distribution established for the specific OD table.
- DynusT will keep track of the park-and-ride utilization by interval.
- DynusT will evaluate the utility function of the drivers in the network to see if transit is more attractive. If the transit option is more attractive and a parking space is available, then travelers could shift mode.

Figure 3-2. Park-and-Ride Lot Average versus Estimated Usage (Vehicles)



[Source: Google Maps.]

References

1. Chiu, Y.-C., J. Bottom, M. Mahut, A. Paz, R. Balakrishna, T. Waller, and J. Hicks, A Primer for Dynamic Traffic Assignment, 2010, Washington, D.C., Transportation Research Board.
2. Mn/DOT, Traffic Data Extract, 2009 [cited 2009, Available from <http://data.dot.state.mn.us/datatools/dataextract.html>].
3. Mn/DOT, All Detector Report, 2009, Available from <http://www.dot.state.mn.us/tmc/trafficinfo/downloads/adr.pdf>.
4. Cambridge Systematics, Inc., AMS Analysis Plan for Pioneer Corridor I-394 in Minneapolis, Minnesota (Final Draft), 2009, U.S. DOT: Oakland.
5. Carey, M., C. Hendrickson, and K. Siddarthan, A Method for Direct Estimation of Origin/Destination Trip Matrices, *Transportation Science*, 1981, 15(1): p. 32-49.
6. Tavana, H., and H. S. Mahmassani, Estimation of Dynamic Origin-Destination Flows from Sensor Data Using Bi-Level Optimization Method, in 82nd Annual Meeting of Transportation Research Board, 2001, Washington, D.C.
7. Lundgren, J. T., and A. Peterson, A Heuristic for the Bilevel Origin-Destination-Matrix Estimation Problem, *Transportation Research Part B: Methodological*, 2008, 42(4): p. 339.
8. Zhou, X., and H. S. Mahmassani, A Structural State Space Model for Real-Time Traffic Origin-Destination Demand Estimation and Prediction in a Day-to-Day Learning Framework, *Transportation Research Part B: Methodological*, 2007, 41(8): p. 823-840.
9. Yang, H., and J. Zhou, Optimal Traffic Counting Locations for Origin-Destination Matrix Estimation, *Transportation Research Part B: Methodological*, 1998, 32(2): p. 109-126.
10. Bell, M. G. H., The Estimation of An Origin-Destination Matrix from Traffic Counts, *Transportation Science*, 1983, 17(2): p. 198-217.
11. Lo, H.P., N. Zhang, and W. H. K. Lam, Estimation of An Origin-Destination Matrix With Random Link Choice Proportions: A Statistical Approach, *Transportation Research Part B: Methodological*, 1996, 30(4): p. 309-324.
12. Lin, P.-W., and G.-L. Chang, A Generalized Model and Solution Algorithm for Estimation of the Dynamic Freeway Origin-Destination Matrix, *Transportation Research Part B: Methodological*, 2007, 41(5): p. 554-572.
13. Zhou, X., and H. Mahmassani, Dynamic Origin-Destination Demand Estimation Using Automatic Vehicle Identification Data, *IEEE Transactions on Intelligent Transportation Systems*, 2006, 7(1): p. 105-114.
14. Lin, P.-W., and G.-L. Chang, Modeling Measurement Errors and Missing Initial Values in Freeway Dynamic Origin-Destination Estimation Systems, *Transportation Research Part C: Emerging Technologies*, 2006, 14(6): p. 384-402.
15. Zhou, X., Dynamic Origin-Destination Demand Estimation and Prediction for Off-Line and on-Line Dynamic Traffic Assignment Operation, in *Civil Engineering*, 2004, University of Maryland: College Park, p. 174.
16. Song, H., Dynamic Traffic Assignment and Estimation and Prediction of Dynamic Origin-Destination Flows, in *Department of Automation Science and Technology*, 2004, Xi'an Jiaotong University: Xi'an.

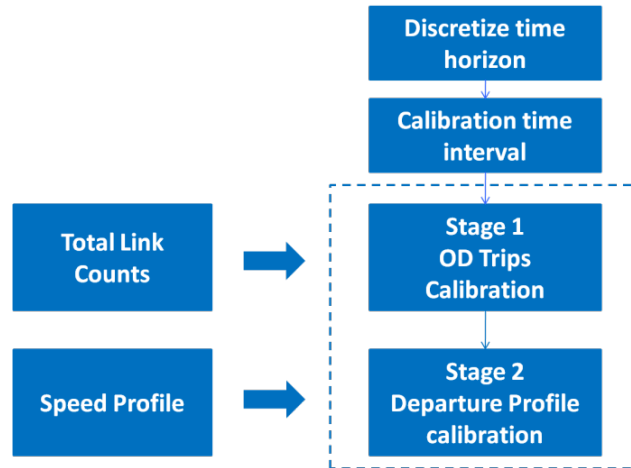
17. Zhou, X., X. Qin, and H. Mahmassani, Dynamic Origin-Destination Demand Estimation with Multiday Link Traffic Counts for Planning Applications, *Transportation Research Record: Journal of the Transportation Research Board*, 2003, 1831: p. 30-38.
18. Lin, Y., Dynamic Origin-Destination Matrix Estimation and Its Application in Intelligent Transportation Systems, in *Automation Science and Technology*, 2003, Xi'an Jiaotong University: Xi'an.
19. Van der Zijpp, N. J., and C. D. R. Lindveld, Estimation of Origin-Destination Demand for Dynamic Assignment With Simultaneous Route and Departure Time Choice, *Journal of the Transportation Research Board*, 2001, 1771(75-82).
20. Tavana, H., Internally-Consistent Estimation of Dynamic Network Origin-Destination Flows from Intelligent Transportation Systems Data Using Bi-Level Optimization, in *Department of Civil Engineering*, 2001, University of Texas at Austin: Austin.
21. Sherali, H. D., and T. Park, Estimation of Dynamic Origin-Destination Trip Tables for a General Network, *Transportation Research Part B: Methodological*, 2001, 35(3): p. 217.
22. Wu, J., and G.-L. Chang, Estimation of Time-Varying Origin-Destination Distributions With Dynamic Screenline Flows, *Transportation Research Part B: Methodological*, 1996, 30(4): p. 277-290.
23. Sherali, H. D., N. Arora, and A. G. Hobeika, Parameter Optimization Methods for Estimating Dynamic Origin-Destination Trip-Tables, *Transportation Research Part B: Methodological*, 1997, 31(2): p. 141.
24. Yang, H., T. Sasaki, Y. Iida, and Y. Asakura, Estimation of Origin-Destination Matrices from Link Traffic Counts on Congested Networks, *Transportation Research Part B: Methodological*, 1992, 26(6): p. 417.
25. Chiu, Y.-C., X. Zhou, and J. Hernandez, Evaluating Urban Downtown One-Way to Two-Way Street Conversion Using a Multiple Resolution Simulation and Assignment Approach, *ASCE Journal of Urban Planning and Development*, 2007, 133(4): p. 222-232.
26. Chiu, Y.-C., E. Nava, H. Zheng, and B. Bustillos, *DynusT User's Manual* (<http://dynust.net/wikibin/doku.php>), 2008.
27. Roess, R. P., E. S. Prassas, and W. McShane, *Traffic Engineering*, Third Edition, 2004.

Appendix A. Time-Dependent Origin-Destination Matrices Calibration Methodology

The OD estimation and calibration problem has long been studied, but most of the solution approaches suffer from two main drawbacks. First, most of the existing studies focus on matching link counts [5-11]. It is widely known that traffic counts are not the suitable congestion descriptor as a flow rate figure corresponds to two different traffic states – free-flow and congested situations. Matching traffic counts do not necessarily lead to a proper match of congestion patterns. Instead, the resulting traffic condition could be quite opposite and counterintuitive. For example, if the simulation model yields fewer counts than the actual data, two explanations are possible: 1) the model OD trips are fewer than they should be in reality, or 2) the model OD trips are much more frequent than the actual trips so the model experiences more severe congestion as well as a lower flow rate.

The second drawback of the existing approaches is that estimating time-dependent OD matrices has been limited to a small network or short time periods due to the explosive problem size. There is no guarantee that the traffic dynamics, such as congestion patterns, can be properly captured by these dynamic OD estimation methods as all these methods focus on matching link counts, incurring the same aforementioned issues [6, 12-22].

The OD calibration method adopted in this ICM study is an innovative approach that circumvents the above issues. The proposed method is a two-stage approach in which the total link count over an extensive time period is matched by solving an optimization model aiming at minimizing the link count deviations. Once the period-long OD matrix is determined, the second stage approach is initiated to update the departure time pattern of the time-dependent OD matrices such that the simulated speed profile properly reflects the actual observations (see Figure A-1).

Figure A-1. Two-Stage OD estimation Framework

Stage 1 Calibration – Match Total Counts

The method presented in this research can be regarded as the bi-level formulation classified by Lundgren and Peterson [7], with the upper-level problem being the minimizing link count deviation problem and the lower-level problem being the dynamic traffic assignment (DTA) problem. The proposed formulation departs from the literature in that the upper-level problem seeks to minimize the absolute difference between the estimated and actual link counts via a one-norm formulation instead of the two-norm (least-square) formulation. Moreover, unlike other prior formulations that minimize the weighted measures of deviation from the base matrix and from the observed counts [7, 21, 23-25], the deviations between the calibrated and the base OD matrices were constrained in the constraint set instead of being specified in the upper-level objective function. These constraints include user-specified tolerable deviations for zone pairs, as well as for total trips. This formulation strategy achieves minimal link count discrepancies while maintaining tolerated deviation between the calibrated and the base OD matrices. Most importantly, this strategy facilitates a transformed linear programming (LP) upper-level formulation that can be solved effectively for a large network.

The lower-level problem is a DTA problem that seeks to obtain the equilibrium assignment matrix or the route choice proportion information. The DTA model used in this study is DynusT [26] with MIVA implementation capable of extended time period simulation and assignment.

It is noteworthy that the proposed OD calibration method includes simultaneous calibration of truck and auto OD matrices. Many planning agencies generate separate auto and truck OD matrices, and autos and trucks are known to have different spatial and temporal distribution patterns. Further, in calibrating the time-dependent OD matrices for autos and trucks, the proportion of total trips allocated to each OD demand time interval was assumed to follow those in the base OD matrices. Doing so ensured that the problem size was manageable while the temporal pattern followed that in the base OD matrices.

Model Formulation

The mathematical notations and model of the OD calibration problem is discussed as follows:

Notations:

N :	Set of OD pairs to which the screen-line counts relates; this is determined by retrieving the volume from the screen-line links after the initial equilibrium procedure and tracing their paths back to their respective OD matrix
M :	Set of screen-line links
$d_{k,n}^a$:	Auto vehicle counts on screen-line link k from OD pair n , determined by the DTA model at the equilibrium
$d_{k,n}^c$:	Truck vehicle counts on screen line link k from OD pair n , determined by the DTA model at the equilibrium
r_n^a :	Number of daily auto trips for OD pair n in the initial OD matrix
r_n^c :	Number of daily truck trips for OD pair n in the initial OD matrix
$r_n^{t,a}$:	Number of auto trips for OD pair n in OD interval t in the initial OD matrix
$r_n^{t,c}$:	Number of truck trips for OD pair n in OD interval t in the initial OD matrix
$r_n^{t,a,l}$:	Number of auto trips for OD pair n in OD interval t in the initial OD matrix estimated at iteration l , $l = 0$ is for initial zonal OD trips
$r_n^{t,c,l}$:	Number of truck trips for OD pair n in OD interval t in the initial OD matrix estimated at iteration l , $l = 0$ is for initial zonal OD trips
x_n^a :	Number of estimated auto trips for OD zone pair n , decision variable
x_n^{ac} :	Number of estimated truck trips for OD zone pair n , decision variable
g_m^a :	Field observed auto counts on link m
g_m^{ac} :	Field observed truck counts on link m
g_m :	Field observed total counts on link m
α^a, α^c :	User-specified tolerable OD zone pair trip deviation percentage for autos and trucks respectively
β^a, β^c :	User-specified tolerable total trip deviation percentage for autos and trucks respectively
λ :	Passenger car equivalent for trucks

The proposed formulation modeling process starts from the algebraic expression of the one-norm linear problem as stated in objective function below:

$$\text{Minimize } \sum_{m=1}^{|M|} \left\{ \left| \sum_{n=1}^{|N|} \left(\frac{d_{mn}^a}{r_n^a} x_n^a \right) - g_m^a \right| + \left| \sum_{n=1}^{|N|} \left(\frac{d_{mn}^c}{r_n^c} x_n^c \right) - g_m^c \right| \right\}$$

The first term of objection function is the absolute value of the auto count deviation and the second is count deviation for trucks. In the case that a truck OD matrix is available but not the link count (e.g.,

typical permanent count station may not produce separate auto and truck counts), the objective function above may be revised as:

$$\text{Minimize } \sum_{m=1}^{|M|} \left\{ \left[\sum_{n=1}^{|N|} \left(\frac{d_{mn}^a}{r_n^a} x_n^a \right) + \lambda \cdot \sum_{n=1}^{|N|} \left(\frac{d_{mn}^c}{r_n^c} x_n^c \right) \right] - g_m \right\}$$

The one-norm minimization objective function can be reformulated to be objective function (1) plus four constraints (2) through (5) by introducing slack variables h_m^a and h_m^c as shown below.

$$\text{Minimize } \sum_{m=1}^{|M|} (h_m^a + h_m^c) \quad (\text{Equation 1})$$

$$\sum_{n=1}^{|N|} \left(\frac{d_{mn}^a}{r_n^a} x_n^a \right) - g_m^a \leq h_m^a \quad (\text{Equation 2})$$

$$-\left[\sum_{n=1}^{|N|} \left(\frac{d_{mn}^a}{r_n^a} x_n^a \right) - g_m^a \right] \leq h_m^a \quad \forall m = 1, \dots, |M| \quad (\text{Equation 3})$$

$$\left[\sum_{n=1}^{|N|} \left(\frac{d_{mn}^c}{r_n^c} x_n^c \right) - g_m^c \right] \leq h_m^c \quad \forall m = 1, \dots, |M| \quad (\text{Equation 4})$$

$$-\left[\sum_{n=1}^{|N|} \left(\frac{d_{mn}^c}{r_n^c} x_n^c \right) - g_m^c \right] \leq h_m^c \quad \forall m = 1, \dots, |M| \quad (\text{Equation 5})$$

Next, from equations (Equation 2) and (Equation 4) two new slack variables v_m^a and v_m^c are introduced to yield equations (Equation 6) and (Equation 7).

$$\sum_{n=1}^{|N|} \left(\frac{d_{mn}^a}{r_n^a} x_n^a \right) - g_m^a - h_m^a + v_m^a = 0 \quad \forall m = 1, \dots, |M| \quad (\text{Equation 6})$$

$$\sum_{n=1}^{|N|} \left(\frac{d_{mn}^c}{r_n^c} x_n^c \right) - g_m^c - h_m^c + v_m^c = 0 \quad \forall m = 1, \dots, |M| \quad (\text{Equation 7})$$

Substitute h_m^a and h_m^c in equations (Equation 1) through (Equation 5) with

$$h_m^a = \sum_{n=1}^{|N|} \left(\frac{d_{mn}^a}{r_n^a} x_n^a \right) - g_m^a + v_m^a = 0 \quad \text{and} \quad h_m^c = \sum_{n=1}^{|N|} \left(\frac{d_{mn}^c}{r_n^c} x_n^c \right) - g_m^c + v_m^c$$

from (Equation 6) and (Equation 7), Equations (Equation 1) through (Equation 5) become (Equation 8) through (Equation 10)

and (Equation 16). The final complete model is presented in equations (Equation 8) through (Equation 18). Equation (Equation 8) is the transformed linear objective function equivalent to the original one-norm formulation. Equations (Equation 11) and (Equation 12) include constraints that ensure the estimated number of trips for each OD pair does not deviate from the user-specified ratio α . Equations (Equation 13) and (Equation 14) represent the constraints ensuring that the estimated total auto trips and truck trips do not deviate from a user-defined ratio β . Equations (19) and (20) are non-negativity constraints. Equation (21) indicates that α or β values are between 0.0 and 1.0. Equation (22) represents a TDUETA process that maps the OD to the screen-line link counts.

$$\text{Minimize } \sum_{m=1}^{|M|} \left\{ \left[\sum_{n=1}^{|N|} \left(\frac{a_{mn}^a}{r_n^a} x_n^a \right) - g_m^a + v_m^a \right] + \left[\sum_{n=1}^{|N|} \left(\frac{a_{mn}^c}{r_n^c} x_n^c \right) - g_m^c + v_m^c \right] \right\} \quad (\text{Equation 8})$$

Subject to:

$$-2 \left[\sum_{n=1}^{|N|} \left(\frac{a_{mn}^a}{r_n^a} x_n^a \right) - g_m^a \right] - v_m^a \leq 0 \quad \forall m = 1, \dots, |M| \quad (\text{Equation 9})$$

$$-2 \left[\sum_{n=1}^{|N|} \left(\frac{a_{mn}^c}{r_n^c} x_n^c \right) - g_m^c \right] - v_m^c \leq 0 \quad \forall m = 1, \dots, |M| \quad (\text{Equation 10})$$

$$(1 - \alpha^a) r_n^a \leq x_n^a \leq (1 + \alpha^a) r_n^a \quad \forall n = 1, \dots, |N| \quad (\text{Equation 11})$$

$$(1 - \alpha^c) r_n^c \leq x_n^c \leq (1 + \alpha^c) r_n^c \quad \forall n = 1, \dots, |N| \quad (\text{Equation 12})$$

$$(1 - \beta^a) \sum_{n=1}^{|N|} r_n^a \leq \sum_{n=1}^{|N|} x_n^a \leq (1 + \beta^a) \sum_{n=1}^{|N|} r_n^a \quad (\text{Equation 13})$$

$$(1 - \beta^c) \sum_{n=1}^{|N|} r_n^c \leq \sum_{n=1}^{|N|} x_n^c \leq (1 + \beta^c) \sum_{n=1}^{|N|} r_n^c \quad (\text{Equation 14})$$

$$x_n^a, x_n^c \geq 0 \quad \forall n = 1, \dots, |N| \quad (\text{Equation 15})$$

$$v_m^a, v_m^c \geq 0 \quad \forall m = 1, \dots, |M| \quad (\text{Equation 16})$$

$$1.0 \geq \alpha \geq 0, 1.0 \geq \beta \geq 0 \quad (\text{Equation 17})$$

$$G = \vartheta(x_n^a, x_n^c, \forall n \in N) \quad (\text{Equation 18})$$

It should be noted that problems (Equation 8) through (Equation 18) determine the optimal zonal OD adjustment for the entire analysis period. This adjustment is allocated to each time-varying OD matrix by distributing x_n^a following the temporal distribution of each OD matrix, that is

$r_n^{t,a} = x_n^a \left(r_n^{a,t,l=0} | r_n^a \right)$ where $r_n^a = \sum_t r_n^{a,t,l=0}$. This means that the temporal patterns of the time-varying OD matrices are maintained. Calibrating the temporal pattern to match the field observed speed profile or density is out of the scope and is omitted from the discussions herein.

Calibration Procedure

As depicted in Figure A-2, the calibration procedure consists of solving for the master one-norm problem, as well as solving a sub-DTA problem. The overall algorithmic steps are briefly discussed below.

Step 0: Set iteration counter $l=0$

Initialization, preparing all input data for DynusT and link count G

Step 1: Set iteration counter $l = l + 1$

Utilize DynusT to perform DTA using the base auto and truck OD matrices. Obtain the output (vehicles and their associated path OD pair).

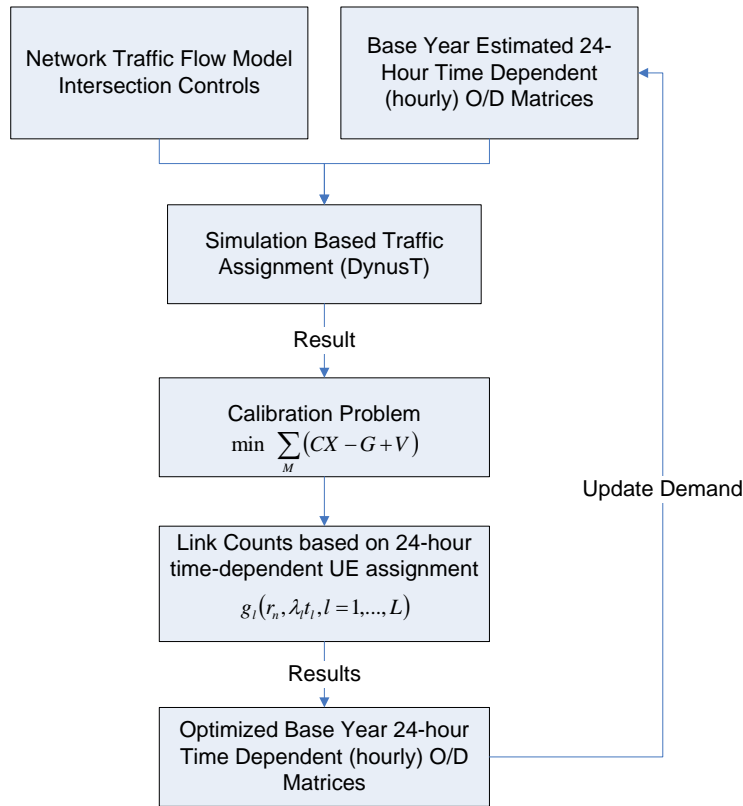
Step 2: Convergence check. Stop if the maximum number of iterations is reached or the convergence criterion is met; otherwise, proceed to Step 3.

Step 3: Prepare all matrix transformations to the standard forms shown in problems (12) through (22).

Step 4: Utilize the optimization solver to solve problems (12) through (22) to obtain the estimated x_n^a, x_n^c for both autos and trucks.

Step 5: Obtain the estimated OD matrices using x_n^a and x_n^c . Update new time-dependent zonal auto trips to be $r_n^{t,a,l=1} = r_n^{a,1}(r_n^{a,t,l=0} | r_n^a)$, and time-dependent zonal truck trips to be $r_n^{t,c,l+1} = x_n^{c,l}(r_n^{c,t,l=0} | r_n^c)$.

Step 6: Go to Step 1.

Figure A-2. OD Demand Calibration Framework

Once the calibration procedure is completed, a single OD matrix for the entire analysis period is obtained. At this point, the Stage 2 calibration is initiated.

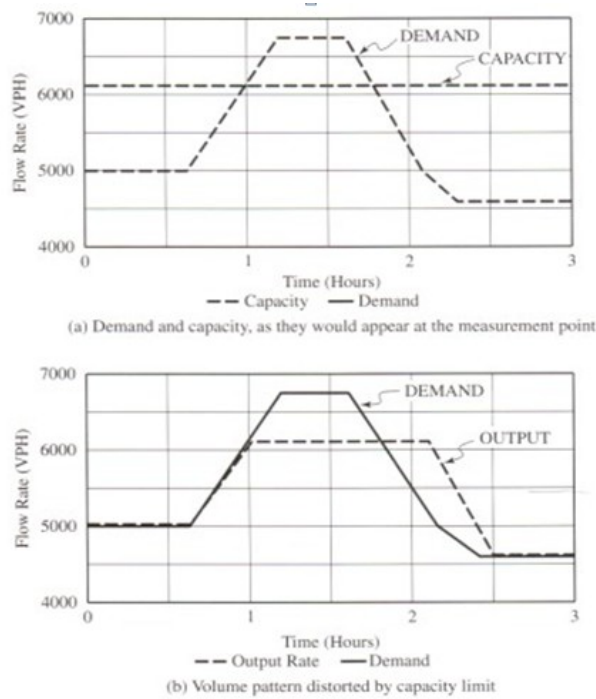
Stage 2 Calibration – Match Speed Profile

After Stage 1 calibration, the total simulated and actual link counts may match well at the analysis period level, but the congestion pattern (e.g., speed or density figures) may still exhibit distinct discrepancies. The purpose of Stage 2 calibration is to adjust the departure pattern based on Stage 1 calibrated OD matrices. After calibration, the total link counts over the analysis period will remain unchanged, but the OD matrices departure pattern will be updated so that after the simulation, the simulated and field observed speed profiles become comparable. The basic concept of Stage 2 calibration is that under congestion, the observed flow rate is actually lower than demand because the observed flow rate is subject to the reduced capacity as shown in Figure A-3. Here *demand* is defined as the number of trips wanting to arrive at the link at a certain time instance, but the actual throughput would be less than demand if demand exceeds capacity of this link. In reality, once this demand/supply imbalance occurs, the speed decreases (and density increases).

However, such demand is unobservable as the traffic data is the observed traffic condition subject to the constraint of the available capacity. The main contribution of this proposed method is to devise an intuitive and theoretically sound approach based on shockwave theory and mapping matrix between the OD and link traffic through DTA – DynusT. The proposed Stage 2 calibration method is aimed at

estimating the demand arriving at the location of interest where a bottleneck is observed, and then linking arriving demand to departing trips, thus updating the time-dependent OD matrices.

Figure A-3. Relationship between Demand, Capacity and Observed Flow [27]



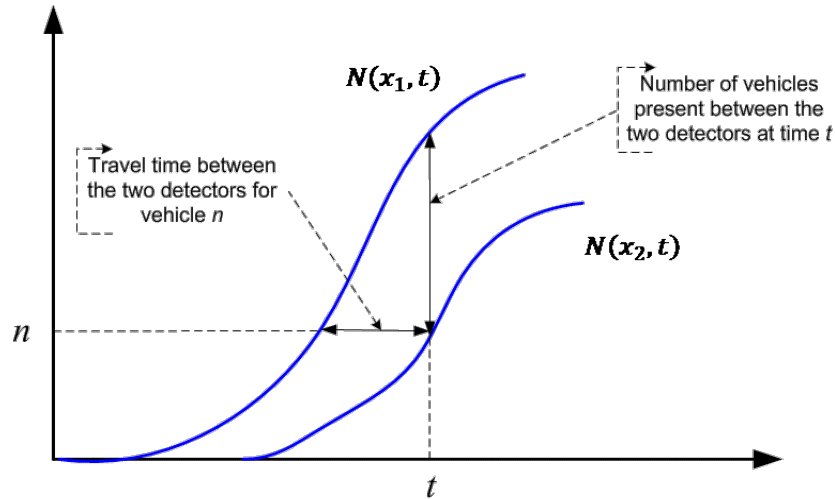
Model Formulation

Cumulative Curves

A typical single- or dual-loop detector (or sensor) generally reports counts, average speed, and occupancy for a pre-specified time period such as 30 seconds. If the count data are processed so that the cumulative count at time t is the sum of all counts in all preceding time steps, then this data is called “cumulative counts” and the curve describing time-varying cumulative counts is called the “cumulative curve.” Mathematically the cumulative count at time T can be expressed by taking the integral of the flow rate over time $[t_0, T]$ as expressed in Equation (Equation 19), where $q^{(t)}$ is the flow rate at time t and t_0 is the start time of data collection.

$$N(T) = \int_{t_0}^T q(t) dt \tag{Equation 19}$$

The cumulative curves representing one upstream and one downstream detector can be illustrated in Figure A-4. Curve $N(x_u, t)$ represents the cumulative flow for the upstream detector located at location x_u . Curve $N(x_d, t)$ represents the cumulative flow for the downstream detector located at location x_d .

Figure A-4. Cumulative Curves for an Upstream Detector and Downstream Detector


Assuming that the distance between the upstream and downstream detector is L , the average density for the link segment between these upstream and downstream detectors at time t can be determined as:

$$k_{x_u \rightarrow x_d}(t) = \frac{N(x_u, t) - N(x_d, T)}{L} \quad (\text{Equation 20})$$

Estimation of Arriving N Curve and Demand Curve

To simplify the discussion, we assume three locations on the one-way uninterrupted roadway. They are denoted as follows and considered congested situations.

- **Location 1.** Upstream end of the roadway, where vehicles are loaded to travel downstream;
- **Location 2:** Location of the fullest extent of the queue propagated from Location 1; and
- **Location 3:** Bottleneck location.

The capacity for the segment from Locations 1 to 2 is assumed to be higher than that at Location 3. Vehicles depart at Location 1 at time-varying rate, some of which exceeds the Location 3 capacity. As a result, when the arriving flow at Location 3 exceeds capacity, queue will be formed and start to propagate upstream.

Because slow-moving vehicles occur only between Locations 2 and 1, the traffic condition between Locations 1 and 2 is free-flowing. This means that the N -curve for Location 2 and that for Location 1 are of identical shape and in parallel to each other. Mathematically, we can express their relationship as follows:

$$N(x_1, t) = N(x_2, t + \Delta t) \quad (\text{Equation 21})$$

where Δt is the free-flow travel time from Location 3 to Location 2.

Rewrite Equation (Equation 20), we have:

$$N(x_2, t) - N(x_3, t) = k_{x_2 \rightarrow x_3}(t)L \quad (\text{Equation 22})$$

By definition, Location 2 is where the fullest extent of the slow-moving queue occurs. The length of the slow-moving queue can be calculated by taking the maximum of the integral of the backward moving shockwave created between the slow-moving queue state and the free-flow arriving flow state. In other words, we have:

$$L = \max_i \left\{ \int_{t_0}^{t_i} \omega(t) dt \mid i = 1, 2, \dots, I \right\} \quad (\text{Equation 23})$$

Where the shockwave speed takes the form of:

$$\omega(t) = \frac{q(x_2, t) - q(x_3, t)}{k(x_2, t) - k(x_3, t)} \quad (\text{Equation 24})$$

Once L is determined the relationship between x_2 and x_3 can be determined, that is:

$$x_3 = x_2 + L$$

Thus, from Equations (Equation 21) and (Equation 22), we could estimate the N -curve at Location 1 to be:

$$N(x_1, t) = N(x_2, t + \Delta t) = N(x_3, t + \Delta t) + k_{x_2 \rightarrow x_3}(t + \Delta t) \cdot \max_i \left\{ \int_{t_0}^{t_i} \omega(t) dt \mid i = 1, 2, \dots, I \right\} \quad (\text{Equation 25})$$

In Equation (25), $N(x_3, t)$ is field measured. L can be calculated by Equation (23), and apply Equation (24) with field measured $q(x_2, t)$ and $q(x_3, t)$ and $k(x_2, t)$ and $k(x_3, t)$.

First, assume the time period to be $[0, T]$ it's clear that we have:

$$N(x_1, T) = \int_{t=0}^T q(x_1, t) dt \quad (\text{Equation 26})$$

$$v(x_1, t) = \frac{q(x_1, t)}{k(x_1, t)} \quad (\text{Equation 27})$$

Where $v(x_1, t)$, $q(x_1, t)$, and $k(x_1, t)$ are average speed, flow, and density at x_1 at time t .

Static Link Counts and Proportion

From Stage 1 calibration, we can obtain the total link counts for the analysis period, let us say $[0, T]$ then we have the following data and their relationship:

$$x_1 = \sum_{n \in N} \sum_k f_k^n \delta_{l,k}^n \quad (\text{Equation 28})$$

$$x_1 = \sum_{n \in N} x_l \delta_{l,k}^n \quad (\text{Equation 29})$$

Where,

N : Set of OD pairs to which the screen-line counts relates, this is determined by retrieving the volume from the screen-line links after the initial equilibrium procedure and tracing their paths back to their respective OD matrix

$$\sum_{n \in N} \delta_l^n = 1$$

δ_l^n : OD pair proportion, it's also clear that
 $\delta_{l,k}^n$: Path flow proportion, equals to one if link $l \in$ path k , zero otherwise;
 f_k^n : Path flow of OD pair n , on path k ;

Mapping of Link Flow to Individual Origins and Departure Times

OD table to link flow: $d_{rs}^{\tau,l,t} \xrightarrow[\text{mapping}]{G(d_{rs}^{\tau,l,t})} x_l^t$

$$d_{rs}^{\tau,l,t} = G^{-1}(x_l^t) \quad (\text{Equation 30})$$

Note: Here we assume a “link” to contain a bottleneck or lane drop, which would usually be expressed by two adjacent links in a network.

$d_{rs}^{\tau,l,t}$: Demand flow from origin r to destination s (OD pair n), departures at time τ arrives at link l at time t ;

x_l^t : Flow of link l at time t .

To simplify, we use $f_{n,\tau}^{l,t}$ to represent $d_{rs}^{\tau,l,t}$ in the following discussion:

$$d_{rs}^{\tau,l,t} = f_{n,\tau}^{l,t} = G^{-1}(x_l^t)$$

By definition of $f_{n,\tau}^{l,t}$, we have:

$$x_l^t = \sum_{\tau \in (0,t)} \sum_{n \in N} f_{n,\tau}^{l,t} \quad (\text{Equation 31})$$

While, flow could also be expressed as:

$$x_l^t = x_l \sum_{\tau \in (0,t)} \sum_{n \in N} \mu_{\tau}^{l,n,t} \quad (\text{Equation 32})$$

Where $\mu_{\tau}^{l,n,t}$: Flow proportion, or flow for OD pair n , departures at time τ , arrives at link l at time t .

From Equation (31) and (32) we have:

$$\sum_{\tau \in (0,t)} \sum_{n \in N} \mu_{\tau}^{l,n,t} = x_l^t / x_l \quad (\text{Equation 33})$$

$$f_{n,\tau}^{l,t} = x_l \mu_{\tau}^{l,n,t} \quad (\text{Equation 34})$$

Actually, $\mu_{\tau}^{l,n,t}$ could also be expressed as:

$$\mu_{\tau}^{l,n,t} = \delta_l^n \gamma_{\tau}^n \quad (\text{Equation 35})$$

Where γ_{τ}^n : departure time proportion for OD pair n ;

δ_l^n : OD pair proportion, get from stage one.

From Equation (33) and (35) we get:

$$x_l^t = x_l \sum_{n \in N} \delta_l^n \left(\sum_{\tau \in (0,t)} \gamma_{\tau}^n \right) \quad (\text{Equation 36})$$

In (19), only γ_{τ}^n is unknown, and our objective is to find an optimal mapping:

$$\gamma_{\tau}^n = G^{-1} \left(x_l^t / x_l, \delta_l^n \right) \quad (\text{Equation 37})$$

Here we introduce an optimization model to find this optimal mapping:

Optimization model: minimize speed deviation:

$$\min \sum_{\tau \in (0,T)} \sum_l |v_l^t - \hat{v}_l^t| = \min \sum_{\tau \in (0,T)} \sum_l \left| \frac{x_l^t}{k_l^t} - \hat{v}_l^t \right| \approx \min \sum_{\tau \in (0,T)} \sum_l \left[\left| \frac{x_l^t}{k_l^t} \right| \right] - \hat{v}_l^t \quad (\text{Equation 38})$$

Where k_l^t and v_l^t are estimated or observed density and speed of link l from field data.

Substitute (19) into this model we get:

$$\min \sum_{\tau \in (0,T)} \sum_l \left| \frac{x_l \sum_{n \in N} \delta_l^n \left(\sum_{\tau \in (0,t)} \gamma_{\tau}^n \right)}{k_l^t} - \hat{v}_l^t \right| \quad (\text{Equation 39})$$

Subject to

$$x_l^t = x_l \sum_{n \in N} \delta_l^n \left(\sum_{\tau \in (0,t)} \gamma_\tau^n \right) \quad (\text{Equation 40})$$

Data:

- x_l^t : From data preprocessing, could be gathered by $x_l^t = dN(t)/dt$, where $N(t)$ is the arriving N -curve.
- x_l : Total link counts on link l , for time period $[0, T]$;
- δ_l^n : OD pair proportion from stage one;
- k_l^t : estimated or observed average density of link l from field data at time t .
- v_l^t : estimated or observed average speed of link l from field data at time t .

Variable:

γ_τ^n : departure time proportion for demand/departure flow of OD pair n .

This model would give us the optimal departure time proportion, then we could get the optimal departure flow, from (34) and (35):

$$f_{n,\tau}^{l,t} = x_l \delta_l^n \gamma_\tau^n \quad (\text{Equation 41})$$

We could also include the path mapping:

$$f_{n,k,\tau}^{l,t} = x_l \delta_l^n \gamma_\tau^n \delta_{l,k}^n \quad (\text{Equation 42})$$

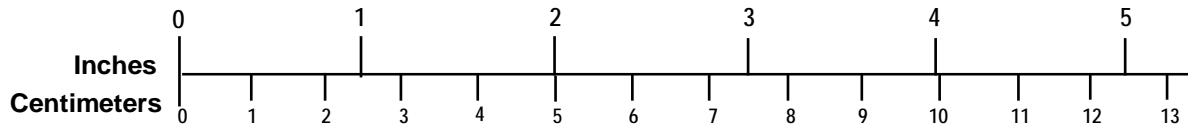
Where $f_{n,k,\tau}^{l,t}$ represents the flow for OD pair n , by path k , at departure time τ , arrives at link l at time t .

After obtaining $f_{n,k,\tau}^{l,t}$, the simulation input vehicle and path files are adjusted accordingly and rerun the simulation to obtain new results.

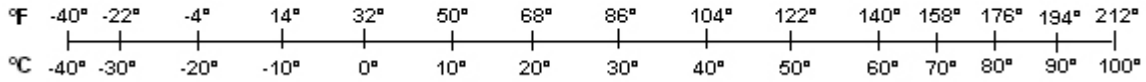
Appendix B. Metric/English Conversion Factors

ENGLISH TO METRIC	METRIC TO ENGLISH
<p>LENGTH (APPROXIMATE)</p> <p>1 inch (in) = 2.5 centimeters (cm) 1 foot (ft) = 30 centimeters (cm) 1 yard (yd) = 0.9 meter (m) 1 mile (mi) = 1.6 kilometers (km)</p>	<p>LENGTH (APPROXIMATE)</p> <p>1 millimeter (mm) = 0.04 inch (in) 1 centimeter (cm) = 0.4 inch (in) 1 meter (m) = 3.3 feet (ft) 1 meter (m) = 1.1 yards (yd) 1 kilometer (km) = 0.6 mile (mi)</p>
<p>AREA (APPROXIMATE)</p> <p>1 square inch (sq in, in²) = 6.5 square centimeters (cm²) 1 square foot (sq ft, ft²) = 0.09 square meter (m²) 1 square yard (sq yd, yd²) = 0.8 square meter (m²) 1 square mile (sq mi, mi²) = 2.6 square kilometers (km²) 1 acre = 0.4 hectare (he) = 4,000 square meters (m²)</p>	<p>AREA (APPROXIMATE)</p> <p>1 square centimeter (cm²) = 0.16 square inch (sq in, in²) 1 square meter (m²) = 1.2 square yards (sq yd, yd²) 1 square kilometer (km²) = 0.4 square mile (sq mi, mi²) 10,000 square meters (m²) = 1 hectare (ha) = 2.5 acres</p>
<p>MASS - WEIGHT (APPROXIMATE)</p> <p>1 ounce (oz) = 28 grams (gm) 1 pound (lb) = 0.45 kilogram (kg) 1 short ton = 2,000 pounds (lb) = 0.9 tonne (t)</p>	<p>MASS - WEIGHT (APPROXIMATE)</p> <p>1 gram (gm) = 0.036 ounce (oz) 1 kilogram (kg) = 2.2 pounds (lb) 1 tonne (t) = 1,000 kilograms (kg) = 1.1 short tons</p>
<p>VOLUME (APPROXIMATE)</p> <p>1 teaspoon (tsp) = 5 milliliters (ml) 1 tablespoon (tbsp) = 15 milliliters (ml) 1 fluid ounce (fl oz) = 30 milliliters (ml) 1 cup (c) = 0.24 liter (l) 1 pint (pt) = 0.47 liter (l) 1 quart (qt) = 0.96 liter (l) 1 gallon (gal) = 3.8 liters (l) 1 cubic foot (cu ft, ft³) = 0.03 cubic meter (m³) 1 cubic yard (cu yd, yd³) = 0.76 cubic meter (m³)</p>	<p>VOLUME (APPROXIMATE)</p> <p>1 milliliter (ml) = 0.03 fluid ounce (fl oz) 1 liter (l) = 2.1 pints (pt) 1 liter (l) = 1.06 quarts (qt) 1 liter (l) = 0.26 gallon (gal) 1 cubic meter (m³) = 36 cubic feet (cu ft, ft³) 1 cubic meter (m³) = 1.3 cubic yards (cu yd, yd³)</p>
<p>TEMPERATURE (EXACT)</p> <p>$[(x-32)(5/9)] \text{ } ^\circ\text{F} = y \text{ } ^\circ\text{C}$</p>	<p>TEMPERATURE (EXACT)</p> <p>$[(9/5)y + 32] \text{ } ^\circ\text{C} = x \text{ } ^\circ\text{F}$</p>

QUICK INCH - CENTIMETER LENGTH CONVERSION



QUICK FAHRENHEIT - CELSIUS TEMPERATURE CONVERSION



For more exact and or other conversion factors, see NIST Miscellaneous Publication 286, Units of Weights and Measures.
Price \$2.50 SD Catalog No. C13 10286

U.S. Department of Transportation
ITS Joint Program Office-HOIT
1200 New Jersey Avenue, SE
Washington, DC 20590

Toll-Free "Help Line" 866-367-7487
www.its.dot.gov

FHWA-JPO-10-036
EDL No. 14943



U.S. Department of Transportation
Research and Innovative Technology
Administration